Control of a Flexible Space Robot Tracking a Moving Target

by

Yifeng Chen

Dissertation submitted to the Faculty of the

Virginia Polytechnic Institute and State University

Partial fulfillment of the requirements for the degree of

Doctor of Philosophy

in

Engineering Mechanics

APPROVED:

L. Meirovitch

L.Meirovitch, Chairman

W. T. Baumann

W.T.Baumann

S. L. Hendricks

S.L.Hendricks

Dean T. Mook

D.T.Mook

Layne T. Watson

L.T.Watson

April 29, 1993

Blacksburg, Virginia

Control of a Flexible Space Robot Tracking a Moving Target

by

Yifeng Chen

Leonard Meirovitch, Committee Chairman

Engineering Mechanics

(Abstract)

This dissertation is concerned with a space robot consisting of a rigid platform, two articulated flexible arms and a rigid end-effector. The task is to ferry some payload and to dock smoothly with an orbiting target whose motion is either known or not known a priori. The dynamical equations for planar motion of the space robot are derived by means of Lagrange's equations. They are then separated into two sets of equations suitable for rigid-body maneuver control design and vibration suppression control design. A perturbation method is used when the target motion is known a priori and direct partitioning is used when the target motion is not known. Both approaches are under the assumption that maneuver motions are much larger than elastic motions.

As far as the rigid-body maneuver control is concerned, optimal trajectory planning is carried out off-line by means of the global optimization method under the assumption that the target motion is known a priori. In contrast, when the target motion is not known a priori, on-line feedback tracking control is carried out by means of an algorithm based on Liapunov-like methodology and using on-line measurements of the target motion.

As far as the vibration suppression control is concerned, the use of the piezoelectric sensor/actuator pairs dispersed along the flexible arms is proposed. Collocated

sensors/actuators for vibration control exhibit good performance. The actuators are designed to compensate for the disturbances caused by the rigid-body maneuver and to realize the LQR feedback control. Assuming that the number of actuators along each flexible arm is equal to the number of modes used to model the beam, the LQR control design is based on a linear time-varying system without persistent disturbances.

Problems related to the digital implementation of the control algorithms are also discussed. Some undesirable effects, such as the bursting pnenomenon and even system instability, can occur if the control algorithms are realized in discrete-time. To prevent these problems, the modified discrete-time control schemes are developed. Numerical examples are used to demonstrate the control algorithms.

Acknowledgements

This dissertation is dedicated to my mother, Jinyuan Dong, and in memory of my father, Shi Chen.

I would like to thank my Ph. D. committee members for their patience and direction. My advisor, Professor L. Meirovitch, deserves special thanks for his invaluable advice, extremely helpful encouragement and criticisms, generous support and understanding during the past four years. Special word of thanks is also directed to Dr. L. T. Watson and Dr. W. T. Baumann who have provided useful discussions and information.

Finally, I express my deepest gratitude to my husband, Zhenhai Chen, who contributed in special ways through his love and support in the best and worst of times.

Table of Contents

Chapter 1 Introduction 1

1.1 Problem Statement 1

1.2 Literature Review 3

1.3 Dissertation Outline 10

Chapter 2 Equations of Motion for a Flexible Space Robot 12

2.1 Equations of Motion 12

2.2 Perturbation Equations 16

2.3 Direct Partitioning Equations 18

Chapter 3 Control Scheme for Tracking a Target Whose Motion is Known A Priori 21

3.1 Inverse Kinematics 21

3.1.1 Robot Redundancy 21

3.1.2 The Global Optimization Method 23

3.1.3 Homotopy Algorithm for Solving Nonlinear TPBV Problem 26

3.2 Inverse Dynamics 29

3.3 Vibration Suppression 29

3.4 Numerical Example 31

Chapter 4 Control Scheme for Tracking a Target Whose Motion is Not Known A Priori 34

4.1 Liapunov-Like Methodology for Tracking Control Algorithm 34

4.1.1 General Idea 34

4.1.2 Modified Algorithm 37

4.2 Vibration Control Algorithm 42

4.2.1 General Control Scheme 42

4.2.2 Discrete-Time Control 44

4.2.3 Modified Discrete-Time Control 45

4.3 Numerical Example 47

Chapter 5 Summary and Conclusions 50

References 53

Appendix A. Matrices in the Original Equations 59

Appendix B. Matrices in the Perturbation Equations 64

Appendix C. Matrices in the Direct Patitioning Equations 69

Figures 72

Vita 101

List of Illustrations

Figure 1. Flexible Space Robot 72

Figure 2. Body Coordinates for Multibody System of Space Robot 73

Figure 3.1a. Time- Lapse Picture of Optimal Robot Configuration Trajectory for Case 1 74

Figure 3.1b. Time- Lapse Picture of Optimal Robot Configuration Trajectory for Case 2 74

Figure 3.2a. Time Histories of the Zero-Order Control Forces 75

Figure 3.2b. Time Histories of the Zero-Order Control Torques 76

Figure 3.2c. Time Histories of the Zero-Order Control Torques 77

Figure 3.3a. Time Histories of Controlled and Uncontrolled Responses 78

Figure 3.3b. Time Histories of Controlled and Uncontrolled Responses 79

Figure 3.3c. Time Histories of Controlled and Uncontrolled Responses 80

Figure 3.3d. Time Histories of Controlled and Uncontrolled Responses 81

Figure 3.4. Time Histories of the Third Elements of the First-Order Control Torques Applied to the Flexible Arms for Disturbance Rejection 82

Figure 3.5a. Time Histories of First-Order Control Forces for LQR Control 83

Figure 3.5b. Time Histories of First-Order Control Torques for LQR Control 84

Figure 3.5c. Time Histories of First-Order Control Torques for LQR Control 85

Figure 3.5d. Time Histories of the Third Elements of the First-Order Control Torques Applied on the Flexible Arms for LQR Control 86

Figure 4.1. Bursting Phenomenon 87

Figure 4.2a. Time- Lapse Picture of Robot Configuration Trajectory for Case 1 88

Figure 4.2b. Time- Lapse Picture of Robot Configuration Trajectory for Case 2 89

Figure 4.3a. Time Histories of Position Error and its Time Derivative 90

Figure 4.3b. Time Histories of Position Error and its Time Derivative 91

Figure 4.3c. Time Histories of Orientation Error and its Time Derivative 92

Figure 4.4. Time Histories of the Tip Elastic Displacements 93

Figure 4.5a. Time Histories of the Control Forces for Rigid-Body Maneuver 94

Figure 4.5b. Time Histories of the Control Torques for Rigid-Body Maneuver 95

Figure 4.5c. Time Histories of the Control Torques for Rigid-Body Maneuver 96

Figure 4.6. Time Histories of the Third Elements of Control Torques Applied to the Flexible Arms for Disturbance Rejection 97

Figure 4.7. Time Histories of the Third Elements of Control Torques Applied to the Flexible Arms for LQR Control 98

Figure 5.1. Block Diagram of the Control Algorithm for a Flexible Space Robot Tracking a Target Whose Motion is Known 99

Figure 5.2. Block Diagram of the Control Algorithm for a Flexible Space Robot Tracking a Target Whose Motion is Not Known 100

Chapter 1 Introduction

Space robots are likely to play an increasingly important role in space missions. They can be used for the collection of space debris, recovery of spacecraft stranded in a useless orbit, repair of orbiting spacecraft, construction of a space station in orbit and servicing the space station while in operation. One of the basic functions of a space robot is to deliver payloads to a target object. In contrast with current remote manipulators, however, space robots must possess the capability of traveling in space and docking with other spacecraft.

Because space robots imply unmanned missions, a well-designed automatic control system must be on board. Together with the complicated dynamics of a space robot itself, the tracking control for a space robot constitutes a very challenging problem.

1.1 Problem Statement

The space robot considered in this dissertation consists of a rigid platform, two articulate flexible arms attached in series to the base, and an end-effector/payload (Fig. 1). The task of the space robot is to track a moving target and deliver payloads accurately and smoothly. To this end, it must have its own control system enabling the platform to translate and rotate and its arms to maneuver.

The equations governing the behavior of space robots are nonlinear and can be expressed in the general form of the state equation

$$\dot{\mathbf{x}} = \mathbf{f}(\mathbf{x}, \mathbf{u}) \tag{1.1a}$$

and the output equation

$$\mathbf{y} = \mathbf{g}(\mathbf{x}) \tag{1.1b}$$

where $\mathbf{x}$ is the state vector, $\mathbf{u}$ is the control force vector and $\mathbf{y}$ is the output vector, usually defined as the position and orientation variables of the end-effector. The target output vector $\mathbf{y}_t$ is defined as the position and orientation variables of the docking port at the target. We can then define the error vector as

$$\mathbf{e} = \mathbf{y}_t - \mathbf{y} \tag{1.2}$$

The problem reduces to that of designing a control law $\mathbf{u}(t)$ so that $\mathbf{e}$ and its time derivative $\dot{\mathbf{e}}$ are driven to zero.

There are two significant differences between industrial robots in current use and space robots considered here. In the first place, industrial robots are mounted on a fixed base, whereas space robots are mounted on space platforms capable of translations and rotations. The second significant difference is that space robots must be very light, and hence very flexible, unlike industrial robots characterized by very bulky and stiff arms. The flexibility of the robot arms causes elastic vibration, which tends to affect adversely the performance of the end-effector. Both characteristics have been considered in this dissertation.

As far as the target motion is concerned, there are two different cases. In the first case, the target motion is assumed to be known a priori. Off-line planning is made to achieve optimality under certain criteria. The control is basically open-loop and the solution is optimal. Because all the *future* information about the target is used for optimality, the whole procedure is sometimes called "planning". The control problem reduces to the solution of a two-point boundary value problem. In the second case, the target motion is not known a priori and the control decision is based on on-line measurement of the *current* state of the system and of the target. This amounts to feedback tracking control.

"Planning" control and "feedback" control can be used in tandem. Indeed,

when the space robot is far from the target and the target motion is known or it can be predicted, planning control can be used to bring the space robot close to the target. Then when the space robot is already close to the target, feedback control can be used for accurate and smooth docking.

In this dissertation, both planning control for tracking a target whose motion is known a priori and feedback control for tracking a target whose motion is not known a priori are investigated.

1.2 Literature Review

Because the research is concerned with two different tracking problems, one in which the target motion is known and one in which the target motion is not known, we review the pertinent literature separately. Moreover, when flexibility is incorporated into space robots, the control problem is significantly more complex than for the rigid-body counterpart, so that a third review section is in order.

i. Planning control

First we discuss tracking control under the assumption that the target motion is known a priori. This is a very common problem in industrial robotics, for which the trajectory of the end-effector for an industrial manipulator is often prescribed. If the robot configuration vector $\mathbf{q} \in R^n$ is related to the end-effector output vector $\mathbf{y} \in R^m$ by means of

$$\mathbf{y} = \mathbf{f}(\mathbf{q}) \tag{1.3}$$

then a desired robot configuration trajectory $\mathbf{q}_d$ and its time rate can be obtained from a desired end-effector trajectory $\mathbf{y}_d$ by means of algorithms based on the following equations

$$\mathbf{q}_d = \mathbf{f}^{-1}(\mathbf{y}_d) \tag{1.4a}$$

$$\dot{\mathbf{q}}_d = J^{\dagger}(\mathbf{q}_d)\dot{\mathbf{y}}_d \tag{1.4b}$$

where $J = \frac{\partial \mathbf{f}}{\partial \mathbf{q}}$ is the Jacobian matrix ($J \in R^{m \times n}$), and $J^{\dagger} \in R^{n \times m}$ is the Moore-Penrose pseudoinverse of J. The procedure of obtaining the desired state $\mathbf{q}_d$ from the prescribed output $\mathbf{y}_d$ is called *inverse kinematics*, sometimes called *trajectory planning*. The control force which can realize the desired state is then computed by certain control algorithms based on the specific robot system equations and this procedure is called *inverse dynamics*. A great deal of research has been carried out on this idea of tracking control.

In the case of space-based robots, extensive research has been carried out on the special problem of free-floating platforms. Longman [1-2] first presented the characteristics of the problem, namely, that the desired robot configuration $\mathbf{q}_d$ cannot be obtained from mere kinematical relations such as that given by Eq. (1.3). He coined the term "forward (inverse) kinetics" to describe the problem. Vafa and Dubowsky [3] developed a new concept, referred to as a "virtual manipulator", to represent the free-floating manipulator system, according to which manipulator path planning and base attitude adjustment can be carried out by cyclic joint motions. Alexander and Cannon [4] presented an extended operational-space control algorithm to calculate appropriate joint torques so as to permit the end-effector to track a desired path while allowing for the free dynamic response of the base vehicle. The main thrust of the research on free-floating space robots is to control the system by merely maneuvering the robot arms. One can realize the desired end-effector trajectory and desired base attitude simultaneously [5], or realize the desired joint angles and desired base attitude simultaneously [6] by actuating joint angles without vehicle attitude control. The research just described is based on the assumption that the robot is free-floating, i.e., there are no external forces and

torques acting on the system, so that the system linear and angular momentum are conserved. For a space robot tracking a moving target, it is unrealistic to make such an assumption, so that algorithms concerned with free-floating space robots are not applicable for our problem.

A space robot system carrying out tracking missions possesses redundancies, i.e., one end-effector trajectory corresponds to an infinity of robot configuration trajectories. The robot redundancy provides an opportunity to optimize the mission. The trajectory associated with the robot configuration can be solved based on a great variety of performance indices or specific requirements, as long as the target trajectory (or desired end-effector trajectory) is known. The approaches used for solving the problem usually falls into two groups, global optimization methods and local optimization methods [7]. De Silva [8] presented a planning space robot trajectory minimizing the base reactions and limiting the end-effector accelerations and jerks to given values. Koivo and Arnautovic [9] presented a method of dynamic optimum control for manipulators with redundancy. Research results have shown that for a robot system with redundancy, such as space robots, not only the tracking can be realized but also certain performance index can be minimized.

In this dissertation, the global optimization method is applied to a tracking control problem for which the target motion is known a priori.

ii. Feedback control

When the target motion is not known a priori, optimal planning is impossible. Even though the target motion is known, it is very likely that some disturbance and unexpected factors can cause errors, so that control based on off-line planning may not work well. In view of this, on-line feedback control for the tracking problem appears more realistic and attractive.

One of the most commonly used techniques for the problem is still the standard one described as follows: First, inverse kinematics is performed from on-line measurements of $\mathbf{y}_d$ to obtain the desired configuration $\mathbf{q}_d$, according to Eq. (1.4). Then, inverse dynamics is performed, i. e., the system equations are used as a nonlinear feedback control algorithm to obtain the control forces so that $\mathbf{q}_d$ is realized in every time step. Because measurements and calculations are performed on-line, the control algorithm must be as simple and as fast as possible. Some investigators have concerned with ways of simplifying the inverse kinematics algorithm [10-12]. Others contributed to a better and simpler control law designed to realize the desired configuration $\mathbf{q}_d$ by various control techniques [13-14].

Because robot tracking is essentially performed by the end-effector, all control algorithms based on tracking the desired configuration $\mathbf{q}_d$ cannot be used before the inverse kinematics problem is first solved. However, on-line calculation of inverse kinematics suffers from problems of computation complexity, robot redundancy and kinematics singularity. Furthermore, the effectiveness of the control is strongly influenced by the accuracy of the inverse kinematics solutions. It follows that approaches to *output* tracking control not based on inverse kinematics are highly desirable. This kind of approaches found in literature can be categoried into four different groups: resolved acceleration control in operational space [4][15], input-output map method [16-17], model following control [18-19] and Liapunov-like methodology[20].

In resolved acceleration control, the control command can be computed typically as

$$\mathbf{F} = M(\mathbf{q})J^{-1}(\mathbf{q})[\ddot{\mathbf{y}}_d + G_1\dot{\mathbf{e}} + G_2\mathbf{e} - \dot{J}(\mathbf{q})\mathbf{q}] + \mathbf{d}(\dot{\mathbf{q}}, \mathbf{q}) \tag{1.5}$$

where $\mathbf{F}$ is the control force vector, M is the mass matrix, $\mathbf{d}$ is the vector grouping of the Coriolis, centrifugal and gravitational forces, G_1 and G_2 are the gain matrices.

$\mathbf{e}$, $\dot{\mathbf{e}}$, $\mathbf{q}$, $\dot{\mathbf{q}}$ and $\ddot{\mathbf{y}}_d$ can be measured and calculated on-line. Strictly speaking, the method amounts to inverse kinematics, because the inverse of Jacobian matrix must still be calculated on-line.

The input-output map technique is based on the invertibility of the input-output map of a nonlinear system equation. Usually it is difficult to find such a map. The corresponding control scheme also involves matrix inversions.

In model-following control, the target trajectory $\mathbf{y}_d$ is regarded as an output of a model dynamical system, so that the plant and output equations are

$$\dot{\mathbf{x}}_m = A_m \mathbf{x}_m + B_m \mathbf{u}_m \tag{1.6a}$$

$$\mathbf{y}_d = C_m \mathbf{x}_m \tag{1.6b}$$

respectively. Tracking is realized by the control $\mathbf{u}$ in Eq. (1.1a), so that $\mathbf{y}$ approached $\mathbf{y}_d$. Model following of linear system has been studied extensively [19]. Optimal model tracking again requires solving two-point boundary value problems off-line [21]. One exception is in the work of Lee et al. [22], in which an optimal decision strategy for aircraft terrain tracking is used. The authors claim that on-line optimal tracking is possible, provided that a fast-converging iteration algorithm proposed in the paper is used.

The Liapunov stability concept has been frequently used in control design. Wang [23] used it to design a guidance law for a spacecraft docking to another spacecraft accurately and smoothly, assuming that the two docking objects are 3-dimensional rigid bodies and have their own control systems on board. Another assumption used in [23] is that the motion of the target object decays to zero with time. Oh et al. [24] presented both theoretical and experimental results of controlling a one-link flexible manipulator using the Liapunov stability principle.

Recently Novakovic [20] presented a technique using Liapunov-like methodology on rigid robot tracking control problem. Compared with other works in the area, his control algorithm exhibits three major advantages:

1) The on-line calculation is simple and it involves neither inverse kinematics nor inverse matrix calculation.
2) The control decision is based on on-line information on the current robot state and target state.
3) Stability is guaranteed no matter how the target motion changes.

In this dissertation, the approach presented in [20] is adopted and modified to solve the problem of flexible space robot tracking control for the case in which the target motion is not known a priori.

iii. Flexible space structure control

In the case of flexible space structures, maneuvering motions excite vibrations of its flexible members. This in turn causes perturbations in the rigid body motions [25]. These coupling effects are highly undesirable, as they can cause the space structures to miss targets.

There are different control schemes for ordinary industrial flexible manipulators. Some control algorithms are based on the linearized models derived from the nonlinear equations of motion of the flexible manipulator. The linearization is performed around the nominal trajectory, which is obtained off-line from the desired tip trajectory. Then linear quadratic regulator (LQR) theory is applied to the linearized model [26-27], as well as other theories such as the variable structure sliding mode control [28-29].

Other researchers attack the problem from another direction. To avoid the complexity resulting from nonlinearity and rigid-flexible motion coupling, they to-

tally abandoned the dynamical equations as the system model. Instead the ARMA model of system identification is used [30-32]. This approach represents essentially adaptive control. Such schemes are useful when accurate dynamical models cannot be obtained. Neither linearization nor state estimation are required, as the control algorithm is based only on the input and output variables, such as tip displacement error, joint angles error and the control force itself. Usually the approach requires computation using on-line recursive tuning and on-line system identification algorithms.

In [33], Bang and Junkins presented a control law for a one-link manipulator derived from Liapunov stability theory in the form

$$u = -g_1(\theta - \theta_d) - g_2\dot{\theta} - g_3(l_0 S_0 - M_0) \tag{1.7}$$

where g_1, g_2 and g_3 are constant gains and $(l_0 S_0 - M_0)$ is the boundary force at the root of link, which can be measured by force sensors or strain gauges. Reference [34] presents a similar control scheme for the general multi-link flexible manipulator. Equation (1.7) represents proportional and derivative control, and it includes the boundary force as a feedback variable. This control scheme is easy to design and implement. However, after a careful examination of the proof in both [33] and [34], it is easy to see that the control scheme is valid only for problems in which the system approaches an equilibrium point in the state space, i.e. $\boldsymbol{\theta} = \boldsymbol{\theta}_d$ and $\dot{\boldsymbol{\theta}} = \mathbf{0}$.

For the space robot with flexible manipulator arms shown in Fig. 1, Murotsu et. [35] proposed a pseudo-resolved acceleration control and reduced-order model control assuming that the space robot is free-floating. Gawrouski et al. [36] proposed a control system consisting of feedforward compensation and feedback control loops based on linearized dynamics. Meirovitch and Lim [37] studied the problem of maneuvering and control of flexible space robots by means of a perturbation

method, whereby the problem is divided into one for the rigid-body maneuvering of the robot and another one for the feedback control of the elastic vibrations and perturbations from the rigid-body motion. The vibration control is carried out by actuators throughout each flexible arm.

In this dissertation, the vibration control design is also based on the assumption that the elastic vibration is small compared to the rigid-body motion. As in [37], the governing equations of motion for the elastic vibration represent a linear time-varying system subjected to persistent disturbances. The vibration control is carried out here by means of piezoelectric sensor/actuator pairs throughout the flexible arms. The major advantage of the piezoelectric sensor/acuator pairs is their collocation property, guaranteeing good control performance [38-40].

1.3 Dissertation Outline

This dissertation is concerned with the control of a two-dimensional flexible space robot tracking a moving target. It is organized as follows:

In Chapter 2, the dynamical equations of motion of a flexible space robot are derived. For the purpose of control design, the original equations are separated into two sets of equations, one governing rigid-body motions and the other the flexible vibration. The separation process differs from one case of target motion to another. In particular, when the target motion is known a priori, a perturbation method is used, and when the target motion is not known a priori, direct partitioning is applied.

Chapter 3 presents a control scheme for a space robot tracking a target whose motion is known a priori. Both the rigid-body tracking maneuver control and the vibration suppression control are developed. A numerical example demonstrates the approach.

Chapter 4 presents the control scheme for a space robot tracking a target whose motion is not known a priori. Again, control algorithms for both tracking and vibration suppression, as well as a numerical example, are presented.

Finally Chapter 5 provides a summary and conclusions.

Chapter 2 Dynamical Equations of Motion for a Flexible Space Robot

The equations of motion for a flexible robot can be derived by means of Lagrange's equations in conjunction with a consistent kinematical scheme. Such equations represent a set of hybrid (ordinary and partial) differential equations involving both rigid-body motions and elastic vibrations, and are nonlinear. In this form, the equations are not suitable for control design. To render them suitable for control design, a discretization procedure is first used, so that the partial differential equations are reduced to sets of ordinary ones. Then, the perturbation method and direct partitioning procedure are applied to the equations resulting in two sets of equations, one governing the rigid-body tracking maneuver and the other governing the elastic vibration control. In this chapter, the equations of motion are first derived and then separated into the rigid-body motion equations and the elastic vibration equations.

2.1 Equations of Motion

The flexible space robot and the coordinate systems are shown in Fig. 2. Body 0 is the robot base, assumed to be rigid. Bodies 1 and 2 are the robot manipulating arms attached in series to Body 0 and they are flexible. Body 3 is the end-effector/payload, also assumed to be rigid. For planar motion, the robot base is capable of two translations, x_0 and y_0, and one rotation θ_0, the two flexible arms are capable of the rotations θ_1 and θ_2 and the elastic vibrations u_1 and u_2 and the end-effector is capable of the rotation θ_3. Referring to Fig. 2, the displacement vector $\mathbf{U}$ and velocity vector $\mathbf{V}$ for a typical point in Body 0 are as follows:

$$\mathbf{U}_0 = \mathbf{R} + C_0^T \mathbf{R}_0 \tag{2.1a}$$

$$\mathbf{V}_0 = \dot{\mathbf{R}} + C_0^T \tilde{\omega}_0 \mathbf{R}_0 \tag{2.1b}$$

Similarly, for Body 1

$$\mathbf{U}_1 = \mathbf{R} + C_0^T \mathbf{L}_0 + C_1^T (\mathbf{r}_1 + \mathbf{u}_1) \tag{2.2a}$$

$$\mathbf{V}_1 = \dot{\mathbf{R}} + C_0^T \tilde{\omega}_0 \mathbf{L}_0 + C_1^T \tilde{\omega}_1 (\mathbf{r}_1 + \mathbf{u}_1) + C_1^T \dot{\mathbf{u}}_1 \tag{2.2b}$$

for Body 2

$$\mathbf{U}_2 = \mathbf{R} + C_0^T \mathbf{L}_0 + C_1^T (\mathbf{L}_1 + \mathbf{u}_{12}) + C_2^T (\mathbf{r}_2 + \mathbf{u}_2) \tag{2.3a}$$

$$\begin{aligned} \mathbf{V}_2 = {} & \dot{\mathbf{R}} + C_0^T \tilde{\omega}_0 \mathbf{L}_0 + C_1^T \tilde{\omega}_1 (\mathbf{L}_1 + \mathbf{u}_{12}) + C_1^T \dot{\mathbf{u}}_{12} \\ & + C_2^T \tilde{\omega}_2 (\mathbf{r}_2 + \mathbf{u}_2) + C_2^T \dot{\mathbf{u}}_2 \end{aligned} \tag{2.3b}$$

and for Body 3

$$\mathbf{U}_3 = \mathbf{R} + C_0^T \mathbf{L}_0 + C_1^T (\mathbf{L}_1 + \mathbf{u}_{12}) + C_2^T (\mathbf{L}_2 + \mathbf{u}_{23}) + C_3^T \mathbf{r}_3 \tag{2.4a}$$

$$\begin{aligned} \mathbf{V}_3 = {} & \dot{\mathbf{R}} + C_0^T \tilde{\omega}_0 \mathbf{L}_0 + C_1^T \tilde{\omega}_1 (\mathbf{L}_1 + \mathbf{u}_{12}) + C_1^T \dot{\mathbf{u}}_{12} \\ & + C_2^T \tilde{\omega}_2 (\mathbf{L}_2 + \mathbf{u}_{23}) + C_2^T \dot{\mathbf{u}}_{23} + C_3^T \tilde{\omega}_3 \mathbf{r}_3 \end{aligned} \tag{2.4b}$$

where

$$C_i = \begin{bmatrix} \cos\theta_i & \sin\theta_i \\ -\sin\theta_i & \cos\theta_i \end{bmatrix} \qquad i = 0, 1, 2, 3 \tag{2.5}$$

are matrices of direction cosines,

$$\tilde{\omega}_i = \begin{bmatrix} 0 & -\dot{\theta}_i \\ \dot{\theta}_i & 0 \end{bmatrix} \qquad i = 0, 1, 2, 3 \tag{2.6}$$

are skew symmetric angular velocity matrices,

$$\mathbf{r}_1 = [\, x_1 \quad 0 \,]^T, \qquad \mathbf{r}_2 = [\, x_2 \quad 0 \,]^T, \qquad \mathbf{R} = [\, x_0 \quad y_0 \,]^T \tag{2.7}$$

are position vectors and

$$\mathbf{u}_1 = [\,0 \quad u_1\,]^T, \qquad \mathbf{u}_2 = [\,0 \quad u_2\,]^T \tag{2.8}$$

are elastic displacement vectors. Moreover,

$$u_{12} = u_1\big|_{x_1=L_1}, \qquad u_{23} = u_2\big|_{x_2=L_2} \tag{2.9}$$

The elastic displacements are discretized as follows:

$$u_i(x,t) = \mathbf{\Phi}_i^T(x_i)\boldsymbol{\xi}_i(t), \qquad i = 1,2 \tag{2.10}$$

where $\mathbf{\Phi}_i(x)$ are vectors of quasi-comparison functions [41] and $\boldsymbol{\xi}_i(t)$ are vectors of generalized displacements. Regarding the robot arms as beams in bending, the quasi-comparison functions can be chosen as linear combination of the admissible functions

$$\phi_k = \cosh\frac{\lambda_k x}{L} - \cos\frac{\lambda_k x}{L} - \sigma_k(\sinh\frac{\lambda_k x}{L} - \sin\frac{\lambda_k x}{L}) \qquad k = 1,2,\ldots \tag{2.11}$$

which represent the eigenfunctions of a clamped-free beam for k odd and clamped-clamped beam for k even, where λ_k's are the nondimensional frequency parameters and σ_k's are the nondimensional parameters.

Using Eqs. (2.1)-(2.11), the kinetic energy of the system can be written as

$$T = \sum_{i=0}^{3} T_i = \frac{1}{2}\sum_{i=0}^{3}\int_{\text{Body } i} \rho_i \mathbf{V}_i^T\mathbf{V}_i dD_i = \frac{1}{2}\dot{\mathbf{q}}^T M\dot{\mathbf{q}} \tag{2.12}$$

where $\mathbf{q} = [\mathbf{R}_0^T \;\; \theta_0 \;\; \theta_1 \;\; \theta_2 \;\; \theta_3 \;\; \boldsymbol{\xi}_1^T \;\; \boldsymbol{\xi}_2^T]^T$ is the configuration vector and M is the mass matrix with entries given in Appendix A.

The potential energy for the system is due entirely to the elasticity of the robot arms and can be written in the form

$$V = \sum_{i=1}^{2}\frac{1}{2}\boldsymbol{\xi}_i^T K_i \boldsymbol{\xi}_i = \frac{1}{2}\mathbf{q}^T K\mathbf{q} \tag{2.13}$$

where

$$K = \text{block}-\text{diag}\,[\,0 \quad \bar{K}_1 \quad \bar{K}_2\,] \tag{2.14}$$

in which

$$\bar{K}_i = \int_0^{L_i} EI_i \Phi_i'' (\Phi_i'')^T dx_i, \qquad i = 1,2 \tag{2.15}$$

are the stiffness matrices for Bodies i, in which EI_i denotes the bending stiffnesses. Note that the gravitational potential is ignored here.

The control forces acting on the robot system include the horizontal and vertical thrusts on the base center, F_x and F_y, an external torque on the base, M_0, the internal joint torques on the joints of two links and end-effector, M_1, M_2 and M_3, and the distributed internal moments created by piezoelectric actuators on links 1 and 2, $\boldsymbol{\tau}_1$ and $\boldsymbol{\tau}_2$. We define the control force vector as $\mathbf{F} = [\,F_x \quad F_y \quad M_0 \quad M_1 \quad M_2 \quad M_3 \quad \boldsymbol{\tau}_1^T \quad \boldsymbol{\tau}_2^T\,]^T$. Then, the virtual work of the system can be written in the form

$$\begin{aligned}
\delta W &= F_x \delta x_0 + F_y \delta y_0 + M_0 \delta\theta_0 + M_1(\delta\theta_1 - \delta\theta_0) \\
&\quad + M_2(\delta\theta_2 - \delta\theta_1 - \Phi_1'^T(L_1)\delta\boldsymbol{\xi}_1) + M_3(\delta\theta_3 - \delta\theta_2 - \Phi_2'^T(L_2)\delta\boldsymbol{\xi}_2) \\
&\quad + \sum_{i=1}^{m_1} \tau_{1i} \Phi_1''^T(x_{1i})\delta\boldsymbol{\xi}_1 + \sum_{i=1}^{m_2} \tau_{2i} \Phi_2''^T(x_{2i})\delta\boldsymbol{\xi}_2 \\
&= \mathbf{Q}^T \delta\mathbf{q}
\end{aligned} \tag{2.16}$$

where $\mathbf{Q}$ is a generalized force vector defined as

$$\mathbf{Q} = G\mathbf{F} \tag{2.17}$$

The entries of the matrix G are given in Appendix A.

Lagrange's equations for the system can be expressed in the symbolic vector form

$$\frac{d}{dt}\left(\frac{\partial T}{\partial \dot{\mathbf{q}}}\right) - \frac{\partial T}{\partial \mathbf{q}} + \frac{\partial V}{\partial \mathbf{q}} = \mathbf{Q} \tag{2.18}$$

Inserting Eqs. (2.12), (2.13) and (2.16) into Eq. (2.18), we obtain the system equations in the matrix form

$$M(\mathbf{q})\ddot{\mathbf{q}} + C(\mathbf{q}, \dot{\mathbf{q}})\dot{\mathbf{q}} + K\mathbf{q} = \mathbf{Q} \tag{2.19}$$

The entries of the matrix C are also given in Appendix A.

Equation (2.19) represents the equation governing the motion of the flexible space robot. It is used for computer simulation of the dynamical system. For the purpose of control design, Eq. (2.19) is conveniently separated into two sets of equations, rigid-body motion equations and elastic vibration equations. To this end, there are two procedures that can be used, depending on the target motion. One is the perturbation method, which is suitable for problems in which the target motion is known a priori. The second is direct partitioning, which is more convenient for problems in which the target motion is not known a priori. The reason for using two different schemes will become obvious later in this chapter.

2.2 Perturbation Equations

Our objective is to track a moving target while suppressing the vibration effects so as to permit accurate and smooth docking. In most cases of interest, elastic motions tend to be small compared to maneuvering motions, particularly when the elastic vibration is controlled. In the perturbation method, the configuration vector and the generalized force vector are separated into the zero-order vector and the first-order vector in the form

$$\mathbf{q}(t) = \mathbf{q}_0(t) + \mathbf{q}_1(t) \tag{2.20a}$$

$$\mathbf{Q}(t) = \mathbf{Q}_0(t) + \mathbf{Q}_1(t) \tag{2.20b}$$

where the subscripts 0 and 1 denote the different orders of magnitude, with the assumption that the zero-order vectors are one order of magnitude larger than the first-order vectors; the elastic vibrations are by definition first-order variables, so that

$$\mathbf{q}_0 = [\, x_{00} \quad y_{00} \quad \theta_{00} \quad \theta_{01} \quad \theta_{02} \quad \theta_{03} \quad \mathbf{0}^T \quad \mathbf{0}^T \,]^T \tag{2.21a}$$

$$\mathbf{q}_1 = [\, x_{10} \quad y_{10} \quad \theta_{10} \quad \theta_{11} \quad \theta_{12} \quad \theta_{13} \quad \boldsymbol{\xi}_1^T \quad \boldsymbol{\xi}_2^T \,]^T \tag{2.21b}$$

Introducing Eqs. (2.20) into Eq. (2.19) and separating quantities of different order of magnitude, the original dynamical system is separated into two systems. One system, referred to as a zero-order system, is concerned with maneuvering of the robot composed of rigid members. The second system, referred to as a first-order system, is concerned with the control of the elastic vibrations and perturbations from the rigid-body maneuvering. The equation defining the zero-order system has the form

$$M_0(\mathbf{q}_0)\ddot{\mathbf{q}}_0 + C_0(\mathbf{q}_0, \dot{\mathbf{q}}_0)\dot{\mathbf{q}}_0 = \mathbf{Q}_0 \tag{2.22}$$

and the equation defining the first-order system is

$$M_1(\mathbf{q}_0)\ddot{\mathbf{q}}_1 + C_1(\mathbf{q}_0, \dot{\mathbf{q}}_0)\dot{\mathbf{q}}_1 + K_1(\mathbf{q}_0, \dot{\mathbf{q}}_0, \ddot{\mathbf{q}}_0)\mathbf{q}_1 + \mathbf{d}(\mathbf{q}_0, \dot{\mathbf{q}}_0, \ddot{\mathbf{q}}_0) = \mathbf{Q}_1 \tag{2.23}$$

where M_0 and M_1 are mass matrices, C_0, C_1 and K_1 are coefficient matrices and $\mathbf{d}$ is a persistent disturbance vector. The explicit expressions for M_0, C_0, M_1, C_1, K_1 and $\mathbf{d}$ are given in Appendix B.

It is clear from above that the zero-order problem can be solved independently of the first-order problem, which is typical of the perturbation method. It means that the zero-order problem is decoupled from the first-order problem. On the other hand, the first-order problem depends on the solution of the zero-order problem, where the dependence manifests itself in the form of time-varying coefficients and

persistent disturbances. The zero-order problem is nonlinear and of relatively low dimension ($n = 6$). In contrast, the first-order problem is linear, time-varying and of relatively large dimension ($n = 6+$ dimension of $\boldsymbol{\xi}_1 +$ dimension of $\boldsymbol{\xi}_2$).

Equations (2.22) and (2.23) obtained by the perturbation method are used for the problem of a flexible space robot tracking a moving target whose motion is known a priori. As mentioned above, when the time history $\mathbf{y}_d(t)$ of a target motion is known, the time history $\mathbf{q}_d(t)$ of the desired robot configuration and the derivatives $\dot{\mathbf{q}}_d(t)$ and $\ddot{\mathbf{q}}_d(t)$ can be obtained from inverse kinematics. Letting $[\,\mathbf{q}_0^T \quad \dot{\mathbf{q}}_0^T \quad \ddot{\mathbf{q}}_0^T\,]^T = [\,\mathbf{q}_d^T \quad \dot{\mathbf{q}}_d^T \quad \ddot{\mathbf{q}}_d^T\,]^T$, $\mathbf{Q}_0$ can be computed directly from Eq. (2.22). On the other hand, $\mathbf{Q}_1$ represents the control vector in the linear time-varying system, Eq. (2.23), designed so as to drive the perturbed system state $\mathbf{q}_1$ to zero. In this sense, we can say that the zero-order equation, Eq. (2.22), is used for the "rigid-body" maneuvering of tracking and the first-order equation, Eq. (2.23), is used for the suppression of vibrations and perturbations from the rigid-body motion.

2.3 Direct Partitioning Equations

Another way of separating the original equation into rigid-body motion equations and elastic vibration equations is to partition Eq. (2.19) directly by writing

$$\mathbf{q} = [\,\mathbf{q}_r^T \quad \mathbf{q}_e^T\,]^T \tag{2.24}$$

where $\mathbf{q}_r = [\,x_0 \quad y_0 \quad \theta_0 \quad \theta_1 \quad \theta_2 \quad \theta_3\,]^T$ is a rigid-body displacement vector, $\mathbf{q}_e = [\,\boldsymbol{\xi}_1^T \quad \boldsymbol{\xi}_2^T\,]^T$ is an elastic displacement vector and $\mathbf{Q}_r$ and $\mathbf{Q}_e$ are corresponding generalized force vectors. Then, Eq. (2.19) can be written in the partitioned matrix form

$$\begin{bmatrix} M_{rr} & M_{re} \\ M_{re}^T & M_{ee} \end{bmatrix} \begin{Bmatrix} \ddot{\mathbf{q}}_r \\ \ddot{\mathbf{q}}_e \end{Bmatrix} + \begin{bmatrix} C_{rr} & C_{re} \\ C_{er} & C_{ee} \end{bmatrix} \begin{Bmatrix} \dot{\mathbf{q}}_r \\ \dot{\mathbf{q}}_e \end{Bmatrix} + \begin{bmatrix} 0 & 0 \\ 0 & K \end{bmatrix} \begin{Bmatrix} \mathbf{q}_r \\ \mathbf{q}_e \end{Bmatrix} = \begin{Bmatrix} \mathbf{Q}_r \\ \mathbf{Q}_e \end{Bmatrix} \tag{2.25}$$

After some algebraic manipulations, and ignoring higher-order terms in the elastic displacements, Eq. (2.25) can be separated into

$$M_r(\mathbf{q}_r)\ddot{\mathbf{q}}_r + C_r(\mathbf{q}_r, \dot{\mathbf{q}}_r)\dot{\mathbf{q}}_r + \mathbf{d}_e(\mathbf{q}, \dot{\mathbf{q}}, \ddot{\mathbf{q}}) = \mathbf{Q}_r \tag{2.26}$$

and

$$M_e(\mathbf{q}_r)\ddot{\mathbf{q}}_e + C_e(\mathbf{q}_r, \dot{\mathbf{q}}_r)\dot{\mathbf{q}}_e + K_e(\mathbf{q}_r, \dot{\mathbf{q}}_r, \ddot{\mathbf{q}}_r)\mathbf{q}_e + \mathbf{d}_r(\mathbf{q}_r, \dot{\mathbf{q}}_r, \ddot{\mathbf{q}}_r) = \mathbf{Q}_e \tag{2.27}$$

where M_r and M_e are mass matrices, C_r, C_e and K_e are coefficient matrices and $\mathbf{d}_e$ and $\mathbf{d}_r$ are disturbance vectors. The entries of the various matrices are given in Appendix C. The term $\mathbf{d}_e$ in Eq. (2.26) is a linear combination of $\mathbf{q}_e$, $\dot{\mathbf{q}}_e$ and $\ddot{\mathbf{q}}_e$. It can be regarded as a disturbance due to the flexibility of the robot arms. The term $\mathbf{d}_r$ in Eq. (2.27) is a function of $\mathbf{q}_r$, $\dot{\mathbf{q}}_r$ and $\ddot{\mathbf{q}}_r$. It can be regarded as a disturbance due to the rigid-body maneuvering of the robot.

Unlike the zero-order equations, Eq. (2.22), and the first-order equations, Eq. (2.23), derived in Sec. 2.2, Eqs. (2.26) and (2.27) are coupled. It is clear that if the robot were rigid, the system dynamical equation would be Eq. (2.26) with $\mathbf{d}_e \equiv 0$. When flexibility of robot arms is introduced into the problem, the coupling between rigid-body motion and flexible vibration is reflected in Eqs. (2.26) and (2.27) in such a way that the persistent disturbance $\mathbf{d}_r$ from the rigid-body motion causes the elastic motion $\mathbf{q}_e$, $\dot{\mathbf{q}}_e$ and $\ddot{\mathbf{q}}_e$ through Eq. (2.27) and $\mathbf{q}_e$ in turn disturbs the rigid-body motion through $\mathbf{d}_e$ in Eq. (2.26).

Equations (2.26) and (2.27) derived from direct partitioning are used for the problem of a flexible space robot tracking a moving target whose motion is not known a priori. As mentioned before, when the target motion is not known a priori, the control decision must be made by means of on-line measurements of the *current* system state and the *current* target state. In Eqs. (2.26) and (2.27), $\mathbf{q}_r$ together

with $\dot{\mathbf{q}}_r$ is the true state of the system and is directly measurable, while in Eqs. (2.22) and (2.23), neither $\mathbf{q}_0$ nor $\mathbf{q}_1$ can be measured directly. This is the major reason we use direct partitioning instead of a perturbation method to separate equations for this particular problem.

Chapter 3 Control Scheme for Tracking a Target Whose Motion is Known A Priori

When the target motion is known a priori, the desired end-effector tip trajectory can be obtained readily. Then, using inverse kinematics, the rigid-body robot configuration corresponding to the desired end-effector trajectory can be calculated. Having the desired robot configuration, the rigid-body dynamical equations can be used to compute the required control forces by means of inverse dynamics. Then, the elastic vibration equations can be used to design the vibration control law for the tracking mission under consideration.

In this chapter, the algorithms for inverse kinematics, inverse dynamics and vibration control are first presented and then demonstrated by means of a numerical example.

3.1 Inverse Kinematics

In this section, we assume that the space robot is made of rigid members. The general idea of the global optimization method for robot redundancy problems is introduced and the corresponding numerical algorithm is presented.

3.1.1 Robot Redundancy

The problem of interest here is the determination of the state vector defining the motion of the robot under the assumption that the tip trajectory of the end-effector is given.

We denote by $\mathbf{y}_e \in R^m$ the end-effector output vector defining the end-effector trajectory and by $\mathbf{q} \in R^n$ the robot configuration vector defining the robot con-

figuration trajectory. When $m < n$, one end-effector trajectory corresponds to an infinity of state trajectories. In this case, the robot is said to possess redundancy.

The kinematical relation between $\mathbf{y}_e$ and $\mathbf{q}$ is given by

$$\mathbf{y}_e = \mathbf{f}(\mathbf{q}) \tag{3.1}$$

Taking the derivatives of Eq. (3.1) with respect to time, we obtain

$$\dot{\mathbf{y}}_e = J(\mathbf{q})\dot{\mathbf{q}} \tag{3.2}$$

$$\ddot{\mathbf{y}}_e = J(\mathbf{q})\ddot{\mathbf{q}} + \dot{J}(\mathbf{q}, \dot{\mathbf{q}})\dot{\mathbf{q}} \tag{3.3}$$

where $J(\mathbf{q}) = \left[\dfrac{\partial \mathbf{f}}{\partial \mathbf{q}}\right]$ is the Jacobian matrix.

The object is to determine a state trajectory $\mathbf{q}$, $\dot{\mathbf{q}}$ corresponding to a given end-effector trajectory $\mathbf{y}_e$. To this end, we invert Eq. (3.2) and write the solution in the form

$$\dot{\mathbf{q}} = J^{\dagger}(\mathbf{q})\dot{\mathbf{y}}_e(t) + (I_n - J^{\dagger}(\mathbf{q})J(\mathbf{q}))\mathbf{y} \tag{3.4}$$

where

$$J^{\dagger} = J^T(JJ^T)^{-1} \tag{3.5}$$

is the Penrose-Moore pseudo-inverse of the matrix J, I_n is the $n \times n$ identity matrix and $\mathbf{y}$ is an arbitrary n-vector. Note that the first term on the right side of Eq. (3.4) represents the minimum-norm solution of Eq. (3.2) and the second term is an arbitrary vector from the Jacobian matrix null space. For a nonredundant robot, i. e., $m = n$, Eq. (3.4) becomes

$$\dot{\mathbf{q}} = J^{-1}(\mathbf{q})\dot{\mathbf{y}}_e(t) \tag{3.6}$$

A space robot is usually redundant due to the motion of its base, so that we must deal with Eq. (3.4) instead of Eq. (3.6), which introduces some complexity in the

problem. However, since $\mathbf{y}$ in Eq. (3.4) is an arbitrary vector, the redundancy also provides the opportunity of optimizing the solutions. The so-called global optimization method is based on this idea.

3.1.2 The Global Optimization Method [7]

The interest lies in a robot configuration trajectory satisfying Eq. (3.4) that is optimal in some sense. First, we introduce the functional

$$L = \int_{t_0}^{t_f} \psi(\mathbf{q}, t)dt \tag{3.7}$$

Then, the determination of $\mathbf{q}(t)$, $t_0 < t < t_f$, can be reduced to the problem of minimizing L among trajectories realizing the desired end-effector trajectory.

Equation (3.4) can be rewritten as

$$\dot{\mathbf{q}} = \mathbf{g}(\mathbf{q}, \mathbf{y}, t) \tag{3.8}$$

so that Eqs. (3.7) and (3.8) can be regarded as representing an optimal control problem for a time-varying nonlinear system, in which $\mathbf{q}$ plays the role of the state vector and $\mathbf{y}$ plays the role of the control vector. Following the established procedure [42], we introduce the Hamiltonian

$$H(\mathbf{q}, \mathbf{p}, \mathbf{y}, t) = \psi(\mathbf{q}, t) + \mathbf{p}^T\mathbf{g}(\mathbf{q}, \mathbf{y}, t) \tag{3.9}$$

in which $\mathbf{p} \in R^n$ is an adjoint n-vector, commonly known as the costate vector. According to Pontryagin's minimum principle, the optimal control extremizes the Hamiltonian at all times. The optimal trajectory is then obtained by solving the $2n$ differential equations

$$\dot{\mathbf{q}} = \frac{\partial H}{\partial \mathbf{p}} \tag{3.10a}$$

$$\dot{\mathbf{p}} = -\frac{\partial H}{\partial \mathbf{q}} \tag{3.10b}$$

Equations (3.10) are subject to $2n$ end conditions specifying the state at the initial and final times, and in particular whether the state is free or fixed. Thus, the problem of determining the optimal trajectory has been reduced to the solution of a two-point boundary value (TPBV) problem.

As an example of interest, we consider

$$\psi(\mathbf{q},t) = \dot{\mathbf{q}}^T\dot{\mathbf{q}} = \mathbf{g}^T\mathbf{g} \tag{3.11}$$

as the function entering into the performance measure L, so that the Hamiltonian becomes

$$H = \mathbf{g}^T\mathbf{g} + \mathbf{p}^T\mathbf{g} \tag{3.12}$$

Then, following the usual steps, we obtain the "control" vector $\mathbf{y}$ minimizing the Hamiltonian in the form

$$\mathbf{y} = -\frac{1}{2}(I_n - J^\dagger J)\mathbf{p} \tag{3.13}$$

Using Eqs. (3.13) and (3.10), we obtain the equations defining the optimal trajectory

$$\dot{\mathbf{q}} = \mathbf{g} \tag{3.14a}$$

$$\dot{\mathbf{p}} = -\left(\frac{\partial \mathbf{g}}{\partial \mathbf{q}}\right)^T (2\mathbf{g} + \mathbf{p}) \tag{3.14b}$$

where

$$\mathbf{g} = J^\dagger\dot{\mathbf{y}}_e(t) - \frac{1}{2}(I_n - J^\dagger J)\mathbf{p} \tag{3.15}$$

In the case in which the integrand ψ in the performance measure is as given by Eq. (3.11), the preceding results can be obtained more readily by using methods of the calculus of variations [43]. To this end, we consider the augmented performance measure

$$L^* = \int_{t_0}^{t_f} [\dot{\mathbf{q}}^T\dot{\mathbf{q}} + \boldsymbol{\lambda}^T(\mathbf{y}_e(t) - \mathbf{f}(\mathbf{q}))]dt = \int_{t_0}^{t_f} \mu(\mathbf{q},\dot{\mathbf{q}},t)dt \tag{3.16}$$

Then, the variation of L^* can be written as

$$\delta L^* = \int_{t_0}^{t_f} \left[\frac{\partial \mu}{\partial \mathbf{q}} - \frac{d}{dt}\left(\frac{\partial \mu}{\partial \dot{\mathbf{q}}}\right)\right]^T \delta\mathbf{q}(t)dt + \left[\frac{\partial \mu}{\partial \dot{\mathbf{q}}(t_f)}\right]^T \delta\mathbf{q}(t_f) - \left[\frac{\partial \mu}{\partial \dot{\mathbf{q}}(t_0)}\right]^T \delta\mathbf{q}(t_0) = 0 \tag{3.17}$$

Equating the coefficient of $\delta\mathbf{q}$ in the integrand to zero, we obtain the vector form of Euler's equation

$$\frac{\partial \mu}{\partial \mathbf{q}} - \frac{d}{dt}\left(\frac{\partial \mu}{\partial \dot{\mathbf{q}}}\right) = \mathbf{0} \tag{3.18}$$

which, upon using Eq. (3.16), leads to

$$J^T\boldsymbol{\lambda} - 2\ddot{\mathbf{q}} = \mathbf{0} \tag{3.19}$$

Using Eqs. (3.19) and (3.3), we have

$$\boldsymbol{\lambda} = 2(JJ^T)^{-1}(\ddot{\mathbf{y}}_e - \dot{J}\dot{\mathbf{q}}) \tag{3.20}$$

Substituting Eq. (3.20) into (3.19) and augmenting the result with the definition $\dot{\mathbf{q}} = \mathbf{v}$, we obtain

$$\dot{\mathbf{q}} = \mathbf{v} \tag{3.21a}$$

$$\dot{\mathbf{v}} = J^{\dagger}(\mathbf{q})(\ddot{\mathbf{y}}_e - \dot{J}\mathbf{v}) \tag{3.21b}$$

Equations (3.21) represent a set of $2n$ first-order differential equations. Comparing Eqs. (3.14) and (3.21), we observe that the first are in terms of $\mathbf{q}$ and $\mathbf{p}$ and the second in terms of $\mathbf{q}$ and $\mathbf{v}$. Equations (3.14) were derived by means of Pontryagin's minimum principle and Eqs. (3.21) by means of the calculus of variations. In spite of their different appearance the two sets of equations yield the same trajectory [43]. Equations (3.21) are simpler to use, but were derived for the special case in which ψ is given by Eq. (3.11). On the other hand, Eqs. (3.14) are broader in scope, and are to be used in the more general case.

3.1.3 Homotopy Algorithm for Solving Nonlinear TPBV Problem

Equations (3.14) or (3.21) in conjunction with the end conditions constitute a nonlinear two-point boundary value problem. The solution of such problems is generally very difficult to obtain, particularly for systems of large dimension. The shooting method [44] reduces the problem to the solution of the nonlinear equation

$$\mathbf{F}(\mathbf{w}) = \mathbf{0} \qquad (\mathbf{F}, \mathbf{w} \in R^n) \tag{3.22}$$

which can be solved by Newton's method. The approach suffers from sensitivity to initial guesses and can lead to divergence. Improving the initial guess is not always feasible, particularly for multivariable systems. As an alternative, consider the continuation method. According to this method, Eq. (3.22) is replaced by a family of problems given by

$$\mathbf{\Gamma}(\alpha, \mathbf{w}) = \alpha\mathbf{F}(\mathbf{w}) + (1 - \alpha)\mathbf{S}(\mathbf{w}) = \mathbf{0} \tag{3.23}$$

where $\alpha \in [0, 1]$ is a parameter and $\mathbf{S}(\mathbf{w})$ is a function such that the equation $\mathbf{S}(\mathbf{w}) = \mathbf{0}$ is relatively easy to solve. This is the equation corresponding to $\alpha = 0$. At $\alpha = 1$, Eq. (3.23) reduces to the equation we would like to solve. The approach consists of solving Eq. (3.23) in a step-by-step manner, beginning with $\alpha = 0$ and finishing with $\alpha = 1$. The solution at every step uses as an initial guess the solution obtained in the previous step. However, if Newton's method is used to solve Eq. (3.23), failure may still occur, because Newton's method postulates that $\mathbf{w} = \mathbf{w}(\alpha)$ in Eq. (3.23), and the zero set of Eq. (3.23) does not necessarily increase monotonically in α.

Quite recently, a new version of the continuation method, known as probability-one homotopy algorithms, has been developed [45]. The algorithms are relatively

insensitive to initial guesses, i.e., they guarantee the convergence to the correct solution even for initial guesses not very close to the solution.

With regard to the algorithm, a homotopy map $\mathbf{\Gamma_a} : [0,1] \times E^n \rightarrow E^n$ is defined by

$$\mathbf{\Gamma_a}(\alpha, \mathbf{w}) = \mathbf{\Gamma}(\mathbf{a}, \alpha, \mathbf{w}) = \alpha \mathbf{F}(\mathbf{w}) + (1-\alpha)(\mathbf{w} - \mathbf{a}) \tag{3.24}$$

According to the homotopy theory, for almost all $\mathbf{a} \in E^n$, there is a zero curve γ of $\mathbf{\Gamma_a}$ emanating from $(0, \mathbf{a})$, along which the Jacobian matrix $D\mathbf{\Gamma_a}$ has full rank. The curve γ is continuously differentiable, does not intersect itself, and is disjoint from all the other zeros of $\mathbf{\Gamma_a}$. Furthermore, γ must either reach a point $(1, \bar{\mathbf{w}})$, in which case $\bar{\mathbf{w}}$ solves Eq. (3.22), or approach infinity. Since γ is smooth, it can be parameterized by the arc length s : $\alpha = \alpha(s)$, $\mathbf{w} = \mathbf{w}(s)$. Then, the zero curve of Eq. (3.24) can be expressed as

$$\mathbf{\Gamma_a}(\alpha(s), \mathbf{w}(s)) = \mathbf{0} \tag{3.25}$$

Thus,

$$\frac{d}{ds}\mathbf{\Gamma_a}(\alpha(s), \mathbf{w}(s)) = \mathbf{0} \tag{3.26}$$

Equation (3.26) can be written as

$$\left[\frac{\partial \mathbf{\Gamma_a}}{\partial \alpha} \quad \frac{\partial \mathbf{\Gamma_a}}{\partial \mathbf{w}} \right] \begin{Bmatrix} \frac{d\alpha}{ds} \\ \frac{d\mathbf{w}}{ds} \end{Bmatrix} = \mathbf{0} \tag{3.27a}$$

$$|| \begin{pmatrix} \frac{d\alpha}{ds} & \frac{d\mathbf{w}}{ds} \end{pmatrix} ||_2 = 1 \tag{3.27b}$$

where $||\ ||_2$ denotes the Euclidean norm. Equation (3.27a) is subject to the initial conditions

$$\begin{aligned} \alpha(0) &= 0 \\ \mathbf{w}(0) &= \mathbf{a} \end{aligned} \tag{3.28}$$

The solution $\bar{\mathbf{w}}(s^*)$ is obtained at the point $s = s^*$ for which $\alpha(s^*) = 1$.

In solving Eq. (3.27a), α is allowed to increase or decrease arbitrarily within $s \in [0, s^*]$, as long as the zero curve γ is followed. This is a distinct advantage over Newton's continuation method, for which α is required to increase monotonically. Based on the homotopy theory, the Jacobian matrix $\left[\frac{\partial \mathbf{\Gamma_a}}{\partial \alpha} \quad \frac{\partial \mathbf{\Gamma_a}}{\partial \mathbf{w}} \right]$ has full rank along the zero curve γ and γ is bounded. This ensures the probability-one convergence for the nonlinear problem.

To apply the algorithm in our inverse kinematics problem, we can express Eq. (3.21) with a specific end condition as a nonlinear two-point boundary value problem as follows

$$\begin{aligned} \dot{\mathbf{q}} &= \mathbf{v} \\ \dot{\mathbf{v}} &= J^{\dagger}(\mathbf{q})(\ddot{\mathbf{y}}_e - \dot{J}\dot{\mathbf{q}}) \\ \mathbf{q}(0) &= \mathbf{c} \\ \mathbf{v}(t_f) &= J^{\dagger}(\mathbf{q}(t_f), t_f)\dot{\mathbf{y}}_e(t_f) \end{aligned} \tag{3.29}$$

It is equivalent to the problem of solving the nonlinear vector equation

$$\mathbf{F}(\mathbf{w}) = \dot{\mathbf{q}}(t_f, \mathbf{w}) - J^{\dagger}(t_f, \mathbf{w})\dot{\mathbf{y}}_e(t_f) = \mathbf{0} \tag{3.30}$$

where $\mathbf{w} = \mathbf{v}(0)$. Note that $\dot{\mathbf{q}}(t_f, \mathbf{w})$ and $J^{\dagger}(t_f, \mathbf{w})$ are functions of $\mathbf{w}$ in an implicit way.

The homotopy map is given by Eq. (3.24), in which $\mathbf{a}$ is an initial guess of $\mathbf{w}$. As long as the solution $\mathbf{w}^*$ of Eq. (3.30) is obtained, $\mathbf{q}^*$ and its derivatives $\dot{\mathbf{q}}^*$ and $\ddot{\mathbf{q}}^*$ can be computed by the ordinary differential equations (3.21) with $2n$ initial conditions $\mathbf{q}(0) = \mathbf{c}$ and $\mathbf{v}(0) = \mathbf{w}^*$. The solution $\mathbf{q}^*(t)$, $\dot{\mathbf{q}}^*(t)$ and $\ddot{\mathbf{q}}^*(t)$, $t \in [0, t_f]$, is the desired robot state trajectory not only realizing the end-effector trajectory $\mathbf{y}_e$ but also optimizing the performance measure L defined by Eq. (3.7).

3.2 Inverse Dynamics

After the desired robot state trajectory, $\mathbf{q}^*(t)$, $\dot{\mathbf{q}}^*(t)$ and $\ddot{\mathbf{q}}^*(t)$, $t \in [0, t_f]$, is obtained through inverse kinematics, the next task is to compute the control forces required to realize the trajectory. Since inverse kinematics is based on the rigid multibody counterpart, the state trajectory cannot be used in a flexible robot system directly. However, referring to section 2.2, we note that we have already derived the zero-order equations of motion (2.22) representing the "rigid-body" maneuver of the flexible robot system. Moreover the zero-order equations are independent of the first-order variables. Therefore, we naturally can assume that

$$\begin{aligned} \mathbf{q}_0(t) &= \mathbf{q}^*(t) \\ \dot{\mathbf{q}}_0(t) &= \dot{\mathbf{q}}^*(t) \qquad\qquad t \in [0, t_f] \\ \ddot{\mathbf{q}}_0(t) &= \ddot{\mathbf{q}}^*(t) \end{aligned} \tag{3.31}$$

With $\mathbf{q}_0$ and its derivatives as known function of time, we can compute the control force trajectory of $\mathbf{Q}_0$ directly by Eq. (2.22). The procedure is referred to as inverse dynamics. Equation (2.22) can be regarded as a control algorithm for the "rigid-body" maneuver of a flexible space robot tracking a known end-effector trajectory. The control is open loop because the inverse kinematics is carried out off-line.

3.3 Vibration Suppression

In the case in which the space robot is composed of rigid members, the above control scheme is sufficient to solve the problem. However, when flexibility of the space robot is considered, we must deal with the elastic vibrations and the perturbations from the rigid-body maneuvering, as indicated in section 2.2. The governing equations of the elastic vibrations and perturbations are the first-order equations, Eqs. (2.23). The first-order variable $\mathbf{q}_1$ is the vector with components correspond-

ing to the elastic vibration and the perturbations from the rigid-body maneuver. The first-order generalized force $\mathbf{Q}_1$ is the force responsible for the suppression of the elastic vibration and the perturbations.

At this point, we introduce the state vector $\mathbf{x} = [\,\mathbf{q}_1^T \quad \dot{\mathbf{q}}_1^T\,]^T$ and the control vector $\mathbf{u} = \mathbf{Q}_1$ and rewrite Eq. (2.23) in the state space form

$$\dot{\mathbf{x}}(t) = A(t)\mathbf{x}(t) + B(t)\mathbf{u}(t) + B(t)\mathbf{d}(t) \tag{3.32}$$

where

$$A = \begin{bmatrix} 0 & I \\ -M_1^{-1}K_1 & -M_1^{-1}C_1 \end{bmatrix} \tag{3.33a}$$

$$B = \begin{bmatrix} 0 \\ M_1^{-1} \end{bmatrix} \tag{3.33b}$$

The matrices M_1, C_1 and K_1 and the vector $\mathbf{d}$ appearing in Eq. (2.23) depend on the zero-order vectors $\mathbf{q}_0$, $\dot{\mathbf{q}}_0$ and $\ddot{\mathbf{q}}_0$, which are the known functions of time obtained from inverse kinematics. Therefore, the matrices A and B and the vector $\mathbf{d}$ are all implicit functions of time. The state equation (3.32) represents a linear, time-varying system with persistent disturbances.

We propose to first compensate for the persistent disturbances open loop and then control the elastic vibrations and rigid-body perturbations in the absence of persistent disturbances closed loop. To this end, we divide the control vector into

$$\mathbf{u} = \mathbf{u}_o + \mathbf{u}_c \tag{3.34}$$

where the open-loop control has the form

$$\mathbf{u}_o(t) = -\mathbf{d}(t) \tag{3.35}$$

so that Eq. (3.32) reduces to

$$\dot{\mathbf{x}}(t) = A(t)\mathbf{x}(t) + B(t)\mathbf{u}_c(t) \tag{3.36}$$

Here the dimension of control vector $\mathbf{u}$ is the same as the dimension of vector $\mathbf{d}$, i. e., the number of control inputs is equal to the number of generalized coordinates.

Finally, we wish to determine the feedback control in an optimal fasion [46]. To this end, we use the LQR theory for which the performance measure has the form

$$L = \mathbf{x}^T(t_f)H_f\mathbf{x}(t_f) + \int_{t_0}^{t_f} [\mathbf{x}^T(t)Q(t)\mathbf{x}(t) + \mathbf{u}_c^T(t)R(t)\mathbf{u}_c(t)]dt \tag{3.37}$$

It is well known that the optimal control law is given by

$$\mathbf{u}_c(t) = -R^{-1}(t)B^T(t)K(t)\mathbf{x}(t) \tag{3.38}$$

where $K(t)$ satisfies the matrix differential Riccati equation

$$\begin{aligned} \dot{K}(t) &= -K(t)A(t) - A^T(t)K(t) - Q(t) + K(t)B(t)R^{-1}(t)B^T(t)K(t) \\ K(t_f) &= H_f \end{aligned} \tag{3.39}$$

3.4 Numerical Example

i) "Rigid-Body" Maneuver

The numerical example is concerned with the robot shown in Fig. 1. As the end-effector output vector, we use $\mathbf{y}_e = [x \;\; y \;\; \varphi]^T$ where x and y are the cartesian components of the end-effector tip and φ is a measure of the orientation of the end-effector. For the sake of this example, we assume that the platform undergoes translation only, $\theta_0 = 0$, so that the configuration vector is $\mathbf{q} = [x_0 \;\; y_0 \;\; \theta_1 \;\; \theta_2 \;\; \theta_3]^T$. At this stage of trajectory planning, we assume that the robot is composed of rigid members. However, for simplicity we omitted the subscript 0 identifying the zero-order quantities in the definition of $\mathbf{q}$. The relation between $\mathbf{y}_e$ and $\mathbf{q}$ is by

components

$$x = x_0 + L_1 \cos\theta_1 + L_2 \cos\theta_2 + L_3 \cos\theta_3$$

$$y = y_0 + L_1 \sin\theta_1 + L_2 \sin\theta_2 + L_3 \sin\theta_3 \tag{3.40}$$

$$\varphi = \cos\theta_3$$

For the purpose of this example, we choose the desired trajectory of $\mathbf{y}_e$ as

$$x = 7.5 \cos 0.2\pi t + 7.5$$

$$y = -7.5 \cos 0.2\pi t + 7.5, \qquad t \in [0, 5.0] \tag{3.41}$$

$$\varphi = \frac{\sqrt{2}}{2} - 0.2\sqrt{2}t$$

so that at $t = 0$ the tip of end-effector starts from the position [15 m 0] and orientation of 45° and at $t = 5.0$ s it ends in the position [0 15 m] and orientation of 135°. The tip velocity is zero at $t = 0$ and $t = 5.0$ s.

The Jacobian matrix is

$$J = \begin{bmatrix} 1 & 0 & -L_1 \sin\theta_1 & -L_2 \sin\theta_2 & -L_3 \sin\theta_3 \\ 0 & 1 & L_1 \cos\theta_1 & L_2 \cos\theta_2 & L_3 \cos\theta_3 \\ 0 & 0 & 0 & 0 & -\sin\theta_3 \end{bmatrix} \tag{3.42}$$

and the performance measure for the optimal trajectory is as given by the Eqs. (3.7) and (3.11). Equation (3.29) is used as the nonlinear two-point boundary value problem.

Letting $L_0 = 2.5$ m, $L_1 = L_2 = 10.0$ m and $L_3 = 2.0$ m, the trajectory is computed for the two cases of different initial configurations:

Case 1: $x_0 = -6.4142$ m $\quad y_0 = -3.9142$ m $\quad \theta_1 = \theta_2 = 0 \quad \theta_3 = \frac{\pi}{4}$

Case 2: $x_0 = -3.4853$ m $\quad y_0 = -10.9853$ m $\quad \theta_1 = 0 \quad \theta_2 = \theta_3 = \frac{\pi}{4}$

Figure 3.1 shows time-lapse pictures of the robot configurations for case 1 and case 2. The results were obtained by the homotopy method. Note that, although the initial configuration is different, in both cases the initial tip position is [15 m 0] and the initial end-effector orientation is 45°, as can be seen from Fig. 3.1.

Using inverse dynamics, the zero-order generalized forces and torques required for rigid-body maneuvering were computed by means of Eq. (2.22). The zero-order real control forces and torques acting on the system were then computed by Eq. (2.17). Their time histories associated with case 2 are displayed in Fig. 3.2.

ii) Vibration and Perturbation Control

Here the results of case 2 are used for simulating the first-order system.

The values of the system parameters are as follows:

$$m_0 = 40.0\,\mathrm{kg} \quad m_1 = m_2 = 10.0\,\mathrm{kg} \quad m_3 = 2.0\,\mathrm{kg}$$

$$L_0 = 2.5\,\mathrm{m} \quad L_1 = L_2 = 10.0\,\mathrm{m} \quad L_3 = 2.0\,\mathrm{m}$$

$$S_x = S_y = 0.0\,\mathrm{kg\,m} \quad I_x = 83.333\,\mathrm{kg\,m^2} \quad I_y = 333.333\,\mathrm{kg\,m^2}$$

$$EI_1 = EI_2 = 10^4\,\mathrm{kg\,m^2}$$

The elastic displacement for the two arms was modeled by means of five quasi-comparison functions [41]. The coefficient matrices for the performance measure in Eq. (3.37), were chosen as

$$Q = diag(\,10^4 \quad \cdots \quad 10^4 \quad 0 \quad \cdots \quad 0\,)$$

$$R = diag(\,1.0 \quad \cdots \quad 1.0\,), \qquad H_f = 0$$

Numerical solutions of the Riccati equation were obtained by an algorithm described in [47]. Time histories of the uncontrolled (dashed lines) and controlled (solid lines) responses are shown in Figs. 3.3a-3.3d. Time histories of the first-order real control forces and torques from the open-loop disturbance rejection control and the closed-loop LQR control are shown in Fig. 3.4 and Figs. 3.5a-3.5d, respectively.

Chapter 4 Control Scheme for Tracking a Target Whose Motion is Not Known A Priori

When the target motion is not known a prior, the tracking and docking operation must be performed in a way that the control decision is based on on-line measurements. Such a control scheme is developed in this chapter. Following a similar pattern to that in chapter 3, we first discuss the tracking control algorithm for the rigid-body maneuver of the space robot and then consider the vibration suppression. Furthermore, the discrete-time version of the control scheme is presented and the problems associated with discretization error are also discussed. Finally a numerical example is used to demonstrate the results of the control scheme.

4.1 Liapunov-Like Methodology for Tracking Control Algorithm

In this section, the general idea of Liapunov-like methodology for tracking control for rigid robots [20] is introduced first. A modified version of the control algorithm is then applied to the flexible space robot for the purpose of discrete-time implementation.

4.1.1 General Idea of Liapunov-Like Methodology for Tracking Control

We introduce the general idea of Liapunov-like methodology by first considering a robot composed of *rigid* members whose dynamical equation is given by

$$M(\mathbf{q})\ddot{\mathbf{q}} + C(\mathbf{q}, \dot{\mathbf{q}})\dot{\mathbf{q}} = \mathbf{Q} \tag{4.1}$$

The kinematic relations are the same as those given by Eqs. (3.1), (3.2) and (3.3).

As mentioned earlier, the tracking is carried out by the end-effector. Thus, the tracking problem is that of driving the error $\mathbf{e} = \mathbf{y}_t - \mathbf{y}_e$ and its time derivative $\dot{\mathbf{e}}$

to zero. To this end, we define a Liapunov function [20]

$$V = \frac{1}{2}\mathbf{z}^T\mathbf{z} \tag{4.2a}$$

$$\mathbf{z} = (\dot{\mathbf{e}} + \beta\mathbf{e}) \tag{4.2b}$$

where β is a positive scalar. If the control is designed in such a way that

$$\dot{V} = -\alpha V, \qquad \alpha = \ln(\frac{V_0}{\epsilon})/t_s \tag{4.3}$$

where ϵ is an arbitrarily small positive scalar and V_0 is the initial value of V, it is guaranteed that for $t > t_s$, the function V remains in the ϵ-neighborhood of zero no matter how the target motion changes. This ensures that the error $\mathbf{e}$ and its derivative $\dot{\mathbf{e}}$ are also very close to zero.

We first define a nonlinear control law $\mathbf{Q}$ as follows:

$$\mathbf{Q} = M(\mathbf{q})\mathbf{u}_r + C(\mathbf{q}, \dot{\mathbf{q}})\dot{\mathbf{q}} \tag{4.4}$$

where $\mathbf{u}_r$ is determined so as to obtain $\dot{V} = -\alpha V$.

From Eq. (4.2), we have

$$\begin{aligned} \dot{V} =& \mathbf{z}^T\dot{\mathbf{z}} = \mathbf{z}^T(\ddot{\mathbf{e}} + \beta\dot{\mathbf{e}}) \\ =& \mathbf{z}^T(\ddot{\mathbf{y}}_t - \ddot{\mathbf{y}}_e + \beta\dot{\mathbf{e}}) \end{aligned} \tag{4.5}$$

Inserting Eq. (3.3) into Eq. (4.5), we can write

$$\dot{V} = \mathbf{z}^T(\ddot{\mathbf{y}}_t - J\ddot{\mathbf{q}} - \dot{J}\dot{\mathbf{q}} + \beta\dot{\mathbf{e}}) \tag{4.6}$$

From Eqs. (4.1) and (4.4), we have

$$\ddot{\mathbf{q}} = \mathbf{u}_r \tag{4.7}$$

Then substituting Eq. (4.7) into Eq. (4.6), we obtain

$$\dot{V} = \mathbf{z}^T(\ddot{\mathbf{y}}_t - \dot{J}\dot{\mathbf{q}} + \beta\dot{\mathbf{e}}) - \mathbf{z}^T J\mathbf{u}_r \tag{4.8}$$

In [20], $\mathbf{u}_r$ is chosen in the form

$$\mathbf{u}_r = \mathbf{w}\frac{h_1 + h_2}{\mathbf{z}^T J\mathbf{w}} \tag{4.9}$$

where

$$h_1 = \mathbf{z}^T(\ddot{\mathbf{y}}_t - \dot{J}\dot{\mathbf{q}} + \beta\dot{\mathbf{e}}) \tag{4.10a}$$

$$h_2 = 0.5\alpha\mathbf{z}^T\mathbf{z} \equiv \alpha V \tag{4.10b}$$

and $\mathbf{w}$ is an arbitrarily chosen vector. Substituting Eqs. (4.9) and (4.10) into Eq. (4.8), we obtain the desired result

$$\dot{V} = -\alpha V \tag{4.11}$$

The control algorithm described above, which consists of Eqs. (4.4), (4.9) and (4.10), possesses the following advantages:

1) The control decision is made using on-line information of the current robot state ($\mathbf{q}$, $\dot{\mathbf{q}}$) and target state ($\mathbf{e}$, $\dot{\mathbf{e}}$ and $\ddot{\mathbf{y}}_t$). The feedback control can automatically counteract the adverse disturbance in space and achieve the final docking in an accurate and smooth way.
2) The on-line calculation is relatively simple, as it involves neither inverse kinematics nor matrix inversions.
3) As can be seen from Eq. (4.11), stability is always guaranteed by Liapunov stability theorem, no matter how the target motion changes.

Applying the above control algorithm directly to our space robot system, the system response was simulated in both continuous and discrete time. Although the performance of the continuous system was as good as that in [20], the results from discrete-time system exhibited some undesirable phenomenon.

As shown in Figure 4.1, in which solid line denotes continuous-time results and dashed line denotes discrete-time results, the control force in discrete time exhibits periods of oscillatory behavior. Further numerical simulation shows that the magnitude of the control force during chattering is bounded, although very large, and its mean value is close to the results of the corresponding continuous time system. Moreover, the occurence of the oscillating period is random, and the length of oscillating periods and the length of the "good performance" periods are both unpredictable. This phenomenon is similar to the so-called "bursting", which appears frequently in discrete-time adaptive system [48] and has been reported for almost a decade.

For our problem, it is important to keep the control force from bursting, otherwise the control can not be realized. Due to the complexity of our space robot system, it is difficult to determine which part of the control algorithm is responsible for the phenomenon. However, because this phenomenon is not reported in [20], where a nonredundant robot system is simulated in discrete time, we can assume that in the case at hand the phenomenon is related to the robot redundancy. In view of this, a modified control algorithm is proposed. In the modified control algorithm, the flexibility of the space robot is also considered.

4.1.2 Modified Tracking Control Algorithm for Flexible Space Robots

To apply Liapunov-like methodology in flexible space robot system, we first derive the kinematical relation given by Eq. (3.1) for the flexible space robot as follows:

$$\begin{aligned} x_e &= x_0 - L_0 \sin\theta_0 + L_1 \cos\theta_1 + L_2 \cos\theta_2 + L_3 \cos\theta_3 - u_{12} \sin\theta_1 - u_{23} \sin\theta_2 \\ y_e &= y_0 + L_0 \cos\theta_0 + L_1 \sin\theta_1 + L_2 \sin\theta_2 + L_3 \sin\theta_3 + u_{12} \cos\theta_1 + u_{23} \cos\theta_2 \\ \theta_e &= \theta_3 \end{aligned} \tag{4.12}$$

For the purpose of kinematical analysis, we define $\bar{\mathbf{q}} = [\,\mathbf{q}_r^T \quad \mathbf{q}_u^T\,]^T$ with $\mathbf{q}_u = [\,u_{12} \quad u_{23}\,]^T$. The Jacobian matrix $\bar{J}$, obtained by differentiating Eq. (4.12) with respect to $\bar{\mathbf{q}}$, has the form

$$\bar{J} = [\,J_r \quad J_u\,] \tag{4.13}$$

where

$$J_r = \begin{bmatrix} 1 & 0 & -L_0\cos\theta_0 & -L_1\sin\theta_1 - u_{12}\cos\theta_1 & -L_2\sin\theta_2 - u_{23}\cos\theta_2 & -L_3\sin\theta_3 \\ 0 & 1 & -L_0\sin\theta_0 & L_1\cos\theta_1 - u_{12}\sin\theta_1 & L_2\cos\theta_2 - u_{23}\sin\theta_2 & L_3\cos\theta_3 \\ 0 & 0 & 0 & 0 & 0 & 1 \end{bmatrix} \tag{4.14a}$$

$$J_u = \begin{bmatrix} -\sin\theta_1 & -\sin\theta_2 \\ \cos\theta_1 & \cos\theta_2 \\ 0 & 0 \end{bmatrix} \tag{4.14b}$$

Therefore, we can write the relations

$$\dot{\mathbf{y}}_e = \bar{J}\dot{\bar{\mathbf{q}}} \tag{4.15}$$

$$\ddot{\mathbf{y}}_e = \bar{J}\ddot{\bar{\mathbf{q}}} + \dot{\bar{J}}\dot{\bar{\mathbf{q}}} \tag{4.16}$$

The dynamical equation for the rigid-body motion of the flexible space robot is given by Eq. (2.26). We can first define a nonlinear control law for $\mathbf{Q}_r$ as follows:

$$\mathbf{Q}_r = M_r(\mathbf{q}_r)\mathbf{u}_r + C_r(\mathbf{q}_r, \dot{\mathbf{q}}_r)\dot{\mathbf{q}}_r \tag{4.17}$$

Using the Liapunov function as in Eqs. (4.2) and following the same procedure as in section 4.1.1, we have

$$\begin{aligned} \dot{V} =& \mathbf{z}^T\dot{\mathbf{z}} = \mathbf{z}^T(\ddot{\mathbf{e}} + \beta\dot{\mathbf{e}}) \\ =& \mathbf{z}^T(\ddot{\mathbf{y}}_t - \bar{J}\ddot{\bar{\mathbf{q}}} - \dot{\bar{J}}\dot{\bar{\mathbf{q}}} + \beta\dot{\mathbf{e}}) \\ =& \mathbf{z}^T(\ddot{\mathbf{y}}_t - \dot{\bar{J}}\dot{\bar{\mathbf{q}}} + \beta\dot{\mathbf{e}}) - \mathbf{z}^T J_r\ddot{\mathbf{q}}_r - \mathbf{z}^T J_u\ddot{\mathbf{q}}_u \end{aligned} \tag{4.18}$$

Substituting Eq. (4.17) into Eq. (2.26), we can write

$$\ddot{\mathbf{q}}_r = \mathbf{u}_r - M_r^{-1}\mathbf{d}_e \tag{4.19}$$

Then substituting Eq. (4.19) into Eq. (4.18), we obtain

$$\dot{V} = \mathbf{z}^T \mathbf{h} - \mathbf{z}^T J_r (\mathbf{u}_r - M_r^{-1} \mathbf{d}_e) \tag{4.20}$$

where

$$\mathbf{h} = \ddot{\mathbf{y}}_t - \dot{\bar{J}} \dot{\bar{\mathbf{q}}} + \beta \dot{\mathbf{e}} - J_u \ddot{\mathbf{q}}_u \tag{4.21}$$

In the following, when implementing the algorithm in discrete-time, we use a decoupled Liapunov function to prevent the bursting phenomenon caused by robot redundancy. Hence, we write

$$V_i = \frac{1}{2} z_i^2, \qquad z_i = \dot{e}_i + \beta e_i, \qquad i = 1, 2, 3 \tag{4.22}$$

so that, using Eqs. (4.20) and (4.21)

$$\dot{V}_i = z_i h_i - z_i ([J_r \mathbf{u}_r]_i - [J_r M_r^{-1} \mathbf{d}_e]_i), \qquad i = 1, 2, 3 \tag{4.23}$$

where $[\ ]_i$ denotes the $i-th$ element of a vector. In Eq. (4.23), because M_r is a positive definite matrix, M_r^{-1} is bounded. Also J_r is bounded. Moreover, from Eq. (C.3) in Appendix C, we can see that $\mathbf{d}_e$ is a linear combination of $\mathbf{q}_e$, $\dot{\mathbf{q}}_e$ and $\ddot{\mathbf{q}}_e$. We then assume that $\mathbf{d}_e$ is bounded according to our ultimate goal of vibration suppression. Hence we can assume that the term $[J_r M_r^{-1} \mathbf{d}_e]_i$ is bounded and satisfies the relation

$$[J_r M_r^{-1} \mathbf{d}_e]_i < \delta_i, \qquad i = 1, 2, 3 \tag{4.24}$$

From (4.24), we have

$$z_i [J_r M_r^{-1} \mathbf{d}_e]_i < |z_i| \delta_i, \qquad i = 1, 2, 3 \tag{4.25}$$

If we can determine a $\mathbf{u}_r$ that satisfies the following conditions:

$$z_i [J_r \mathbf{u}_r]_i = z_i h_i + \frac{1}{2} \alpha_i z_i^2 + |z_i| \delta_i, \qquad i = 1, 2, 3 \tag{4.26}$$

then

$$\dot{V}_i = -\frac{1}{2}\alpha_i z_i^2 + [J_r M_r^{-1}\mathbf{d}_e]_i - |z_i|\delta_i < -\frac{1}{2}\alpha_i z_i^2 = -\alpha_i V_i, \qquad i = 1,2,3 \tag{4.27}$$

According to Liapunov stability theorem, Eq. (4.26) is the sufficient condition for our tracking problem. We further simplify Eq. (4.26) by assuming $z_i \neq 0$, so that

$$[J_r \mathbf{u}_r]_i = h_i + \frac{1}{2}\alpha_i z_i + sgn(z_i)\delta_i, \qquad i = 1,2,3 \tag{4.28}$$

or

$$[J_r \mathbf{u}_r]_i = s_i, \qquad i = 1,2,3 \tag{4.29}$$

with

$$s_i = \ddot{y}_{ti} - [\dot{\bar{J}}\dot{\mathbf{q}}]_i + \beta\dot{e}_i - [J_u\ddot{\mathbf{q}}_u]_i + \frac{1}{2}\alpha_i z_i + sgn(z_i)\delta_i \tag{4.30}$$

Equation (4.29) can be expressed in the matrix form

$$J_r \mathbf{u}_r = \mathbf{s} \tag{4.31}$$

where $\mathbf{s} = [\, s_1 \quad s_2 \quad s_3 \,]^T$ and J_r is a 3×6 matrix. The solution of Eq. (4.31) does not yield a unique $\mathbf{u}_r$. This agrees with Eq. (4.9) in the original control scheme in which $\mathbf{w}$ is an arbitrarily chosen vector. Here we can simply prescribe the redundant degrees of freedom and then solve Eq. (4.31) accordingly.

Using Eq.(4.14a), we expand Eq. (4.31) as follows:

$$\begin{aligned}
&u_{r1} - L_0\cos\theta_0 u_{r3} - (L_1\sin\theta_1 + u_{12}\cos\theta_1)u_{r4} \\
&\quad -(L_2\sin\theta_2 + u_{23}\cos\theta_2)u_{r5} - L_3\sin\theta_3 u_{r6} = s_1 \\
&u_{r2} - L_0\sin\theta_0 u_{r3} + (L_1\cos\theta_1 - u_{12}\sin\theta_1)u_{r4} \\
&\quad +(L_2\cos\theta_2 - u_{23}\sin\theta_2)u_{r5} + L_3\cos\theta_3 u_{r6} = s_2 \\
&\qquad\qquad\qquad\qquad\qquad\qquad\qquad\qquad u_{r6} = s_3
\end{aligned} \tag{4.32}$$

As a simple example, we can constraint three elements of $\mathbf{u}_r$ by taking

$$u_{r3} = u_{r4} = u_{r5} = 0 \tag{4.33}$$

for the entire tracking period and use Eqs. (4.32) to solve for the other three elements of $\mathbf{u}_r$ on-line, with the result

$$\begin{aligned} u_{r1} &= s_1 + L_3 \sin\theta_3 u_{r6} \\ u_{r2} &= s_2 - L_3 \cos\theta_3 u_{r6} \\ u_{r6} &= s_3 \end{aligned} \tag{4.34}$$

The above algorithm for $\mathbf{u}_r$ together with Eq. (4.17) represents the maneuver control for a flexible space robot tracking a moving target whose motion is not known a priori. The control algorithm requires that the following conditions be satisfied:

1) The output error vector $\mathbf{e}$ and its time derivative $\dot{\mathbf{e}}$ can be measured on-line.
2) The target output acceleration $\ddot{\mathbf{y}}_t$ can be measured or estimated on-line.
3) The robot rigid-body displacement vector $\mathbf{q}_r$ and its time derivative $\dot{\mathbf{q}}_r$ can be measured on-line.
4) The elastic tip displacement vector $\mathbf{q}_u$ and its time derivatives $\dot{\mathbf{q}}_u$ and $\ddot{\mathbf{q}}_u$ can be measured on-line.
5) The elastic vibration of the robot arms should be controlled so that a reasonable value for the upper bound δ_i can be set.

In addition to the advantages of the original algorithm mentioned in section 4.1.1, the modified control algorithm presented here provides two extensions from the original one. The first extension is that the flexible effect of the robot arms is incorporated into the control algorithm. It is reflected in the kinematic relations expressed by Eqs. (4.12) and in the term $sgn(z_i)\delta_i$ in Eq. (4.30), which is associated

with the vibration disturbance vector $\mathbf{d}_e$ in Eq. (2.26). The second extension consists of the use of the decoupled Liapunov function, Eq. (4.22), to eliminate the bursting phenomenon (section 4.1.1) when the control algorithm is implemented in discrete-time.

4.2 Vibration Control Algorithm

Because of the coupling of the rigid-body motions and the elastic vibration, the performance of tracking control is closely related to how well the vibration suppression is done. Without vibration control, the tracking cannot be realized for a flexible space robot.

4.2.1 General Control Scheme

Our objective is to drive the elastic motion state $\mathbf{q}_e$, $\dot{\mathbf{q}}_e$ close to zero during the tracking and docking operation. Recall that Eq. (2.27) represents the motion of the elastic vibration of the space robot and it describes a linear time-varying system with a persistent disturbance term $\mathbf{d}_r$ due to the rigid-body motions. Using the same idea as in the vibration control scheme presented in section 3.3, we separate the generalized control force $\mathbf{Q}_e$ into:

$$\mathbf{Q}_e = \mathbf{Q}_{er} + \mathbf{Q}_{ee} \tag{4.35}$$

where $\mathbf{Q}_{er}$ is used to compensate the disturbance term $\mathbf{d}_r$, i. e.,

$$\mathbf{Q}_{er} = \mathbf{d}_r(\mathbf{q}_r, \dot{\mathbf{q}}_r, \ddot{\mathbf{q}}_r) \tag{4.36}$$

Then Eq. (2.27) becomes

$$M_e(\mathbf{q}_r)\ddot{\mathbf{q}}_e + C_e(\mathbf{q}_r, \dot{\mathbf{q}}_r)\dot{\mathbf{q}}_e + K_e(\mathbf{q}_r, \dot{\mathbf{q}}_r, \ddot{\mathbf{q}}_r)\mathbf{q}_e = \mathbf{Q}_{ee} \tag{4.37}$$

Letting $\mathbf{x} = [\,\mathbf{q}_e^T \quad \dot{\mathbf{q}}_e^T\,]^T$ be the state vector and $\mathbf{u} = \mathbf{Q}_{ee}$ the control vector, we can rewrite Eq. (4.37) in the state space form

$$\dot{\mathbf{x}} = A(t)\mathbf{x} + B(t)\mathbf{u} \tag{4.38}$$

where

$$A(t) = \begin{bmatrix} 0 & I \\ -M_e^{-1}K_e & -M_e^{-1}C_e \end{bmatrix} \qquad B = \begin{bmatrix} 0 \\ M_e^{-1} \end{bmatrix} \tag{4.39}$$

Introducing the quadratic performance measure

$$J = \frac{1}{2}\mathbf{x}^T(t_f)H_f\mathbf{x}(t_f) + \frac{1}{2}\int_{t_0}^{t_f}[\mathbf{x}^T(t)Q\mathbf{x}(t) + \mathbf{u}^T(t)R\mathbf{u}(t)]dt \tag{4.40}$$

the control vector minimizing J can be obtained by LQR theory as

$$\mathbf{u} = -R^{-1}B^T(t)K(t)\mathbf{x} \tag{4.41}$$

where $K(t)$ satisfies the differential Riccati equation

$$\dot{K}(t) = -Q - K(t)A(t) - A^T(t)K(t) + K(t)B(t)R^{-1}B^T(t)K(t), \qquad K(t_f) = H_f \tag{4.42}$$

However, the above LQR control scheme does not work in the case in which the target motion is not known a priori. In Eq. (4.38), $A(t)$ and $B(t)$ depend on time through rigid-body motion variables $\mathbf{q}_r$, $\dot{\mathbf{q}}_r$ and $\ddot{\mathbf{q}}_r$ which can only be obtained through on-line measurement. But the solution for $K(t)$ requires that $K(t_f)$, as well as both $A(t)$ and $B(t)$ over the time interval $t \in [0, t_f]$, be known a priori, because the integration of Eq. (4.42) is performed backward in time. To resolve the problem, a discrete-time version of the vibration control algorithm is proposed whereby $K(t)$ is assumed to be constant over small time intervals $t \in [kT, (k+1)T]$ over which only an algebraic Riccati equation need be solved. Indeed, for practical reasons, the control algorithm is usually implemented digitally.

4.2.2 The Discrete-Time Control Algorithm

The discrete-time control algorithm for disturbance rejection is expressed as

$$\mathbf{Q}_{er}(k) = \mathbf{d}_r(\mathbf{q}_r(k), \dot{\mathbf{q}}_r(k), \ddot{\mathbf{q}}_r(k)) \tag{4.43}$$

The discretized form of Eq. (4.38) is given by

$$\mathbf{x}(k+1) = \hat{A}(k)\mathbf{x}(k) + \hat{B}(k)\mathbf{u}(k) \tag{4.44}$$

where

$$\hat{A}(k) = e^{A(kT)} \tag{4.45a}$$

$$\hat{B}(k) = (e^{A(kT)} - I)A^T(kT)B(kT) \tag{4.45b}$$

Based on the discrete-time form of the LQR theory [49], the performance index of Eq. (4.40) becomes

$$\hat{J} = \frac{1}{2}\sum_{k=0}^{N}[\mathbf{x}^T(k)Q\mathbf{x}(k) + \mathbf{u}^T(k)R\mathbf{u}(k)] \tag{4.46}$$

The discrete-time algebraic Riccati equation is

$$\hat{K}(k) = \hat{A}^T(k)[\hat{K}(k) - \hat{K}(k)\hat{B}(k)(R + \hat{B}^T(k)\hat{K}(k)\hat{B}(k))^{-1}\hat{B}^T(k)\hat{K}(k)]\hat{A}(k) + Q \tag{4.47}$$

and the control law is

$$\mathbf{u}(k) = -(R + \hat{B}(k)\hat{K}(k)\hat{B}(k))^{-1}\hat{B}^T(k)\hat{K}(k)\hat{A}(k)\mathbf{x}(k) \tag{4.48}$$

Note that the state vector $\mathbf{x}(k) = [\,\mathbf{q}_e^T(k) \quad \dot{\mathbf{q}}_e^T(k)\,]^T$ can be estimated or calculated directly from the measured elastic displacements (velocities) along the flexible arms at every sampling period T and the control vector $\mathbf{u}(k) = \mathbf{Q}_{ee}(k)$, as well as $\mathbf{Q}_{er}(k)$ in Eq. (4.43), is held constant during every sampling period.

However, direct application of the discrete-time control algorithm described by Eqs. (4.43) and (4.48) to our problem causes a severe instability problem. The reason is that the discrete-time control force $\mathbf{Q}_{er}$ in Eq. (4.43) is not able to cancel the continuous disturbance term $\mathbf{d}_r$ in Eq. (2.27) perfectly. Thus, the LQR control design based on Eq. (4.37), in which the disturbance is absent, is no longer appropriate. The error accumulates with time and finally results in instability. To resolve this problem, a modified vibration control algorithm is proposed in the next section.

4.2.3 Modified Discrete-Time Control Algorithm

An examination of the disturbance term $\mathbf{d}_r$ in Eq. (C.14) in Appendix C, i.e., an examination of

$$\mathbf{d}_r = M_{re}^T \ddot{\mathbf{q}}_r + C_{er} \dot{\mathbf{q}}_r \tag{4.49}$$

reveals that $\ddot{\mathbf{q}}_r$ in the first term is the major cause of the system instability. Usually $\ddot{\mathbf{q}}_r(k)$ is not available and $\ddot{\mathbf{q}}_r(k-1)$ is used as the estimation of $\ddot{\mathbf{q}}_r(k)$. Stable performance of the system can be achieved only if $\ddot{\mathbf{q}}_r(k)$ can be measured or estimated perfectly. Even a very small error in $\ddot{\mathbf{q}}_r$ appearing in Eq. (4.43) can result in failure of the LQR design. To avoid use of $\ddot{\mathbf{q}}_r$ in Eq. (4.43), we replace $\ddot{\mathbf{q}}_r$ by $\mathbf{u}_r$, so that the disturbance rejection control scheme becomes

$$\begin{aligned} \mathbf{Q}_{er}(k) &= \mathbf{d}_r(\mathbf{q}_r(k), \dot{\mathbf{q}}_r(k), \mathbf{u}_r(k)) \\ &= M_{re}^T(\mathbf{q}_r(k))\mathbf{u}_r(k) + C_{er}(\mathbf{q}_r(k), \dot{\mathbf{q}}_r(k))\dot{\mathbf{q}}_r(k) \end{aligned} \tag{4.50}$$

where $\mathbf{u}_r(k)$ is calculated by the tracking control algorithm of Eq. (4.31). We then substitute Eqs. (4.49), (4.50) and (4.19) into Eq. (2.27) and obtain the system equation as follows:

$$M_e(\mathbf{q}_r)\ddot{\mathbf{q}}_e + C_e(\mathbf{q}_r, \dot{\mathbf{q}}_r)\dot{\mathbf{q}}_e + K_e(\mathbf{q}_r, \dot{\mathbf{q}}_r, \ddot{\mathbf{q}}_r)\mathbf{q}_e - M_{re}^T M_r^{-1}\mathbf{d}_e = \mathbf{Q}_{ee} \tag{4.51}$$

As shown in Appendix C, $\mathbf{d}_e$ can be expressed as

$$\mathbf{d}_e = M_{re}\ddot{\mathbf{q}}_e + C_{re}\dot{\mathbf{q}}_e + (K_M^e + K_C^e)\mathbf{q}_e \tag{4.52}$$

Substituting Eq. (4.52) into Eq. (4.51), we obtain the modified linear time-varying system

$$M_e^*(\mathbf{q}_r)\ddot{\mathbf{q}}_e + C_e^*(\mathbf{q}_r, \dot{\mathbf{q}}_r)\dot{\mathbf{q}}_e + K_e^*(\mathbf{q}_r, \dot{\mathbf{q}}_r, \ddot{\mathbf{q}}_r)\mathbf{q}_e = \mathbf{Q}_{ee} \tag{4.53}$$

where, comparing Eqs. (4.37) and (4.53), we observe that matrices M_e^*, C_e^* and K_e^* represent modified coefficient matrices given by

$$M_e^* = M_e - M_{re}^T M_r^{-1} M_{re} \tag{4.54a}$$

$$C_e^* = C_e - M_{re}^T M_r^{-1} C_{re} \tag{4.54b}$$

$$K_e^* = K_e - M_{re}^T M_r^{-1} (K_M^e + K_C^e) \tag{4.54c}$$

Based on Eq. (4.53) together with Eqs. (4.54), we can follow the same procedure as for the LQR design in section 4.2.2 to obtain the control law for $\mathbf{Q}_{ee}$. The simulation results showed a stable performance of the system under the modified control scheme. Further numerical simulation showed that even in the case of a system with only the mass matrix M_e modified, i. e., a system described by

$$M_e^*(\mathbf{q}_r)\ddot{\mathbf{q}}_e + C_e(\mathbf{q}_r, \dot{\mathbf{q}}_r)\dot{\mathbf{q}}_e + K_e(\mathbf{q}_r, \dot{\mathbf{q}}_r, \ddot{\mathbf{q}}_r)\mathbf{q}_e = \mathbf{Q}_{ee} \tag{4.55}$$

the control law from LQR design still is able to produce good system performance. This is because the first term of the right side of Eq. (4.52) is dominant, and using the original C_e and K_e is equivalent to dropping the second and third terms in Eq. (4.52), which does not affect the system performance very much.

In view of the above, a new discrete-time vibration control $\mathbf{Q}_e$ can be expressed as

$$\mathbf{Q}_e(k) = \mathbf{Q}_{er}(k) + \mathbf{Q}_{ee}(k) \tag{4.56}$$

with $\mathbf{Q}_{er}(k)$ satisfying Eq. (4.50), in which $\mathbf{u}_r$ is determined in tracking control algorithm, and $\mathbf{Q}_{ee}(k)$ satisfying feedback control law given by Eq. (4.48), in which the gain matrix is obtained by means of the LQR optimal control algorithm based on the linear time-varying system described by Eq. (4.55).

4.3 Numerical Example

A numerical example involving the flexible space robot shown in Fig. 1 demonstrate the approach. The values of the system parameters are the same as in the example of section 3.4.

The target motion is not known a priori and must be measured on-line. However, for simulation purposes, we choose an example target trajectory as follows:

$$\begin{aligned} x_t(t) &= 10.0\sin(\frac{\pi}{10}t) \\ y_t(t) &= 10.0 + 10.0\sin(\frac{\pi}{10}t), \qquad t \in [0, 5.0\,\mathrm{s}] \\ \theta_t(t) &= \frac{3\pi}{20}t \end{aligned} \tag{4.57}$$

The initial conditions of the space robot are given by:

$$\begin{aligned} \mathbf{q}_r(0) &= [\,0.0 \quad -15.0 \quad 0.0 \quad 0.5\pi \quad 0.4775\pi \quad 0.25\pi\,]^T \\ \dot{\mathbf{q}}_r(0) &= \mathbf{0} \\ \mathbf{q}_e(0) &= [\,0.01 \quad \cdots \quad 0.01\,]^T \\ \dot{\mathbf{q}}_e(0) &= \mathbf{0} \end{aligned}$$

The parameters of the control synthesis design are

$$\beta = 20.0, \quad \epsilon = 10^{-3}, \quad t_s = 2.5\,\mathrm{s}, \quad \delta_i = 20, \ i = 1, 2, 3$$

We prescribe the three redundant degrees of freedom in $\mathbf{u}_r$ as u_{r3}, u_{r4} and u_{r5}. They are defined in two different cases as follows:

Case 1:

$$u_{r3} = u_{r4} = u_{r5} = 0 \qquad 0 \leq t \leq 5.0 \tag{4.58}$$

Case 2:

$$u_{r3} = \begin{cases} 0 & t \leq 0 \\ 4\Delta\theta_0/t_f^2 & 0 < t \leq t_f/2 \\ -4\Delta\theta_0/t_f^2 & t_f/2 < t \leq t_f \\ 0 & t > t_f \end{cases} \tag{4.59a}$$

$$u_{r4} = \begin{cases} 0 & t \leq 0 \\ 4\Delta\theta_1/t_f^2 & 0 < t \leq t_f/2 \\ -4\Delta\theta_1/t_f^2 & t_f/2 < t \leq t_f \\ 0 & t > t_f \end{cases} \tag{4.59b}$$

$$u_{r5} = \begin{cases} 0 & t \leq 0 \\ 4\Delta\theta_2/t_f^2 & 0 < t \leq t_f/2 \\ -4\Delta\theta_2/t_f^2 & t_f/2 < t \leq t_f \\ 0 & t > t_f \end{cases} \tag{4.59c}$$

where $t_f = 4.0$s, $\Delta\theta_0 = \frac{\pi}{6}$, $\Delta\theta_1 = \frac{\pi}{4}$, and $\Delta\theta_2 = -\frac{\pi}{6}$.

For a rigid space robot, Eqs. (4.58) and (4.59) represent constraints on the acceleration of the robot configuration. In case 1, the mission amounts to keeping the base attitude θ_0 and the two joint angles θ_1 and θ_2 constant while tracking a moving target. In case 2, the mission implies bang-bang maneuvers involving a base attitude change of $\Delta\theta_0$ and arms angle changes of $\Delta\theta_1$ and $\Delta\theta_2$ while tracking a moving target.

The constraints cannot be realized perfectly for a flexible space robot due to vibration disturbances. However, the performance can be improved by vibration suppression control. Because the major objective here is to track the moving target, we use the constraint equations, Eqs. (4.58) and (4.59), to eliminate the robot redundancy.

For vibration control, the LQR design parameters are chosen as

$$R = \begin{bmatrix} I_{n\times n} & 0 \\ 0 & I_{n\times n} \end{bmatrix}$$

$$Q = \begin{bmatrix} 2.0 \times 10^4 I_{n\times n} & & & \\ & 10^4 I_{n\times n} & & \\ & & 2.0 \times 10^4 I_{n\times n} & \\ & & & 10^4 I_{n\times n} \end{bmatrix}$$

The elastic displacement for each of the two arms was modeled by means of five quasi-comparison functions.

The system performance under the tracking and docking maneuver is simulated over 5.0 seconds. To this end, the tracking control algorithm presented in section 4.1.2 and the vibration control algorithm presented in section 4.2.3 are used. The simulation is performed in discrete-time with a sampling period $T = 0.001$ s.

Figures 4.2a and 4.2b show time-lapse pictures of the robot configurations for cases 1 and 2, respectively. For case 2, time histories of the tracking error $\mathbf{e}$ and its time derivative $\dot{\mathbf{e}}$ are shown in Figs. 4.3a-4.3c, time histories of the tip elastic displacements of the two flexible links are shown in Fig. 4.4, time histories of the control forces and torques for rigid-body maneuver are displayed in Figs. 4.5a-4.5c. Time histories of the control torques acting on the flexible arms for disturbance rejection and LQR control are shown in Fig. 4.6 and Fig. 4.7, respectively.

Chapter 5 Summary and Conclusions

This dissertation is concerned with a planar space robot consisting of a rigid platform, two articulated flexible arms and a rigid end-effector. The task is to ferry some payload and to dock smoothly with an orbiting target whose motion is either known or not known a priori.

The dynamical equations of motion for the space robot are derived by means of Lagrange's equations. They are then separated into two sets of equations permitting rigid-body maneuver control and vibration suppression control to be designed separately. When the target motion is known a priori, a perturbation method is used. When the target motion is not known a priori, direct partitioning is used. Both approaches are based on the assumption that maneuver motions are much larger than elastic motions.

As far as the rigid-body maneuver control is concerned, optimal trajectory planning is carried out off-line by means of the global optimization method under the assumption that the target motion is known. In contrast, on-line feedback tracking control is performed when the target motion is not known a priori.

The vibration suppression control is carried out by means of piezoelectric sensor/actuator pairs dispersed along the flexible arms. Collocated sensors/actuators for vibration control exhibit good performance. The actuators are designed to compensate for the disturbances caused by the rigid-body maneuver and to realize the LQR feedback control. Assuming that the number of actuators along each flexible arm is equal to the number of modes used to model the beam, the LQR control design is based on a linear time-varying system without persistent disturbances.

The control schemes for the rigid-body maneuver and vibration suppression are

combined in the block diagrams of Figs. 5.1 and 5.2 for two different problems, the first in which the target motion is known and the second in which it is not known.

The problem considered in this dissertation is unique in the sense that both kinematical redundancy and the effect of flexibility are included. The target motion can be either known or not known a priori. The latter case requires a control algorithm capable of using on-line measurements of the target motion, which has not been considered before. The major contributions of this dissertation are as follows:

1) The equations of motion are separated in various ways so as to fit different types of target motion.
2) Optimal trajectory planning is carried out by means of the global optimization method in the kinematically redundant space robot, and the algorithm is realized numerically by the homotopy method.
3) An on-line tracking control algorithm using Liapunov-like methodology in the flexible space robot is developed. The bursting phenomenon associated with the original algorithm in [20] when implemented discrete-time has been encountered here as well, and a modified version using decoupled Liapunov function was developed to totally eliminate the phenomenon.
4) A modified disturbance rejection control and a LQR control associated with the on-line tracking maneuver are developed in a way that the discrete-time version of the algorithm is free of system instability.

As shown in Fig. 5.1, the optimal trajectory control associated with the known motion of the target is an open-loop control, and so is the corresponding disturbance rejection control. The corresponding LQR vibration control is a closed-loop control, with the feedback gain depending on the target trajectory and calculated off-line. The problem of digital implementation of the algorithm and the construction of the

state observers have been studied by Lim in [50]. As shown in Fig. 5.2, the feedback tracking control associated with the unknown motion of the target is a closed-loop control, and so are the corresponding disturbance rejection and the LQR vibration control. For the LQR control in this case, the feedback gains are calculated on-line. It is reasonable to assume that, with the increased capability of future computers, such computation load will not cause much difficulty. However, it is advisable to explore some other control schemes in the future so as to fully utilize the properties of piezoelectric materials to further simplify the on-line process.

The control algorithms presented in this dissertation can be applied directly to three-dimensional problems. For optimal trajectory planning, when the target motion is known a priori, it turns out that the proposed algorithm is capable of solving a great variety of problems by defining appropriate performance indices to achieve certain goals, such as collision avoidance, minimum time or minimum energy. For feedback tracking algorithm, when the target motion is not known a priori, the proposed algorithm has the flexibility of solving different problems by defining appropriate output variables. For example, if the mission involves tracking and docking with an orbiting target while its base attitude is to be kept at constant, we can define the output vector as $\mathbf{y}_e = [\, x_e \quad y_e \quad \theta_e \quad \theta_0 \,]^T$ and the target output vector as $\mathbf{y}_t = [\, x_t \quad y_t \quad \theta_t \quad 0 \,]^T$, and then use the proposed control algorithm to drive the error vector $\mathbf{e} = \mathbf{y}_t - \mathbf{y}_e$ and its time derivative $\dot{\mathbf{e}}$ to zero.

The numerical examples presented in chapters 3 and 4 have shown the good system performance in both the rigid-body maneuver and the vibration suppression. Although planar problems with specific performance index or output variable definition were used in simulations, the control algorithm can be extended to more general cases involving three-dimensional motions.

References

1 Longman, R. W., "The Kinetics and Workspace of a Satellite-Mounted Robot," *Journal of the Astronautical Sciences*, Vol. 38, No. 4, 1990, pp. 423-439.

2 Lindberg, R. E., Longman, R. W., and Zedd, M. F., "Kinematic and Dynamic Properties of an Elbow Manipulator Mounted on a Satellite," *Journal of the Astronautical Sciences*, Vol. 38, No. 4, 1990, pp. 397-421.

3 Vafa, Z., and Dubowsky, S., "On the Dynamics of Space Manipulators Using the Virtual Manipulator, with Applications to Path Planning," *Journal of the Astronautical Sciences*, Vol. 38, No. 4, 1990, pp. 441-472.

4 Alexander, H. L., and Cannon, R. H., "An Extended Operational-Space Control Algorithm for Satellite Manipulators," *Journal of the Astronautical Sciences*, Vol. 38, No. 4, 1990, pp. 473-486.

5 Nenchev, D., Umetani, Y., and Yoshida, K., "Analysis of a Redundant Free-Flying Spacecraft/Manipulator System," *IEEE Transactions on Robotics and Automation*, Vol. 8, No. 1, 1992, pp. 1-6.

6 Nakamura, Y., and Mukherjee, R., "Nonholonomic Path Planning via a Bidirectional Approach," *IEEE Transactions on Robotics and Automation*, Vol. 7, No. 4, 1991, pp. 500-514.

7 Nakamura, Y., *Advanced Robotics: Redundancy and Optimization*, Addison-Wesley, Reading, Massachusetts, 1991.

8 de Silva, C. W., "Trajectory Design for Robotic Manipulators in Space Applications," *Journal of Guidance, Control, and Dynamics*, Vol. 14, No. 3, 1991, pp. 670-674.

9 Koivo, A. J., and Arnautovic, S. H., "Dynamic Optimum Control of Redundant Manipulators," *Proceedings of the 1991 IEEE International Conference*

on Robotics and Automation, Sacramento, CA, April 1991, pp. 466-471.

10 Lee, S., and Bejczy, A. K., "Redundant Arm Kinematic Control Based on Parameterization", *Proceedings of the 1991 IEEE International Conference on Robotics and Automation*, Sacramento, CA, April, 1991, pp. 458-465.

11 Cheng, H., and Gupta, K. C., "A Study of Robot Inverse Kinematics Based on the Solution of Differential Equation", *Journal of Robotics System*, Vol. 8, No. 2, 1991, pp. 159-175.

12 Dubey, R. V., Euler, J. A., and Babcock, S. M., "Real-Time Implementation of an Optimization Scheme for Seven-Degree-of-Freedom Redundant Manipulators", *IEEE Transactions on Robotics and Automation*, Vol. 7, No. 5, Oct. 1991, pp. 579-588.

13 Tarokh, M., and Seraji, H., "A Multivariable Control Scheme for Robot Manipulators", *Journal of Robotics System*, Vol. 8, No. 1, 1991, pp. 1-19.

14 Leung, T.-P., Zhou, Q.-J., and Su, C.-Y., "An Adaptive Variable Structure Model Following Control Design for Robot Manipulators", *IEEE TRansactions on Automatic Control*, Vol. 36, No. 3, March, 1991, pp. 347-352.

15 Umetani, Y., and Yoshida, K., "Theoretical and Experimental Study on In-Orbit Capture Operation with Satellite Mounted Manipulator", *IFAC Automatic Control in Aerospace*, Tsukuba, Japan, 1989, pp. 121-126.

16 Behtash, S., "Robust Output Tracking for Nonlinear Systems", *International Journal of Control*, Vol. 51, No. 6, 1990, pp. 1381-1407.

17 Liao, T., Fu, L., and Hsu, C., "Adaptive Robust Tracking of Nonlinear Systems and with an Application to a Robotic Manipulator," *System and Control Letter*, Vol. 15, 1990, pp. 339-348.

18 Tyler, J. S. Jr., "The Characteristics of Model-Following Systems as Synthesized by Optimal Control", *IEEE Transactions on Automatic Control*, Vol.

AC-9, Oct. 1964, pp. 485-498.

19 Erzberger, H., "Analysis and Design of Model Following Control System by State Space Techniques", *Proceedings of Joint Automatic Control Conference*, 1968, pp. 572-581.

20 Novakovic, Z. R., "Lyapunov-like Methodology for Robot Tracking Control Synthesis", *International Journal of Control*, Vol. 51, No. 3, 1990, pp. 567-583.

21 Long, T. W., and Carrington, C. K., "A New Nonlinear Optimal Control Method: the Tracking and Relative Direction Imbedded System," *International Journal of Control*, Vol. 54, No. 2, 1991, pp. 417-433.

22 Lee, S. M., Bien, Z., and Park, S. O., "On-line Optimal Terrain Tracking System," *Optimal Control Applications and Methods*, Vol. 11, 1990, pp. 289-306.

23 Wang, P. K. C., "Automatic Assembly of Space Station," *Proceedings of the Workshop on Identification and Control of Flexible Space Structures*, San Diego, CA, April, 1985, Vol. 1, pp 67-101.

24 Oh, H., Vadali, S. R., and Junkins, J. L., "Use of the Work-Energy Rate Principle for Designing Feedback Control Laws", *Journal of Guidance, Control, and Dynamics*, Vol. 15, No. 1, Jan-Feb. 1992, pp. 275-277.

25 Meirovitch, L., and Kwak, M. K., "Dynamics and Control of Spacecraft with Retargeting Flexible Antennas," *Journal of Guidance, Control, and Dynamics*, Vol. 13, No. 2, 1990, pp. 241-248.

26 Krishnamurthy, K., and Lu, M.-S., "Feedback control of a Flexible Cylindrical Manipulator", *Computers and Structures*, Vol. 36, No. 6, 1990, pp. 987-992

27 Modi, V. J., and Chan, J. K., "Performance of an Orbiting Flexible Mobile Manipulator", *Transactions of the ASME: Journal of Mechanical Design*, Vol.

113, Dec. 1991, pp. 516-524.

28 Qian, W. T., and Ma, C.C. H., "A New Controller Design for a Flexible One-Link Manipulator", *IEEE Transactions on Automatic Control*, Vol. 37, No. 1, Jan. 1992, pp. 132-137.

29 Yeung, K. S., and Chen, Y. P., "Sliding-Mode Controller Design of a Single-link Flexible Manipulator under Gravity", *International Journal of Control*, Vol. 52, No. 1, 1990, pp. 101-117.

30 Yurkovich, S., and Pacheco, F. E., "On Controller Tuning for a Flexible-Link Manipulator with Varying Payload", *Journal of Robotics Systems*, Vol. 6, No. 3, 1989, pp. 233-254.

31 Yang, Y.-P., and Huang, K.-M., "Adaptive Lattice Estimation and Control of a Manipulator with One Flexible Forearm", *IEE Proceedings-D: Control Theory and Applications*, Vol. 139, No. 3, May 1992, pp. 237-244.

32 Koivo, A. J., and Lee, K. S., "Self-Tuning Control of a Two-Link Manipulator with a Flexible Forearm", *The International Journal of Robotics Research*, Vol. 11, No. 4, Aug. 1992, pp. 383-395.

33 Bang, H., and Junkins, J. L., "Liapunov Optimal Control Laws for Flexible Structures Maneuver and Vibration control", *Advances in the Astronautical Sciences*, Vol. 75, Part I, 1990, p563.

34 Lee, H. G., Kawamura, S., Miyazaki, F., and Arimoto, S., "External Sensory Feedback Control for End-Effector of Flexible Multilink Manipulators", *Proceedings of 1990 IEEE International Conference on Robotics and Automation*, Cincinnati, OH, May 1990, pp. 1796-1802.

35 Murotsu, Y., Tsujio, S., Senda, K., and Hayashi, M., "Trajectory Control of Flexible Manipulators on a Free-Flying Space Robot", *IEEE Control System Magazine*, June, 1992, pp. 51-57.

36 Gawronski, W., Ih, C.-H. C., and Wang, S. J., "On Dynamics and Control of Multi-Link Flexible Space Manipulators", *AIAA-90-3396-CP*, pp. 725-734.

37 Meirovitch, L., and Lim, S., "Maneuvering and Control of Flexible Space Robots," *NASA Workshop on Distributed Parameter Modeling and Control of Flexible Aerospace System*, Williamsburg, VA, June 8-10, 1992.

38 Lee, C.-K., Chiang, W.-W., and O'sullivan, T. C., "Piezoelectric Model Sensor/Actuator Pairs for Critical Active Damping Vibration Control", *Journal of Acoustical Society of America*, Vol. 90, No. 1, July 1990, pp. 374-384.

39 Tzou, H. S., and Tseng, C. T., "Distributed Piezoelectric Sensor/Actuator Design for Dynamic Measurement/Control of Distributed Parameter Systems: A Piezoelectric Finite Element Approach", *Journal of Sound and Vibration*, Vol. 138, No. 1, 1990, pp. 17-34.

40 Dosch, J. J., and Inman, D. J., "A Self-Sensing Piezoelectric Actuator for Collocated Control", *Journal of Intelligent Material Systems and Structures*, Vol. 3, Jan. 1992, pp. 166-185.

41 Meirovitch, L., and Kwak, M. K., "Rayleigh-Ritz Based Substructure Synthesis for Flexible Multibody Systems", *AIAA Journal*, Vol. 19, No. 10, 1991, pp. 1709-1719.

42 Kirk, D. E., *Optimal Control Theory: An Introduction*, Prentice Hall, New Jersey, 1970.

43 Kazerounian, K., and Wang, Z., "Global versus Local Optimization in Redundancy Resolution of Robotic Manipulators," *International Journal of Robotics Research*, Vol. 7, No. 5, 1988, pp. 3-12.

44 Ascher, U., Mattheij, R., and Russell, R., *Numerical Solution of Boundary Value Problems for Ordinary Differential Equations*, Prentice Hall, New Jersey, 1988.

45 Watson, L. T., "Globally Convergent Homotopy Algorithms for Nonlinear Systems of Equations," *Nonlinear Dynamics*, Vol. 1, 1990, pp. 143-191.

46 Meirovitch, L., *Dynamics and Control of Structures*, Wiley-Interscience, New York, NY, 1990.

47 Kenney, R. S., and Leipnik, R. B., "Numerical Integration of the Differential Matrix Riccati Equation," *IEEE Transactions on Automatic Control*, Vol. 30, No. 10, 1990, pp. 962-970.

48 Anderson, B. D. O., " Adaptive Systems, Lack of Persistency of Excitation and Bursting Phenomena", *Automatica*, Vol. 21, No. 3, 1985, pp. 247-258.

49 Franklin, G. F., Powell, J. D. and Workman, M. L., *Digital Control of Dynamic Systems*, Addison-Wesley Publishing Company, New York, 1990.

50 Lim, S., "Position and Vibration Control of Flexible Space Robots", Ph.D. Dissertation, VPI&SU, 1992.

Appendix A: Matrices in the Original Equations

The mass matrix M in Eq. (2.12), as well as in Eq. (2.19), is defined as

$$M = \begin{bmatrix} & & & m_{17} & m_{18} \\ & & & m_{27} & m_{28} \\ & \bar{M}_0 & & m_{37} & m_{38} \\ & & & m_{47} & m_{48} + \mathbf{b}_1 \\ & & & m_{57} + \mathbf{b}_2 & m_{58} \\ & & & m_{67} & m_{68} \\ m_{17}^T & \dots & m_{67}^T & m_{77} & m_{78} \\ m_{18}^T & \dots & m_{68}^T & m_{78}^T & m_{88} \end{bmatrix} \tag{A.1}$$

with

$$\bar{M}_0 = \begin{bmatrix} m_t & 0 & -S_{tx} & a_1 & a_2 & -S_3 s_3 \\ 0 & m_t & -S_{ty} & a_3 & a_4 & S_3 c_3 \\ -S_{tx} & -S_{ty} & I_{t0} & a_5 & a_6 & S_3 L_0 s_{30} \\ a_1 & a_3 & a_5 & \bar{I}_1 & a_7 & a_8 \\ a_2 & a_4 & a_6 & a_7 & \bar{I}_2 & a_9 \\ -S_3 s_3 & S_3 c_3 & S_3 L_0 s_{30} & a_8 & a_9 & I_3 \end{bmatrix} \tag{A.2}$$

in which

$$\begin{aligned} a_1 &= -S_{t1} s_1 - \bar{\Phi}_{t1}^T \xi_1 c_1, \qquad a_2 = -S_{t2} s_2 - \bar{\Phi}_{t2}^T \xi_2 c_2 \\ a_3 &= S_{t1} c_1 - \bar{\Phi}_{t1}^T \xi_1 s_1, \qquad a_4 = S_{t2} c_2 - \bar{\Phi}_{t2}^T \xi_2 s_2 \\ a_5 &= S_{t1} L_0 s_{10} + \bar{\Phi}_{t1}^T \xi_1 L_0 c_{10}, \qquad a_6 = S_{t2} L_0 s_{20} + \bar{\Phi}_{t2}^T \xi_2 L_0 c_{20} \\ a_7 &= S_{t2} L_1 c_{21} + S_{t2} \Phi_{12}^T \xi_1 s_{21} - \bar{\Phi}_{t2}^T \xi_2 L_1 s_{21} + \bar{\Phi}_{t2}^T \xi_2 \Phi_{12}^T \xi_1 c_{21} \\ a_8 &= S_3 L_1 c_{31} + S_3 \Phi_{12}^T \xi_1 s_{31}, \qquad a_9 = S_3 L_2 c_{32} + S_3 \Phi_{23}^T \xi_2 s_{32} \\ \mathbf{b}_1 &= \bar{\Phi}_{t2}^T \Phi_{12}^T \xi_1 s_{21}, \qquad \mathbf{b}_2 = -\Phi_{12}^T \bar{\Phi}_{t2}^T \xi_2 s_{21} \\ \bar{I}_1 &= I_{t1} + \xi_1^T m_{77} \xi_1, \qquad \bar{I}_2 = I_{t2} + \xi_2^T m_{88} \xi_2 \end{aligned} \tag{A.3}$$

and

$$
\begin{aligned}
&m_{17} = -\bar{\Phi}_{t1}^T s_1, \qquad m_{27} = \bar{\Phi}_{t1}^T c_1, \qquad m_{37} = \bar{\Phi}_{t1}^T L_0 s_{10} \\
&m_{47} = \tilde{\Phi}_1^T + (m_2 + m_3) L_1 \Phi_{12}^T, \qquad m_{57} = S_{t2} \Phi_{12}^T c_{21}, \qquad m_{67} = S_3 \Phi_{12}^T c_{31} \\
&m_{18} = -\bar{\Phi}_{t2}^T s_2, \qquad m_{28} = \bar{\Phi}_{t2}^T c_2, \qquad m_{38} = \bar{\Phi}_{t2}^T L_0 s_{20} \\
&m_{48} = \bar{\Phi}_{t2}^T L_1 c_{21}, \qquad m_{58} = \tilde{\Phi}_2^T + m_3 L_2 \Phi_{23}^T, \qquad m_{68} = S_3 \Phi_{23}^T c_{32} \\
&m_{77} = \Lambda_1 + (m_2 + m_3) \Phi_{12} \Phi_{12}^T, \qquad m_{78} = \Phi_{12} \bar{\Phi}_{t2}^T c_{21} \\
&m_{88} = \Lambda_2 + m_3 \Phi_{23} \Phi_{23}^T
\end{aligned}
\tag{A.4}
$$

and we note that $s_i = \sin\theta_i$, $c_i = \cos\theta_i$, $s_{ij} = \sin(\theta_i - \theta_j)$ and $c_{ij} = \cos(\theta_i - \theta_j)$. Moreover, we have used the following definitions:

$$
\begin{aligned}
&m_t = m_0 + m_1 + m_2 + m_3 \\
&S_{tx} = S_{0x} \sin\theta_0 + S_{0y} \cos\theta_0 + (m_1 + m_2 + m_3) L_0 \cos\theta_0 \\
&S_{ty} = -S_{0x} \cos\theta_0 + S_{0y} \sin\theta_0 + (m_1 + m_2 + m_3) L_0 \sin\theta_0 \\
&S_{t1} = S_1 + (m_2 + m_3) L_1, \qquad S_{t2} = S_2 + m_3 L_2 \\
&I_{t0} = I_{0x} + I_{0y} + (m_1 + m_2 + m_3) L_0^2 \\
&I_{t1} = I_1 + (m_2 + m_3) L_1^2, \qquad I_{t2} = I_2 + m_3 L_2^2 \\
&\bar{\Phi}_{t1} = \bar{\Phi}_1 + (m_2 + m_3) \Phi_{12}, \qquad \bar{\Phi}_{t2} = \bar{\Phi}_2 + m_3 \Phi_{23}
\end{aligned}
$$

in which

$$
\begin{aligned}
m_i &= \int_{\text{Body } i} \rho_i dD_i \qquad i = 0,1,2,3 \\
S_i &= \int_{\text{Body } i} \rho_i x_i dD_i \qquad I_i = \int_{\text{Body } i} \rho_i x_i^2 dD_i \qquad i = 1,2,3 \\
S_{0x} &= \int_{\text{Body } 0} \rho_0 x dD_0 \qquad S_{0y} = \int_{\text{Body } 0} \rho_0 y dD_0 \\
I_{0x} &= \int_{\text{Body } 0} \rho_0 x^2 dD_0 \qquad I_{0y} = \int_{\text{Body } 0} \rho_0 y^2 dD_0
\end{aligned}
$$

$$\bar{\mathbf{\Phi}}_i = \int_{\text{Body } i} \rho_i \mathbf{\Phi}_i dD_i \qquad \tilde{\mathbf{\Phi}}_i = \int_{\text{Body } i} \rho_i x_i \mathbf{\Phi}_i dD_i$$

$$\Lambda_i = \int_{\text{Body } i} \rho_i \mathbf{\Phi}_i \mathbf{\Phi}_i^T dD_i \qquad i = 1, 2$$

$$\mathbf{\Phi}_{12} = \mathbf{\Phi}_1(x_1)\big|_{x_1=L_1} \qquad \mathbf{\Phi}_{23} = \mathbf{\Phi}_2(x_2)\big|_{x_2=L_2}$$

The matrix G in Eq. (2.17) is defined as

$$G = \begin{bmatrix} 1 & 0 & 0 & 0 & 0 & 0 & \mathbf{0}^T & \mathbf{0}^T \\ 0 & 1 & 0 & 0 & 0 & 0 & \mathbf{0}^T & \mathbf{0}^T \\ 0 & 0 & 1 & -1 & 0 & 0 & \mathbf{0}^T & \mathbf{0}^T \\ 0 & 0 & 0 & 1 & -1 & 0 & \mathbf{0}^T & \mathbf{0}^T \\ 0 & 0 & 0 & 0 & 1 & -1 & \mathbf{0}^T & \mathbf{0}^T \\ 0 & 0 & 0 & 0 & 0 & 1 & \mathbf{0}^T & \mathbf{0}^T \\ \mathbf{0} & \mathbf{0} & \mathbf{0} & \mathbf{0} & -\mathbf{\Phi}_1'(L_1) & \mathbf{0} & G_1 & 0 \\ \mathbf{0} & \mathbf{0} & \mathbf{0} & \mathbf{0} & \mathbf{0} & -\mathbf{\Phi}_2'(L_2) & 0 & G_2 \end{bmatrix} \tag{A.5}$$

in which

$$G_i = [\, \mathbf{\Phi}_i''(x_{i1}) \quad \cdots \quad \mathbf{\Phi}_i''(x_{im}) \,] \qquad i = 1, 2 \tag{A.6}$$

m is the number of actuators on each link. Here m equals the number of modes and the G_i's are square matrices.

The coefficient matrix C in Eq. (2.19) is defined as

$$C = \begin{bmatrix} 0 & 0 & C_{13} & C_{14} & C_{15} & C_{16} & C_{17} & C_{18} \\ 0 & 0 & C_{23} & C_{24} & C_{25} & C_{26} & C_{27} & C_{28} \\ 0 & 0 & 0 & C_{34} & C_{35} & C_{36} & C_{37} & C_{38} \\ 0 & 0 & C_{43} & 0 & C_{45} & C_{46} & C_{47} & C_{48} \\ 0 & 0 & C_{53} & C_{54} & 0 & C_{56} & C_{57} & C_{58} \\ 0 & 0 & C_{63} & C_{64} & C_{65} & 0 & C_{67} & C_{68} \\ \mathbf{0} & \mathbf{0} & C_{73} & C_{74} & C_{75} & C_{76} & 0 & C_{78} \\ \mathbf{0} & \mathbf{0} & C_{83} & C_{84} & C_{85} & C_{86} & C_{87} & 0 \end{bmatrix} \tag{A.7}$$

where

$$C_{13} = S_{ty}\dot{\theta}_0$$

$$C_{14} = (-S_{t1}c_1 + \bar{\mathbf{\Phi}}_{t1}^T \boldsymbol{\xi}_1 s_1)\dot{\theta}_1$$

$$C_{15} = (-S_{t2}c_2 + \bar{\mathbf{\Phi}}_{t2}^T \boldsymbol{\xi}_2 s_2)\dot{\theta}_2$$

$$C_{16} = -\, S_3 c_3 \dot{\theta}_3$$

$$C_{17} = -2.0\bar{\Phi}_{t1}^T c_1 \dot{\theta}_1$$

$$C_{18} = -2.0\bar{\Phi}_{t2}^T c_2 \dot{\theta}_2$$

$$C_{23} = -S_{tx}\dot{\theta}_0$$

$$C_{24} = (-S_{t1}s_1 - \bar{\Phi}_{t1}^T \xi_1 c_1)\dot{\theta}_1$$

$$C_{25} = (-S_{t2}s_2 - \bar{\Phi}_{t2}^T \xi_2 c_2)\dot{\theta}_2$$

$$C_{26} = -S_3 s_3 \dot{\theta}_3$$

$$C_{27} = -2.0\bar{\Phi}_{t1}^T s_1 \dot{\theta}_1$$

$$C_{28} = -2.0\bar{\Phi}_{t2}^T s_2 \dot{\theta}_2$$

$$C_{34} = (S_{t1}L_0 c_{10} - \bar{\Phi}_{t1}^T \xi_1 L_0 s_{10})\dot{\theta}_1$$

$$C_{35} = (S_{t2}L_0 c_{20} - \bar{\Phi}_{t2}^T \xi_2 L_0 s_{20})\dot{\theta}_2$$

$$C_{36} = S_3 L_0 c_{30}\dot{\theta}_3$$

$$C_{37} = 2.0\bar{\Phi}_{t1}^T L_0 c_{10}\dot{\theta}_1$$

$$C_{38} = 2.0\bar{\Phi}_{t2}^T L_0 c_{20}\dot{\theta}_2$$

$$C_{43} = (-S_{t1}L_0 c_{10} + \bar{\Phi}_{t1}^T \xi_1 L_0 s_{10})\dot{\theta}_0$$

$$C_{45} = (-S_{t2}L_1 s_{21} - \bar{\Phi}_{t2}^T \xi_2 L_1 c_{21} + S_{t2}\Phi_{12}^T \xi_1 c_{21} - \bar{\Phi}_{t2}^T \xi_2 \Phi_{12}^T \xi_1 s_{21})\dot{\theta}_2$$

$$C_{46} = (-S_3 L_1 s_{31} + S_3 \Phi_{12}^T \xi_1 c_{31})\dot{\theta}_3$$

$$C_{47} = 2.0\xi_1^T(\Lambda_1 + (m_2 + m_3)\Phi_{12}\Phi_{12}^T)\dot{\theta}_1$$

$$C_{48} = 2.0(-L_1 s_{21}\bar{\Phi}_{t2}^T + \Phi_{12}^T \xi_1 c_{21}\bar{\Phi}_{t2}^T)\dot{\theta}_2$$

$$C_{53} = (-S_{t2}L_0 c_{20} + \bar{\Phi}_{t2}^T \xi_2 L_0 s_{20})\dot{\theta}_0$$

$$C_{54} = (S_{t2}L_1 s_{21} + \bar{\Phi}_{t2}^T \xi_2 L_1 c_{21} - S_{t2}\Phi_{12}^T \xi_1 c_{21} + \bar{\Phi}_{t2}^T \xi_2 \Phi_{12}^T \xi_1 s_{21})\dot{\theta}_1$$

$$C_{56} = (-S_3 L_2 s_{32} + S_3 \Phi_{23}^T \xi_2 c_{32})\dot{\theta}_3$$

$$C_{57} = 2.0(S_{t2}s_{21}\Phi_{12}^T + \bar{\Phi}_{t2}^T \xi_2 c_{21}\Phi_{12}^T)\dot{\theta}_1$$

$$C_{58} = 2.0\boldsymbol{\xi}_2^T(\Lambda_2 + m_3\boldsymbol{\Phi}_{23}\boldsymbol{\Phi}_{23}^T)\dot{\theta}_2$$

$$C_{63} = -S_3 L_0 c_{30}\dot{\theta}_0$$

$$C_{64} = (S_3 L_1 s_{31} - S_3\boldsymbol{\Phi}_{12}^T\boldsymbol{\xi}_1 c_{31})\dot{\theta}_1$$

$$C_{65} = (S_3 L_2 s_{32} - S_3\boldsymbol{\Phi}_{23}^T\boldsymbol{\xi}_2 c_{32})\dot{\theta}_2$$

$$C_{67} = 2.0 S_3 s_{31}\boldsymbol{\Phi}_{12}^T\dot{\theta}_1$$

$$C_{68} = 2.0 S_3 s_{32}\boldsymbol{\Phi}_{23}^T\dot{\theta}_2$$

$$C_{73} = -\bar{\boldsymbol{\Phi}}_{t1} L_0 c_{10}\dot{\theta}_0$$

$$C_{74} = -(\Lambda_1 + (m_2 + m_3)\boldsymbol{\Phi}_{12}\boldsymbol{\Phi}_{12}^T)\boldsymbol{\xi}_1\dot{\theta}_1$$

$$C_{75} = (-S_{t2} s_{21}\boldsymbol{\Phi}_{12} - \bar{\boldsymbol{\Phi}}_{t2}^T\boldsymbol{\xi}_2 c_{21}\boldsymbol{\Phi}_{12})\dot{\theta}_2$$

$$C_{76} = -S_3 s_{31}\boldsymbol{\Phi}_{12}\dot{\theta}_3$$

$$C_{78} = -2.0\boldsymbol{\Phi}_{12}\bar{\boldsymbol{\Phi}}_{t2}^T s_{21}\dot{\theta}_2$$

$$C_{83} = -\bar{\boldsymbol{\Phi}}_{t2} L_0 c_{20}\dot{\theta}_0$$

$$C_{84} = (L_1 s_{21}\bar{\boldsymbol{\Phi}}_{t2} - \boldsymbol{\Phi}_{12}^T\boldsymbol{\xi}_1 c_{21}\bar{\boldsymbol{\Phi}}_{t2})\dot{\theta}_1$$

$$C_{85} = -(\Lambda_2 + m_3\boldsymbol{\Phi}_{23}\boldsymbol{\Phi}_{23}^T)\boldsymbol{\xi}_2\dot{\theta}_2$$

$$C_{86} = -S_3 s_{32}\boldsymbol{\Phi}_{23}\dot{\theta}_3$$

$$C_{87} = 2.0\bar{\boldsymbol{\Phi}}_{t2}\boldsymbol{\Phi}_{12}^T s_{21}\dot{\theta}_1$$

Appendix B: Matrices in the Perturbation Equations

Throughout this Appendix, the configuration variables represent the zero-order variables. But the subscript 0 is dropped for the sake of simplicity.

The mass matrix M_0 in Eq. (2.22), the zero-order equations of motion, is defined as

$$M_0 = \begin{bmatrix} m_t & 0 & -S_{tx} & -S_{t1}s_1 & -S_{t2}s_2 & -S_3 s_3 \\ 0 & m_t & -S_{ty} & S_{t1}c_1 & S_{t2}c_2 & S_3 c_3 \\ -S_{tx} & -S_{ty} & I_{t0} & S_{t1}L_0 s_{10} & S_{t2}L_0 s_{20} & S_3 L_0 s_{30} \\ -S_{t1}s_1 & S_{t1}c_1 & S_{t1}L_0 s_{10} & I_{t1} & S_{t2}L_1 c_{21} & S_3 L_1 c_{31} \\ -S_{t2}s_2 & S_{t2}c_2 & S_{t2}L_0 s_{20} & S_{t2}L_1 c_{21} & I_{t2} & S_3 L_2 c_{32} \\ -S_3 s_3 & S_3 c_3 & S_3 L_0 s_{30} & S_3 L_1 c_{31} & S_3 L_2 c_{32} & I_3 \end{bmatrix} \tag{B.1}$$

The coefficient matrix C_0 in Eq. (2.22) is defined as

$$C_0 = \begin{bmatrix} 0 & 0 & S_{ty}\dot{\theta}_0 & -S_{t1}c_1\dot{\theta}_1 & -S_{t2}c_2\dot{\theta}_2 & -S_3 c_3\dot{\theta}_3 \\ 0 & 0 & -S_{tx}\dot{\theta}_0 & -S_{t1}s_1\dot{\theta}_1 & -S_{t2}s_2\dot{\theta}_2 & -S_3 s_3\dot{\theta}_3 \\ 0 & 0 & 0 & S_{t1}L_0 c_{10}\dot{\theta}_1 & S_{t2}L_0 c_{20}\dot{\theta}_2 & S_3 L_0 c_{30}\dot{\theta}_3 \\ 0 & 0 & -S_{t1}L_0 c_{10}\dot{\theta}_0 & 0 & -S_{t2}L_1 s_{21}\dot{\theta}_2 & -S_3 L_1 s_{31}\dot{\theta}_3 \\ 0 & 0 & -S_{t2}L_0 c_{20}\dot{\theta}_0 & S_{t2}L_1 s_{21}\dot{\theta}_1 & 0 & -S_3 L_2 s_{32}\dot{\theta}_3 \\ 0 & 0 & -S_3 L_0 c_{30}\dot{\theta}_0 & S_3 L_1 s_{31}\dot{\theta}_1 & S_3 L_2 s_{32}\dot{\theta}_2 & 0 \end{bmatrix} \tag{B.2}$$

The mass matrix M_1 in Eq. (2.23), the first-order equations, is defined as

$$M_1 = \begin{bmatrix} & & & m_{17} & m_{18} \\ & M_0 & & \vdots & \vdots \\ & & & m_{67} & m_{68} \\ m_{17}^T & \dots & m_{67}^T & m_{77} & m_{78} \\ m_{18}^T & \dots & m_{68}^T & m_{78}^T & m_{88} \end{bmatrix} \tag{B.3}$$

where $m_{17}, \dots, m_{88}$ are given in Eqs. (A.4) in Appendix A.

The coefficient matrices C_1 and K_1 in Eq. (2.23) are defined as

$$C_1 = \begin{bmatrix} & & & & & & c_{17} & c_{18} \\ & & & & & & c_{27} & c_{28} \\ & & & 2C_0 & & & c_{37} & c_{38} \\ & & & & & & 0 & c_{48} \\ & & & & & & c_{57} & 0 \\ & & & & & & c_{67} & c_{68} \\ 0 & 0 & c_{73} & 0 & c_{75} & c_{76} & 0 & c_{78} \\ 0 & 0 & c_{83} & c_{84} & 0 & c_{86} & c_{87} & 0 \end{bmatrix} \tag{B.4}$$

where

$$c_{17} = -2\bar{\Phi}_{t1}^T c_1 \dot{\theta}_1, \qquad c_{18} = -2\bar{\Phi}_{t2}^T c_2 \dot{\theta}_2, \qquad c_{27} = -2\bar{\Phi}_{t1}^T s_1 \dot{\theta}_1$$

$$c_{28} = -2\bar{\Phi}_{t2}^T s_2 \dot{\theta}_2, \qquad c_{37} = 2\bar{\Phi}_{t1}^T L_0 c_{10} \dot{\theta}_1, \qquad c_{38} = 2\bar{\Phi}_{t2}^T L_0 c_{20} \dot{\theta}_2$$

$$c_{48} = -2\bar{\Phi}_{t2}^T L_1 s_{21} \dot{\theta}_2, \qquad c_{57} = 2S_{t2} \Phi_{12}^T s_{21} \dot{\theta}_1, \qquad c_{67} = 2S_3 \Phi_{12}^T s_{31} \dot{\theta}_1$$

$$c_{68} = 2S_3 \Phi_{23}^T s_{32} \dot{\theta}_2, \qquad c_{73} = -2\bar{\Phi}_{t1} L_0 c_{10} \dot{\theta}_0, \qquad c_{75} = -2S_{t2} \Phi_{12} s_{21} \dot{\theta}_2$$

$$c_{76} = -2S_3 \Phi_{12} s_{31} \dot{\theta}_3, \qquad c_{83} = 2\bar{\Phi}_{t2} L_0 s_{20} \dot{\theta}_0, \qquad c_{84} = 2\bar{\Phi}_{t2} L_1 s_{21} \dot{\theta}_1$$

$$c_{86} = -2S_3 \Phi_{23} s_{32} \dot{\theta}_3, \qquad c_{78} = -2\Phi_{12} \bar{\Phi}_{t2}^T s_{21} \dot{\theta}_2, \qquad c_{87} = 2\bar{\Phi}_{t2} \Phi_{12}^T s_{21} \dot{\theta}_1$$

and

$$K_1 = \begin{bmatrix} 0 & 0 & K_{13} & K_{14} & K_{15} & K_{16} & K_{17} & K_{18} \\ 0 & 0 & K_{23} & K_{24} & K_{25} & K_{26} & K_{27} & K_{28} \\ 0 & 0 & K_{33} & K_{34} & K_{35} & K_{36} & K_{37} & K_{38} \\ 0 & 0 & K_{43} & K_{44} & K_{45} & K_{46} & K_{47} & K_{48} \\ 0 & 0 & K_{53} & K_{54} & K_{55} & K_{56} & K_{57} & K_{58} \\ 0 & 0 & K_{63} & K_{64} & K_{65} & K_{66} & K_{67} & K_{68} \\ 0 & 0 & K_{73} & K_{74} & K_{75} & K_{76} & K_{77} + \bar{K}_1 & K_{78} \\ 0 & 0 & K_{83} & K_{84} & K_{85} & K_{86} & K_{87} & K_{88} + \bar{K}_2 \end{bmatrix} \tag{B.5}$$

where

$$K_{13} = S_{ty} \ddot{\theta}_0 + S_{tx} \dot{\theta}_0^2$$

$$K_{14} = -S_{t1} c_1 \ddot{\theta}_1 + S_{t1} s_1 \dot{\theta}_1^2$$

$$K_{15} = -S_{t2} c_2 \ddot{\theta}_2 + S_{t2} s_2 \dot{\theta}_2^2$$

$$K_{16} = -S_3 c_3 \ddot{\theta}_3 + S_3 s_3 \dot{\theta}_3^2$$

$$K_{17} = -\bar{\Phi}_{t1}^T c_1 \ddot{\theta}_1 + \bar{\Phi}_{t1}^T s_1 \dot{\theta}_1^2$$

$$K_{18} = -\bar{\Phi}_{t2}^T c_2 \ddot{\theta}_2 + \bar{\Phi}_{t2}^T s_2 \dot{\theta}_2^2$$

$$K_{23} = -S_{tx} \ddot{\theta}_0 + S_{ty} \dot{\theta}_0^2$$

$$K_{24} = -S_{t1} s_1 \ddot{\theta}_1 - S_{t1} c_1 \dot{\theta}_1^2$$

$$K_{25} = -S_{t2} s_2 \ddot{\theta}_2 - S_{t2} c_2 \dot{\theta}_2^2$$

$$K_{26} = -S_3 s_3 \ddot{\theta}_3 - S_3 c_3 \dot{\theta}_3^2$$

$$K_{27} = -\bar{\Phi}_{t1}^T s_1 \ddot{\theta}_1 - \bar{\Phi}_{t1}^T c_1 \dot{\theta}_1^2$$

$$K_{28} = -\bar{\Phi}_{t2}^T s_2 \ddot{\theta}_2 - \bar{\Phi}_{t2}^T c_2 \dot{\theta}_2^2$$

$$\begin{aligned} K_{33} =& S_{ty}\ddot{x}_0 - S_{tx}\ddot{y}_0 - S_{t1}L_0 c_{10}\ddot{\theta}_1 - S_{t2}L_0 c_{20}\ddot{\theta}_2 - S_3 L_0 c_{30}\ddot{\theta}_3 \\ & + S_{t1}L_0 s_{10}\dot{\theta}_1^2 + S_{t2}L_0 s_{20}\dot{\theta}_2^2 + S_3 L_0 s_{30}\dot{\theta}_3^2 \end{aligned}$$

$$K_{34} = S_{t1}L_0 c_{10}\ddot{\theta}_1 - S_{t1}L_0 s_{10}\dot{\theta}_1^2$$

$$K_{35} = S_{t2}L_0 c_{20}\ddot{\theta}_2 - S_{t2}L_0 s_{20}\dot{\theta}_2^2$$

$$K_{36} = S_3 L_0 c_{30}\ddot{\theta}_3 - S_3 L_0 s_{30}\dot{\theta}_3^2$$

$$K_{37} = \bar{\Phi}_{t1}^T L_0 c_{10}\ddot{\theta}_1 - \bar{\Phi}_{t1}^T L_0 s_{10}\dot{\theta}_1^2$$

$$K_{38} = \bar{\Phi}_{t2}^T L_0 c_{20}\ddot{\theta}_2 - \bar{\Phi}_{t2}^T L_0 s_{20}\dot{\theta}_2^2$$

$$K_{43} = -S_{t1}L_0 c_{10}\ddot{\theta}_0 - S_{t1}L_0 s_{10}\dot{\theta}_0^2$$

$$\begin{aligned} K_{44} =& -S_{t1}c_1\ddot{x}_0 - S_{t1}s_1\ddot{y}_0 + S_{t1}L_0 c_{10}\ddot{\theta}_0 + S_{t2}L_1 s_{21}\ddot{\theta}_2 + S_3 L_1 s_{31}\ddot{\theta}_3 \\ & + S_{t1}L_0 s_{10}\dot{\theta}_0^2 + S_{t2}L_1 c_{21}\dot{\theta}_2^2 + S_3 L_1 c_{31}\dot{\theta}_3^2 \end{aligned}$$

$$K_{45} = -S_{t2}L_1 s_{21}\ddot{\theta}_2 - S_{t2}L_1 c_{21}\dot{\theta}_2^2$$

$$K_{46} = -S_3 L_1 s_{31}\ddot{\theta}_3 - S_3 L_1 c_{31}\dot{\theta}_3^2$$

$$\begin{aligned} K_{47} =& -\bar{\Phi}_{t1}^T c_1\ddot{x}_0 - \bar{\Phi}_{t1}^T s_1\ddot{y}_0 + \bar{\Phi}_{t1}^T L_0 c_{10}\ddot{\theta}_0 + S_{t2}\Phi_{12}^T s_{21}\ddot{\theta}_2 + S_3\Phi_{12}^T s_{31}\ddot{\theta}_3 \\ & + \bar{\Phi}_{t1}^T L_0 s_{10}\dot{\theta}_0^2 + S_{t2}\Phi_{12}^T c_{21}\dot{\theta}_2^2 + S_3\Phi_{12}^T c_{31}\dot{\theta}_3^2 \end{aligned}$$

$$K_{48} = -\bar{\Phi}_{t2}^T L_1 s_{21}\ddot{\theta}_2 - \bar{\Phi}_{t2}^T L_1 c_{21}\dot{\theta}_2^2$$

$$K_{53} = -S_{t2}L_0 c_{20}\ddot{\theta}_0 - S_{t2}L_0 s_{20}\dot{\theta}_0^2$$

$$K_{54} = S_{t2}L_1 s_{21}\ddot{\theta}_1 - S_{t2}L_1 c_{21}\dot{\theta}_1^2$$

$$\begin{aligned} K_{55} =& -S_{t2}c_2\ddot{x}_0 - S_{t2}s_2\ddot{y}_0 + S_{t2}L_0 c_{20}\ddot{\theta}_0 - S_{t2}L_1 s_{21}\ddot{\theta}_1 + S_3 L_2 s_{32}\ddot{\theta}_3 \\ & + S_{t2}L_0 s_{20}\dot{\theta}_0^2 + S_{t2}L_1 c_{21}\dot{\theta}_1^2 + S_3 L_2 c_{32}\dot{\theta}_3^2 \end{aligned}$$

$$K_{56} = -S_3 L_2 s_{32}\ddot{\theta}_3 - S_3 L_2 c_{32}\dot{\theta}_3^2$$

$$K_{57} = S_{t2}\Phi_{12}^T s_{21}\ddot{\theta}_1 - S_{t2}\Phi_{12}^T c_{21}\dot{\theta}_1^2$$

$$K_{58} = -\bar{\Phi}_{t2}^T c_2\ddot{x}_0 - \bar{\Phi}_{t2}^T s_2\ddot{y}_0 + \bar{\Phi}_{t2}^T L_0 c_{20}\ddot{\theta}_0 - \bar{\Phi}_{t2}^T L_1 s_{21}\ddot{\theta}_1 + S_3\Phi_{23}^T s_{32}\ddot{\theta}_3$$
$$+ \bar{\Phi}_{t2}^T L_0 s_{20}\dot{\theta}_0^2 + \bar{\Phi}_{t2}^T L_1 c_{21}\dot{\theta}_1^2 + S_3\Phi_{23}^T c_{32}\dot{\theta}_3^2$$

$$K_{63} = -S_3 L_0 c_{30}\ddot{\theta}_0 - S_3 L_0 s_{30}\dot{\theta}_0^2$$

$$K_{64} = S_3 L_1 s_{31}\ddot{\theta}_1 - S_3 L_1 c_{31}\dot{\theta}_1^2$$

$$K_{65} = S_3 L_2 s_{32}\ddot{\theta}_2 - S_3 L_2 c_{32}\dot{\theta}_2^2$$

$$K_{66} = -S_3 c_3\ddot{x}_0 - S_3 s_3\ddot{y}_0 + S_3 L_0 c_{30}\ddot{\theta}_0 - S_3 L_1 s_{31}\ddot{\theta}_1 - S_3 L_2 s_{32}\ddot{\theta}_2$$
$$+ S_3 L_0 s_{30}\dot{\theta}_0^2 + S_3 L_1 c_{31}\dot{\theta}_1^2 + S_3 L_2 c_{32}\dot{\theta}_2^2$$

$$K_{67} = S_3\Phi_{12}^T s_{31}\ddot{\theta}_1 - S_3\Phi_{12}^T c_{31}\dot{\theta}_1^2$$

$$K_{68} = S_3\Phi_{23}^T s_{32}\ddot{\theta}_2 - S_3\Phi_{23}^T c_{32}\dot{\theta}_2^2$$

$$K_{73} = -\bar{\Phi}_{t1} L_0 c_{10}\ddot{\theta}_0 - \bar{\Phi}_{t1} L_0 s_{10}\dot{\theta}_0^2$$

$$K_{74} = -\bar{\Phi}_{t1} c_1\ddot{x}_0 - \bar{\Phi}_{t1} s_1\ddot{y}_0 + \bar{\Phi}_{t1} L_0 c_{10}\ddot{\theta}_0 + S_{t2}\Phi_{12} s_{21}\ddot{\theta}_2 + S_3\Phi_{12} s_{31}\ddot{\theta}_3$$
$$+ \bar{\Phi}_{t1} L_0 s_{10}\dot{\theta}_0^2 + S_{t2}\Phi_{12} c_{21}\dot{\theta}_2^2 + S_3\Phi_{12} c_{31}\dot{\theta}_3^2$$

$$K_{75} = -S_{t2}\Phi_{12} s_{21}\ddot{\theta}_2 - S_{t2}\Phi_{12} c_{21}\dot{\theta}_2^2$$

$$K_{76} = -S_3\Phi_{12} s_{31}\ddot{\theta}_3 - S_3\Phi_{12} c_{31}\dot{\theta}_3^2$$

$$K_{77} = -[\Lambda_1 + (m_2 + m_3)\Phi_{12}\Phi_{12}^T]\dot{\theta}_1^2$$

$$K_{78} = -\Phi_{12}\bar{\Phi}_{t2}^T(s_{21}\ddot{\theta}_2 + c_{21}\dot{\theta}_2^2)$$

$$K_{83} = \bar{\Phi}_{t2} L_0 s_{20}\ddot{\theta}_0 - \bar{\Phi}_{t2} L_0 c_{20}\dot{\theta}_0^2$$

$$K_{84} = \bar{\Phi}_{t2} L_1 s_{21}\ddot{\theta}_1 - \bar{\Phi}_{t2} L_1 c_{21}\dot{\theta}_1^2$$

$$K_{85} = -\bar{\Phi}_{t2} c_2\ddot{x}_0 - \bar{\Phi}_{t2} s_2\ddot{y}_0 - \bar{\Phi}_{t2} L_0 s_{20}\ddot{\theta}_0 - \bar{\Phi}_{t2} L_1 s_{21}\ddot{\theta}_1$$
$$+ S_3\Phi_{23} s_{32}\ddot{\theta}_3 + \bar{\Phi}_{t2} L_0 c_{20}\dot{\theta}_0^2 + \bar{\Phi}_{t2} L_1 c_{21}\dot{\theta}_1^2 + S_3\Phi_{23} c_{32}\dot{\theta}_3^2$$

$$K_{86} = -S_3\Phi_{23} s_{32}\ddot{\theta}_3 - S_3\Phi_{23} c_{32}\dot{\theta}_3^2$$

$$K_{87} = \bar{\Phi}_{t2}\Phi_{12}^T(s_{21}\ddot{\theta}_1 - c_{21}\dot{\theta}_1^2)$$

$$K_{88} = -[\Lambda_2 + m_3\Phi_{23}\Phi_{23}^T]\dot{\theta}_2^2$$

The disturbance vector $\mathbf{d}$ in Eq. (2.23) is defined as

$$\mathbf{d} = [0 \quad 0 \quad 0 \quad 0 \quad 0 \quad 0 \quad \mathbf{d}_7^T \quad \mathbf{d}_8^T]^T \tag{B.6}$$

where

$$\begin{aligned}\mathbf{d}_7 =&[\tilde{\Phi}_1 + (m_2 + m_3)L_1\Phi_{12}]\ddot{\theta}_1 + \bar{\Phi}_{t1}(-s_1\ddot{x}_0 + c_1\ddot{y}_0 + L_0 s_{10}\ddot{\theta}_0 - L_0 c_{10}\dot{\theta}_0^2) \\ &+ S_{t2}\Phi_{12}(c_{21}\ddot{\theta}_2 - s_{21}\dot{\theta}_2^2) + S_3\Phi_{12}(c_{31}\ddot{\theta}_3 - s_{31}\dot{\theta}_3^2) \\ \mathbf{d}_8 =&[\tilde{\Phi}_2 + m_3 L_2\Phi_{23}]\ddot{\theta}_2 + \bar{\Phi}_{t2}(-s_2\ddot{x}_0 + c_2\ddot{y}_0 + L_0 c_{20}\ddot{\theta}_0 + L_0 s_{20}\dot{\theta}_0^2 \\ &+ L_1 c_{21}\ddot{\theta}_1 + L_1 s_{21}\dot{\theta}_1^2) + S_3\Phi_{23}(c_{32}\ddot{\theta}_3 - s_{32}\dot{\theta}_3^2)\end{aligned}$$

Appendix C: Matrices in the Direct Partitioning Equations

The mass matrix M_r and the coefficient matrix C_r in Eq. (2.26) are defined as

$$M_r = M_0 \tag{C.1}$$

$$C_r = C_0 \tag{C.2}$$

where M_0 and C_0 are given in Eqs. (B.1) and (B.2) respectively in Appendix B. The disturbance vector $\mathbf{d}_e$ in Eq. (2.26) is defined as

$$\mathbf{d}_e = M_{re}\ddot{\mathbf{q}}_e + C_{re}\dot{\mathbf{q}}_e + (K_M^e + K_C^e)\mathbf{q}_e \tag{C.3}$$

where

$$M_{re} = \begin{bmatrix} m_{17} & m_{18} \\ m_{27} & m_{28} \\ \vdots & \vdots \\ m_{67} & m_{68} \end{bmatrix} \tag{C.4}$$

$$C_{re} = \begin{bmatrix} -2\bar{\Phi}_{t1}^T c_1 \dot{\theta}_1 & -2\bar{\Phi}_{t2}^T c_2 \dot{\theta}_2 \\ -2\bar{\Phi}_{t1}^T s_1 \dot{\theta}_1 & -2\bar{\Phi}_{t2}^T s_2 \dot{\theta}_2 \\ 2\bar{\Phi}_{t1}^T L_0 c_{10} \dot{\theta}_1 & 2\bar{\Phi}_{t2}^T L_0 c_{20} \dot{\theta}_2 \\ 0 & -2\bar{\Phi}_{t2}^T L_1 s_{21} \dot{\theta}_2 \\ 2\Phi_{12}^T S_{t2} s_{21} \dot{\theta}_1 & 0 \\ 2\Phi_{12}^T S_3 s_{31} \dot{\theta}_1 & 2\Phi_{23}^T S_3 s_{32} \dot{\theta}_2 \end{bmatrix} \tag{C.5}$$

$$K_M^e = \begin{bmatrix} -\bar{\Phi}_{t1}^T c_1 \ddot{\theta}_1 & -\bar{\Phi}_{t2}^T c_2 \ddot{\theta}_2 \\ -\bar{\Phi}_{t1}^T s_1 \ddot{\theta}_1 & -\bar{\Phi}_{t2}^T s_2 \ddot{\theta}_2 \\ \bar{\Phi}_{t1}^T L_0 c_{10} \ddot{\theta}_1 & \bar{\Phi}_{t2}^T L_0 c_{20} \ddot{\theta}_2 \\ \mathbf{k}_{M1} & -\bar{\Phi}_{t2}^T L_1 s_{21} \ddot{\theta}_2 \\ \Phi_{12}^T S_{t2} s_{21} \ddot{\theta}_1 & \mathbf{k}_{M2} \\ \Phi_{12}^T S_3 s_{31} \ddot{\theta}_1 & \Phi_{23}^T S_3 s_{32} \ddot{\theta}_2 \end{bmatrix} \tag{C.6}$$

in which

$$\mathbf{k}_{M1} = -\bar{\Phi}_{t1}^T (c_1 \ddot{x}_0 + s_1 \ddot{y}_0 - L_0 c_{10} \ddot{\theta}_0) + \Phi_{12}^T (S_{t2} s_{21} \ddot{\theta}_2 + S_3 s_{31} \ddot{\theta}_3)$$

$$\mathbf{k}_{M2} = -\bar{\Phi}_{t2}^T (c_2 \ddot{x}_0 + s_2 \ddot{y}_0 - L_0 c_{20} \ddot{\theta}_0) - \bar{\Phi}_{t2}^T L_1 s_{21} \ddot{\theta}_1 + \Phi_{23} S_3 s_{32} \ddot{\theta}_3$$

and

$$K_C^e = \begin{bmatrix} \bar{\Phi}_{t1}^T s_1 \dot{\theta}_1^2 & \bar{\Phi}_{t2}^T s_2 \dot{\theta}_2^2 \\ -\bar{\Phi}_{t1}^T c_1 \dot{\theta}_1^2 & -\bar{\Phi}_{t2}^T c_2 \dot{\theta}_2^2 \\ -\bar{\Phi}_{t1}^T L_0 s_{10} \dot{\theta}_1^2 & -\bar{\Phi}_{t2}^T L_0 s_{20} \dot{\theta}_2^2 \\ \mathbf{k}_{C1} & -\bar{\Phi}_{t2}^T L_1 c_{21} \dot{\theta}_2^2 \\ -\Phi_{12}^T S_{t2} c_{21} \dot{\theta}_1^2 & \mathbf{k}_{C2} \\ -\Phi_{12}^T S_3 c_{31} \dot{\theta}_1^2 & -\Phi_{23}^T S_3 c_{32} \dot{\theta}_2^2 \end{bmatrix} \tag{C.7}$$

in which

$$\mathbf{k}_{C1} = \bar{\Phi}_{t1}^T L_0 s_{10} \dot{\theta}_0^2 + \Phi_{12}^T S_{t2} c_{21} \dot{\theta}_2^2 + \Phi_{12}^T S_3 c_{31} \dot{\theta}_3^2$$

$$\mathbf{k}_{C2} = \bar{\Phi}_{t2}^T L_0 s_{20} \dot{\theta}_0^2 + \bar{\Phi}_{t2}^T L_1 c_{21} \dot{\theta}_1^2 + \Phi_{23}^T S_3 c_{32} \dot{\theta}_3^2$$

The mass matrix M_e and the coefficient matrix C_e are defined as

$$M_e = \begin{bmatrix} \Lambda_1 + (m_2 + m_3) \Phi_{12} \Phi_{12}^T & \Phi_{12} \bar{\Phi}_{t2}^T c_{21} \\ \bar{\Phi}_{t2} \Phi_{12}^T c_{21} & \Lambda_2 + m_3 \Phi_{23} \Phi_{23}^T \end{bmatrix} \tag{C.8}$$

and

$$C_e = \begin{bmatrix} 0 & -2\Phi_{12} \bar{\Phi}_{t2}^T s_{21} \dot{\theta}_2 \\ 2\bar{\Phi}_{t2} \Phi_{12}^T s_{21} \dot{\theta}_1 & 0 \end{bmatrix} \tag{C.9}$$

The coefficient matrix K_e is defined as

$$K_e = K + K_M + K_C \tag{C.10}$$

where

$$K = \begin{bmatrix} \bar{K}_1 & 0 \\ 0 & \bar{K}_2 \end{bmatrix} \tag{C.11}$$

$$K_M = \begin{bmatrix} 0 & -\mathbf{\Phi}_{12}\bar{\mathbf{\Phi}}_{t2}^T s_{21}\ddot{\theta}_2 \\ \bar{\mathbf{\Phi}}_{t2}\mathbf{\Phi}_{12}^T s_{21}\ddot{\theta}_1 & 0 \end{bmatrix} \tag{C.12}$$

and

$$K_C = \begin{bmatrix} -(\Lambda_1 + (m_2+m_3)\mathbf{\Phi}_{12}\mathbf{\Phi}_{12}^T)\dot{\theta}_1^2 & -\mathbf{\Phi}_{12}\bar{\mathbf{\Phi}}_{t2}^T c_{21}\dot{\theta}_2^2 \\ -\bar{\mathbf{\Phi}}_{t2}\mathbf{\Phi}_{12}^T c_{21}\dot{\theta}_1^2 & -(\Lambda_2 + m_3\mathbf{\Phi}_{23}\mathbf{\Phi}_{23}^T)\dot{\theta}_2^2 \end{bmatrix} \tag{C.13}$$

The disturbance vector $\mathbf{d}_r$ is defined as

$$\mathbf{d}_r = M_{re}^T\ddot{\mathbf{q}}_r + C_{er}\dot{\mathbf{q}}_r \tag{C.14}$$

with M_{re} given in Eq. (C.4) and

$$C_{er} = \begin{bmatrix} 0 & 0 & -\bar{\mathbf{\Phi}}_{t1}L_0 c_{10}\dot{\theta}_0 & 0 & -\mathbf{\Phi}_{12}S_{t2}s_{21}\dot{\theta}_2 & -\mathbf{\Phi}_{12}S_3 s_{31}\dot{\theta}_3 \\ 0 & 0 & -\bar{\mathbf{\Phi}}_{t2}L_0 c_{20}\dot{\theta}_0 & \bar{\mathbf{\Phi}}_{t2}L_1 s_{21}\dot{\theta}_1 & 0 & -\mathbf{\Phi}_{23}S_3 s_{32}\dot{\theta}_3 \end{bmatrix} \tag{C.15}$$

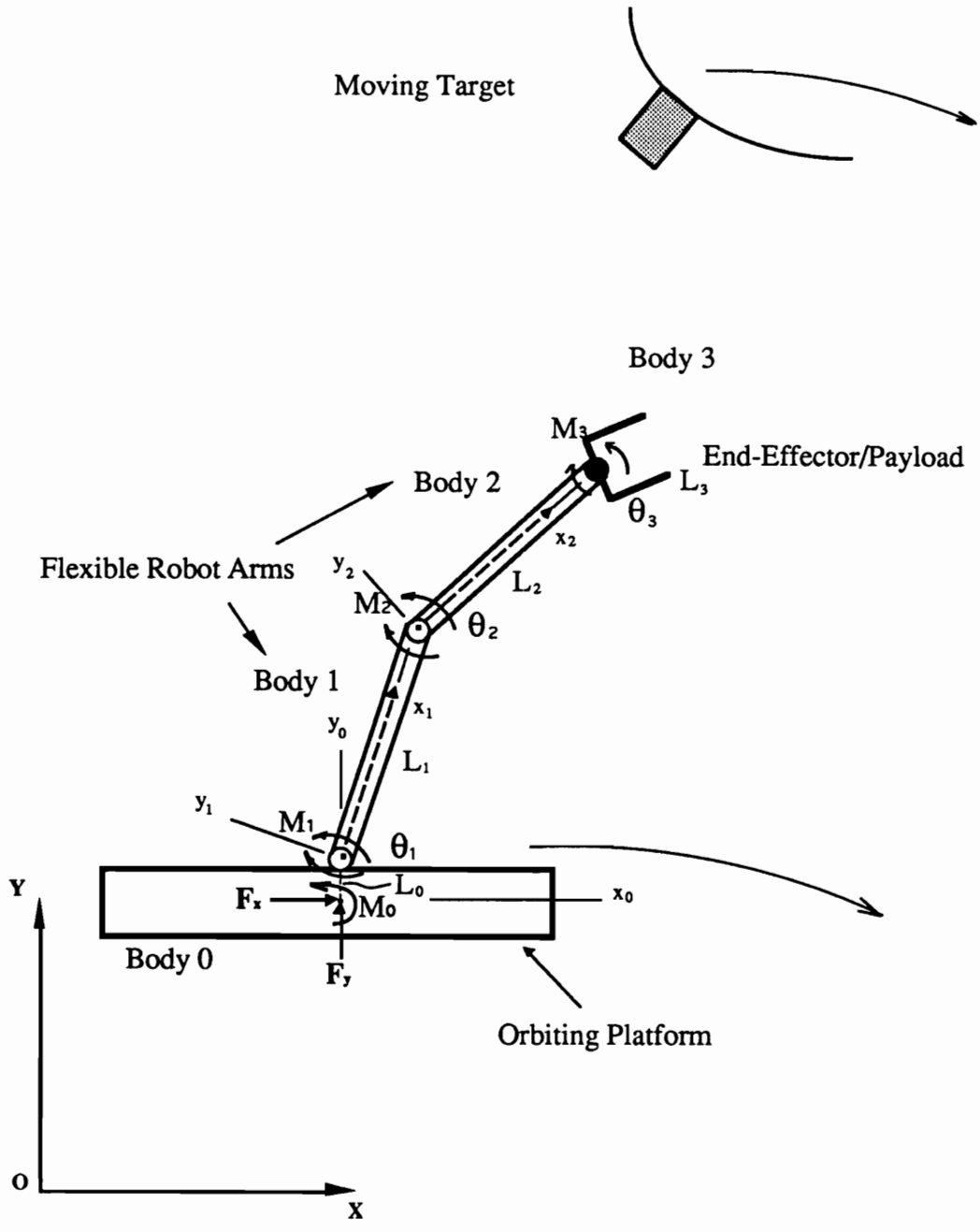

Figure 1. Flexible Space Robot

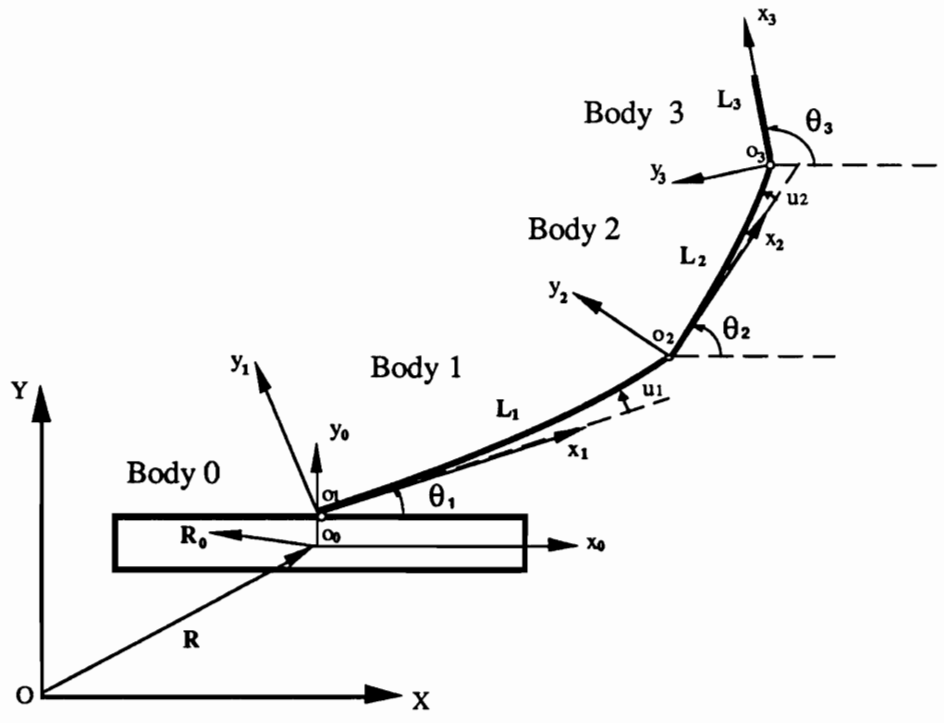

XOY: Inertial coordinate system.

$x_0o_0y_0$: Coordinate system attached to Body 0 with o_0o_1 as y_0 axis.

$x_1o_1y_1$: Coordinate system attached to Body 1 with x_1 axis tangent to Body 1 at o_1.

$x_2o_2y_2$: Coordinate system attached to Body 2 with x_2 axis tangent to Body 2 at o_2.

$x_3o_3y_3$: Coordinate system attached to Body 3.

Figure 2. Body Coordinates for Multibody System of Space Robot

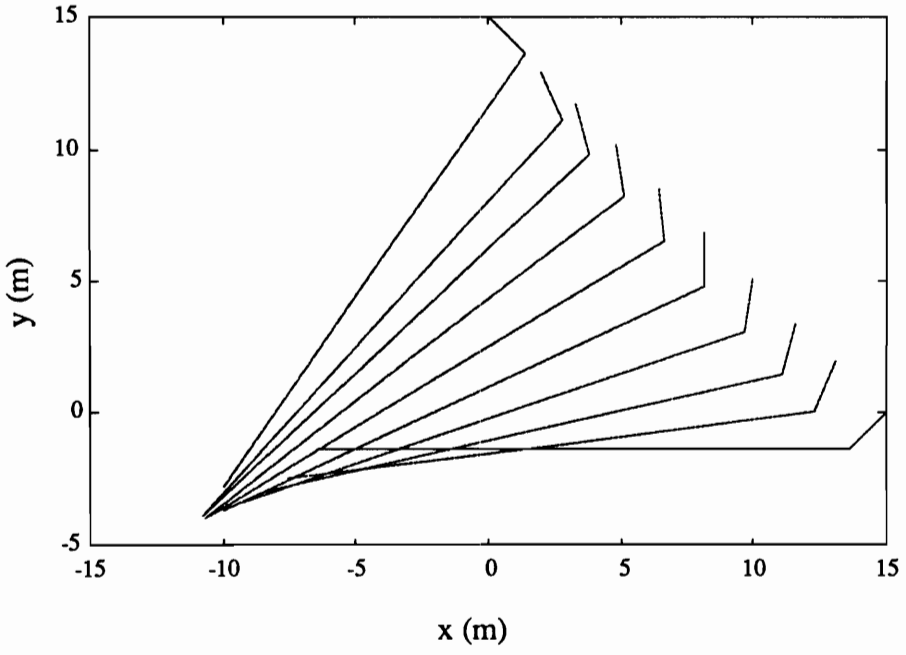

Figure 3.1a. Time-Lapse Picture of Optimal Robot Configuration Trajectory for Case 1

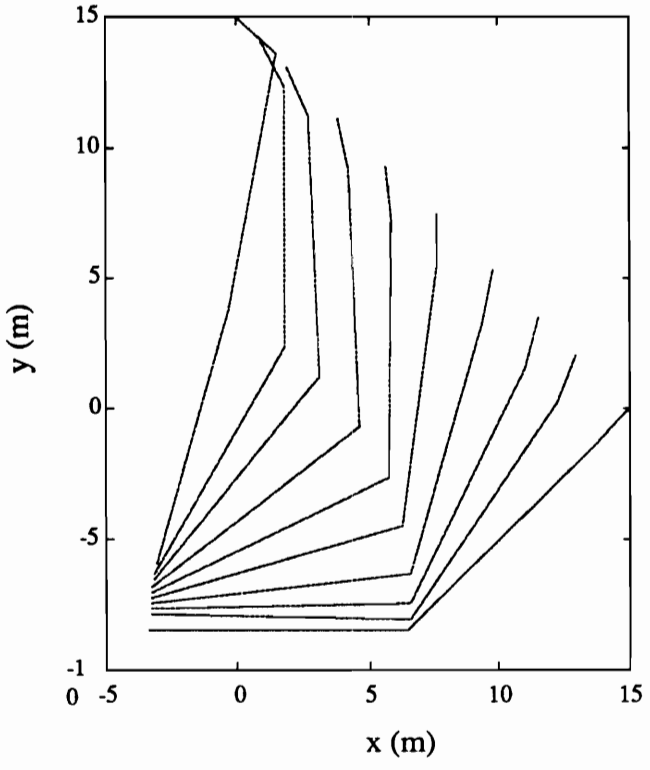

Figure 3.1b. Time-Lapse Picture of Optimal Robot Configuration Trajectory for Case 2

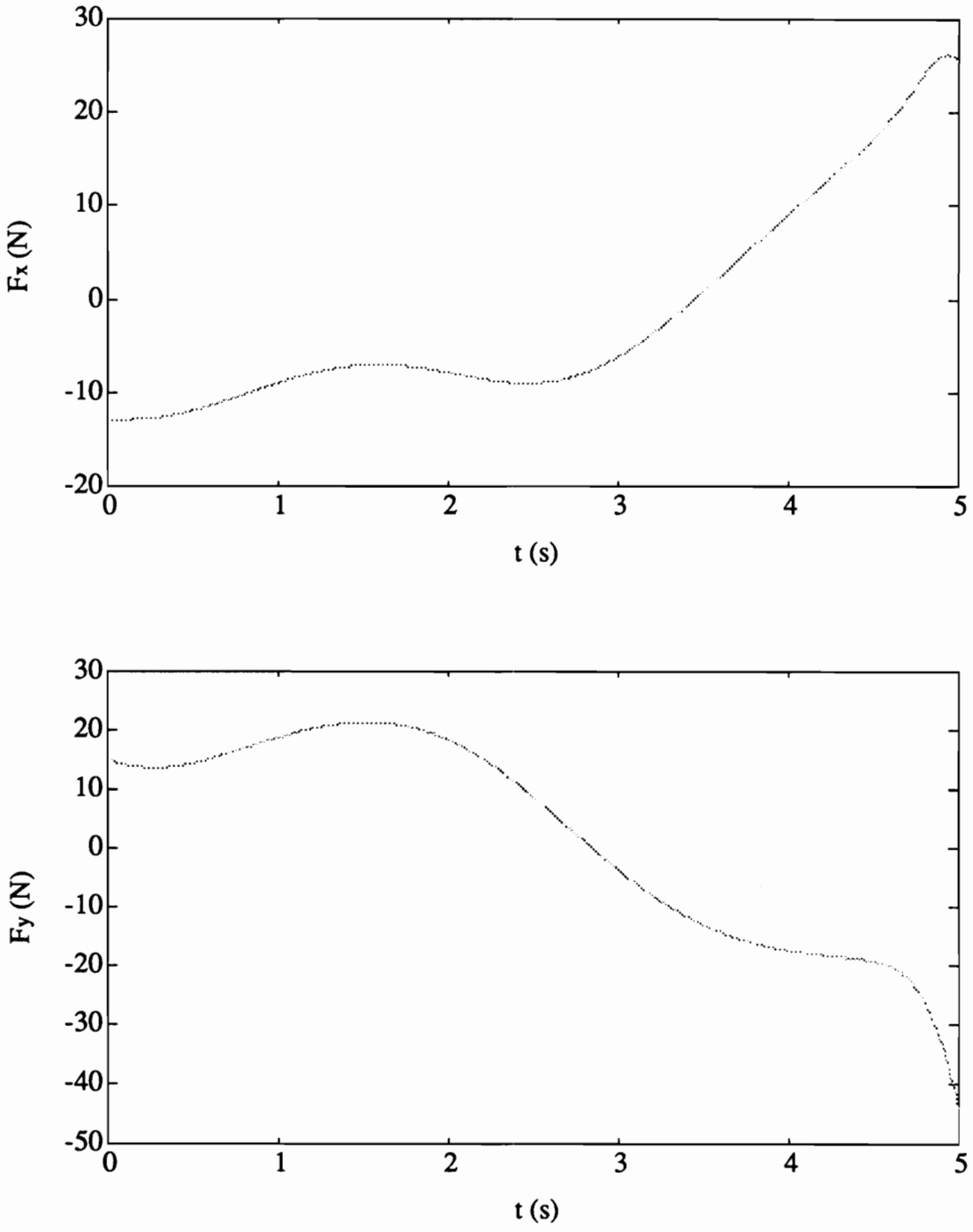

Figure 3.2a. Time Histories of The Zero-Order Control Forces

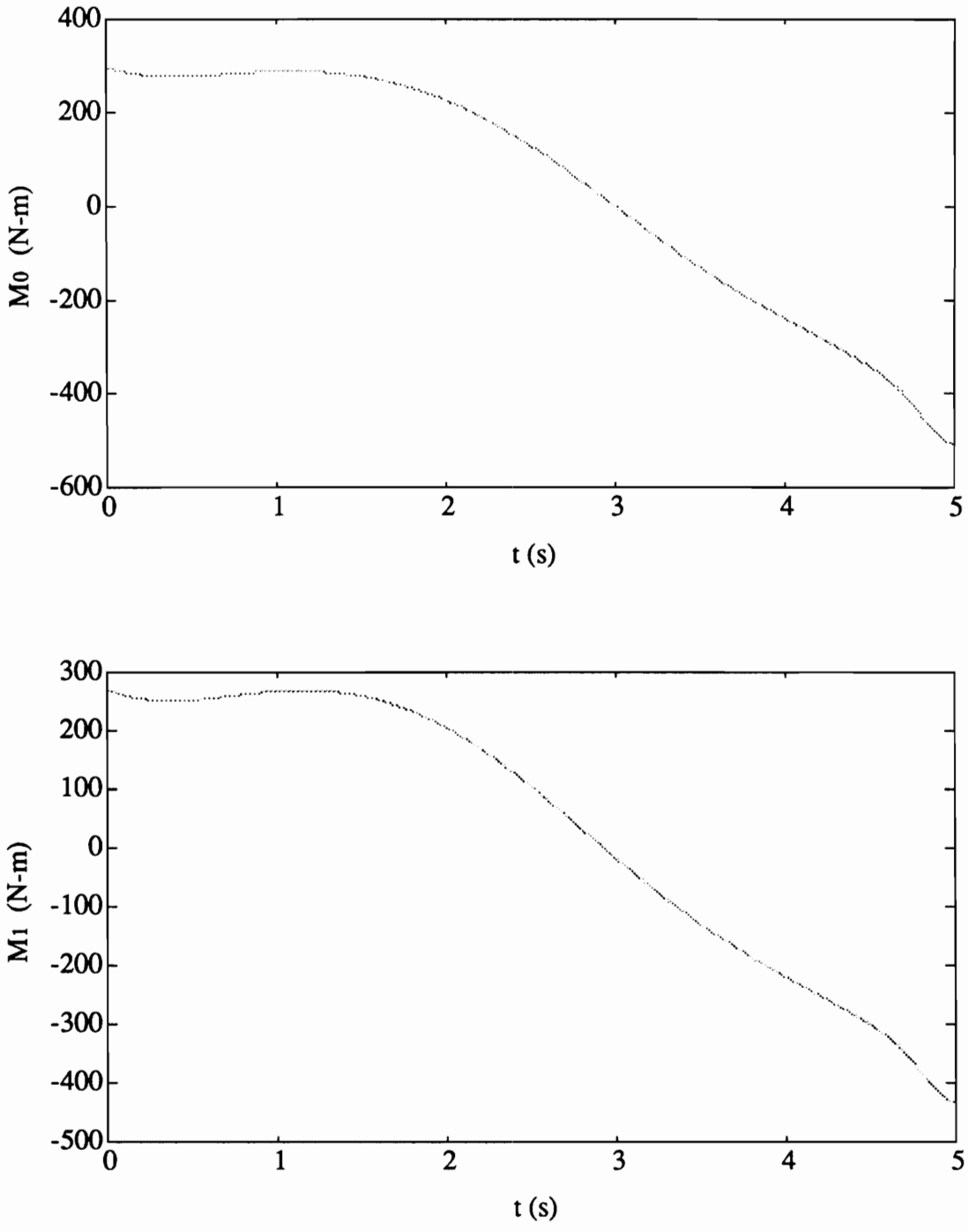

Figure 3.2b. Time Histories of The Zero-Order Control Torques

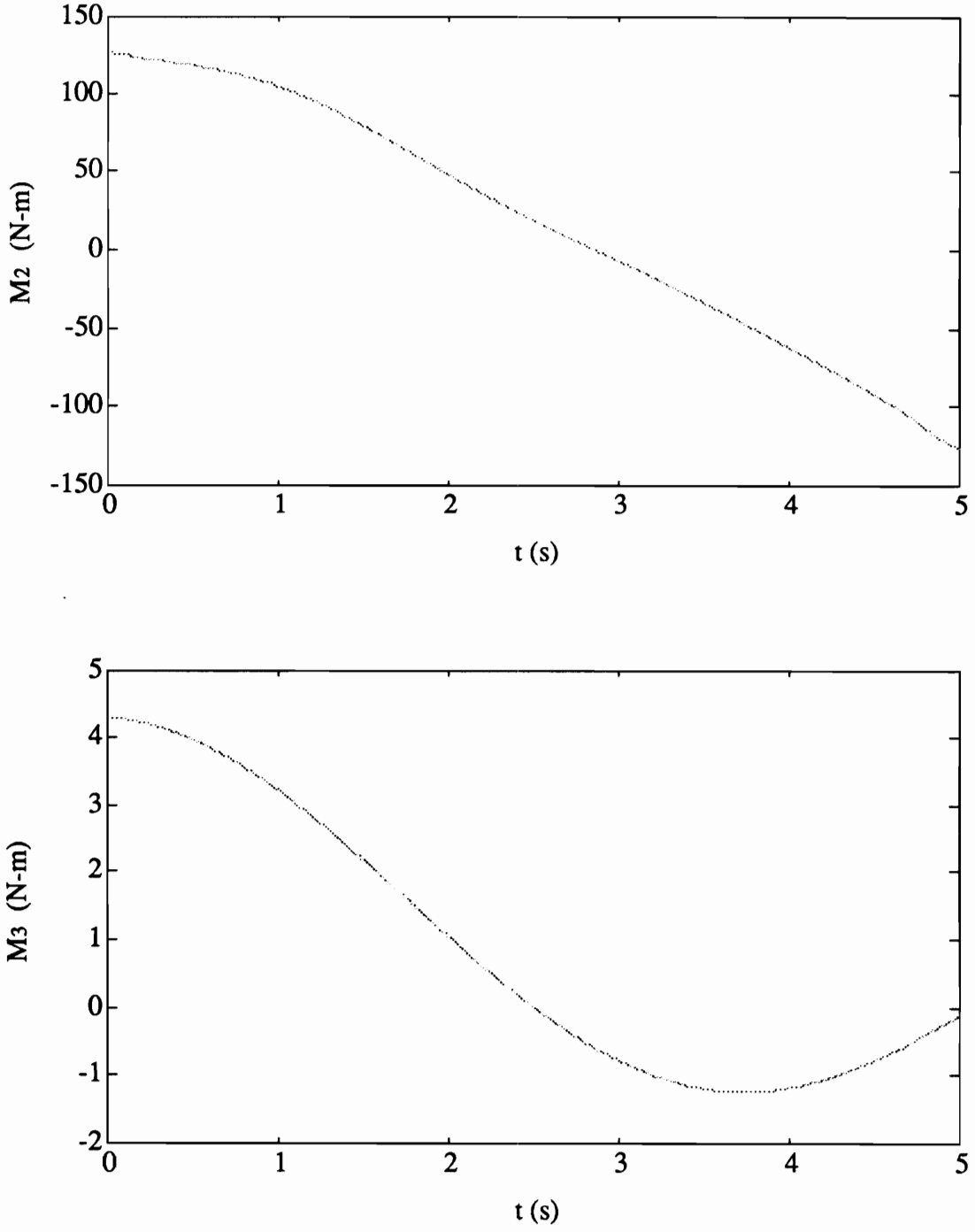

Figure 3.2c. Time Histories of The Zero-Order Control Torques

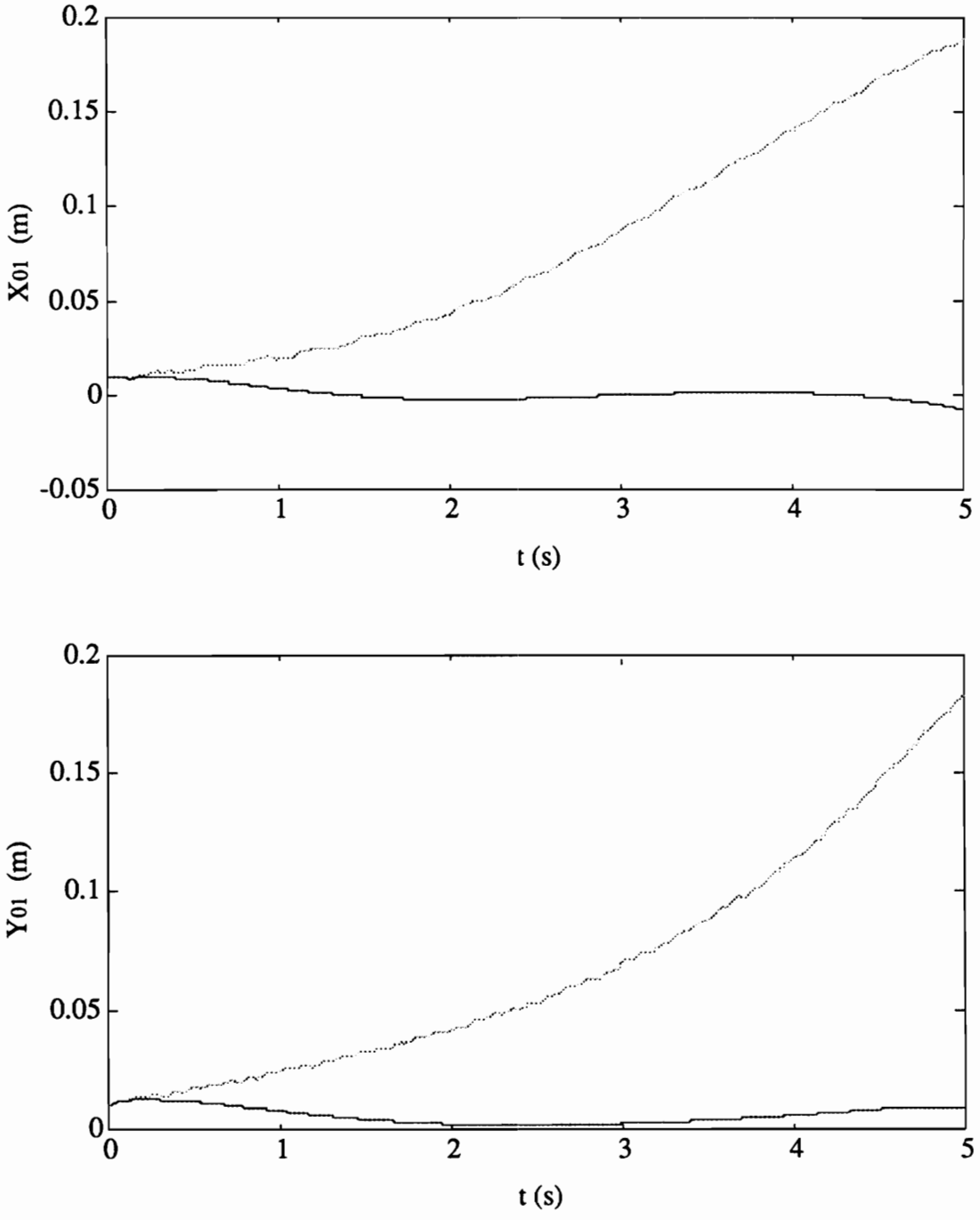

Figure 3.3a. Time Histories of Controlled (——) and Uncontrolled (.....) Responses

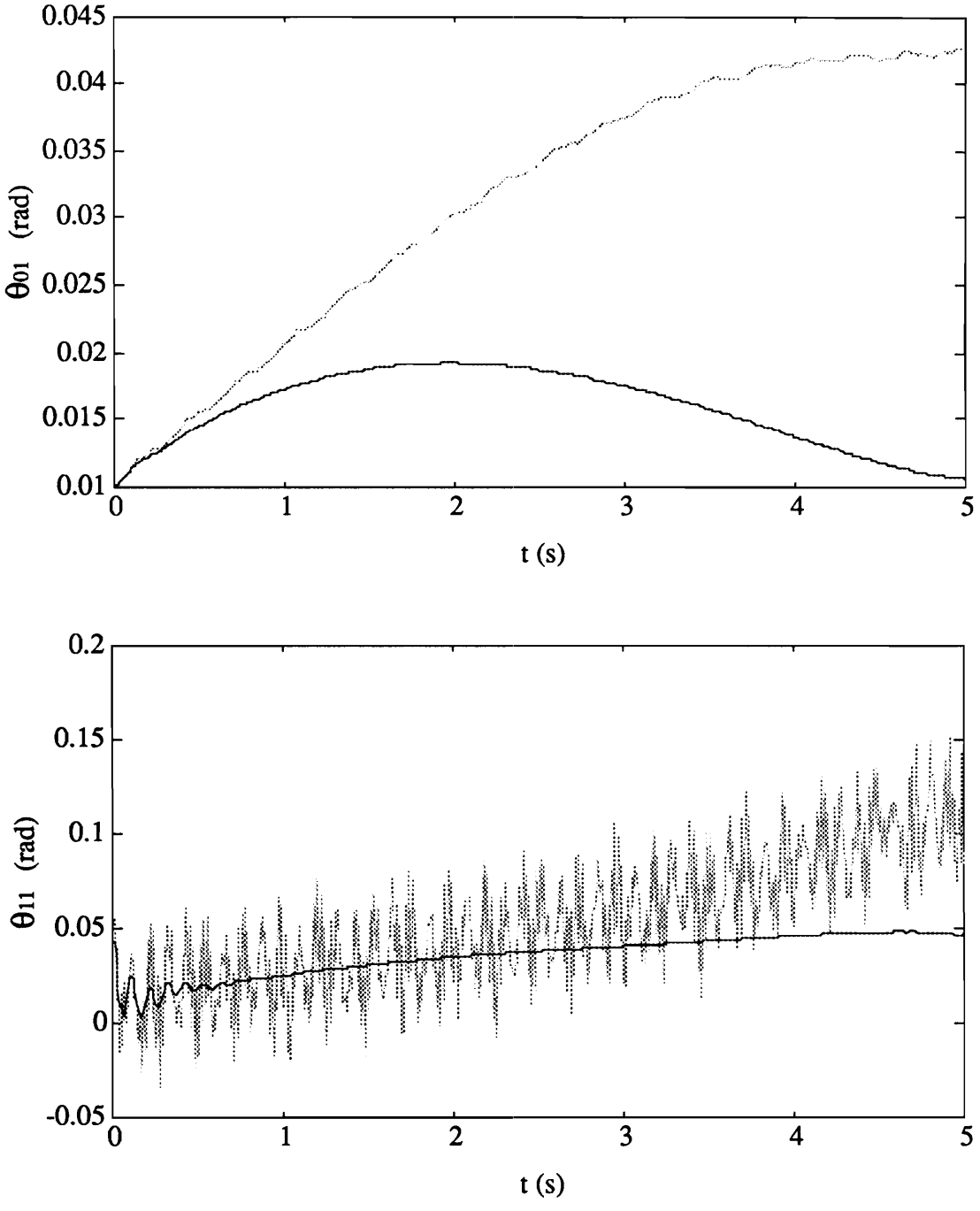

Figure 3.3b. Time Histories of Controlled (——) and Uncontrolled (·····) Responses

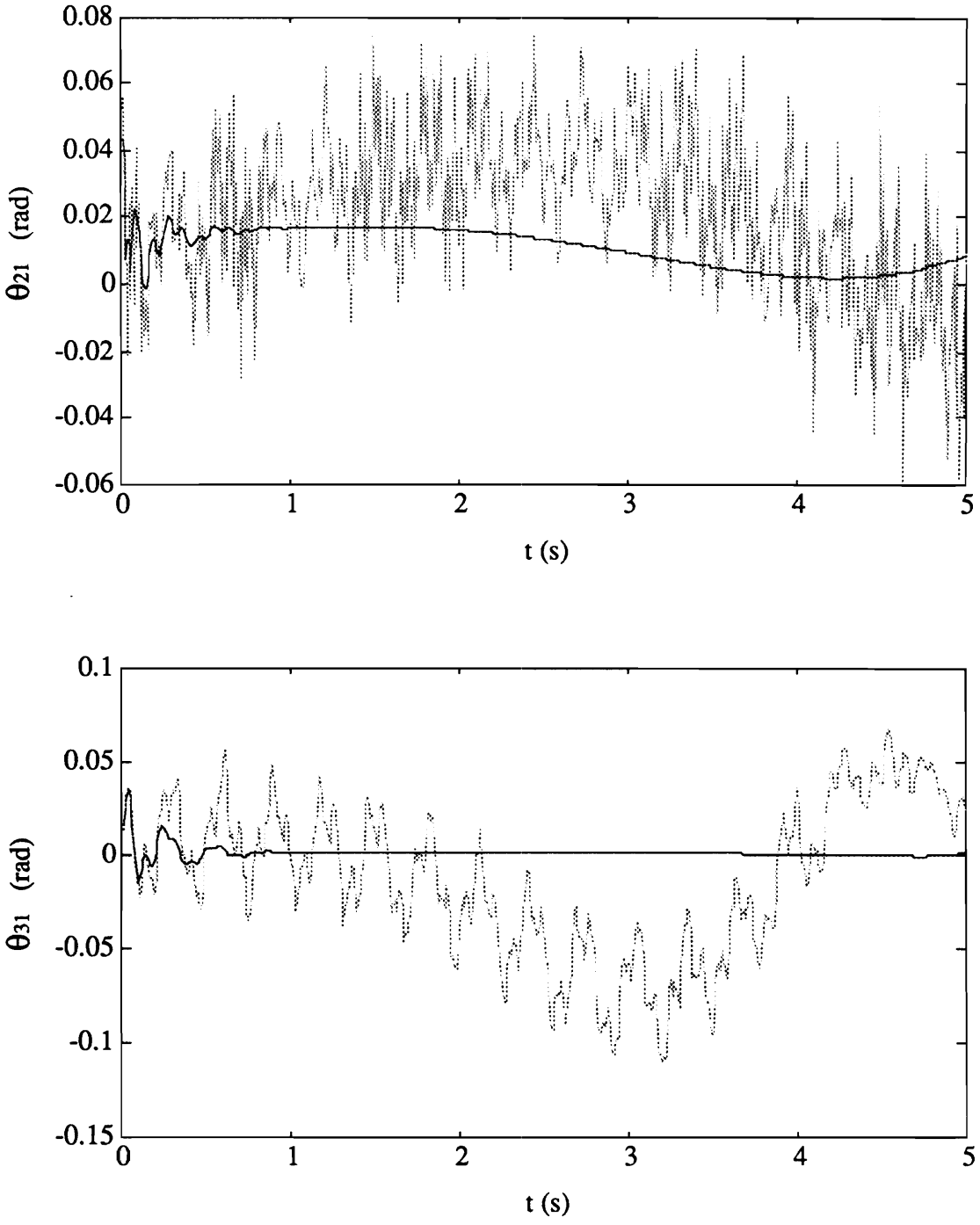

Figure 3.3c. Time Histories of Controlled (——) and Uncontrolled (·····) Responses

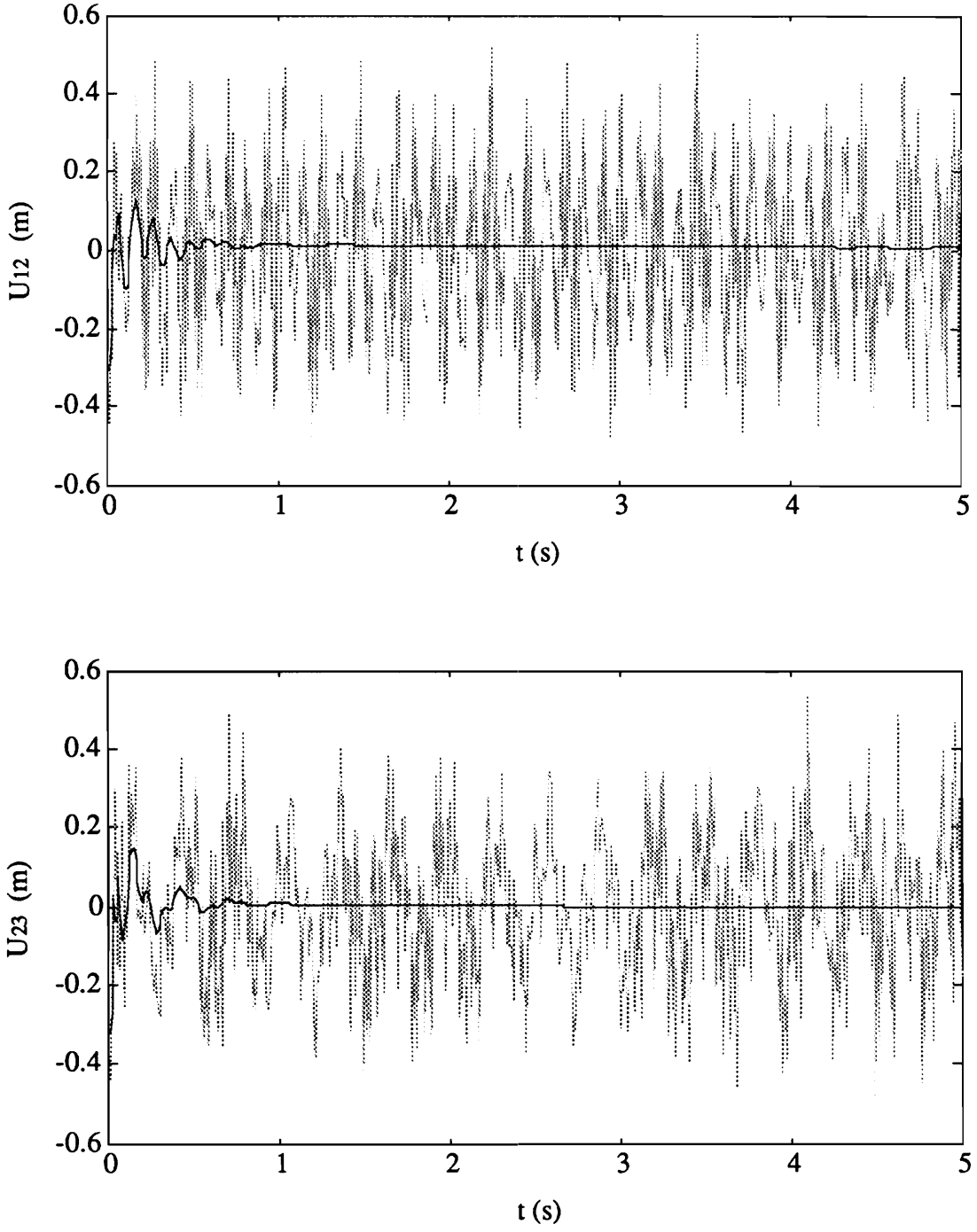

Figure 3.3d. Time Histories of Controlled (——) and Uncontrolled (·····) Responses

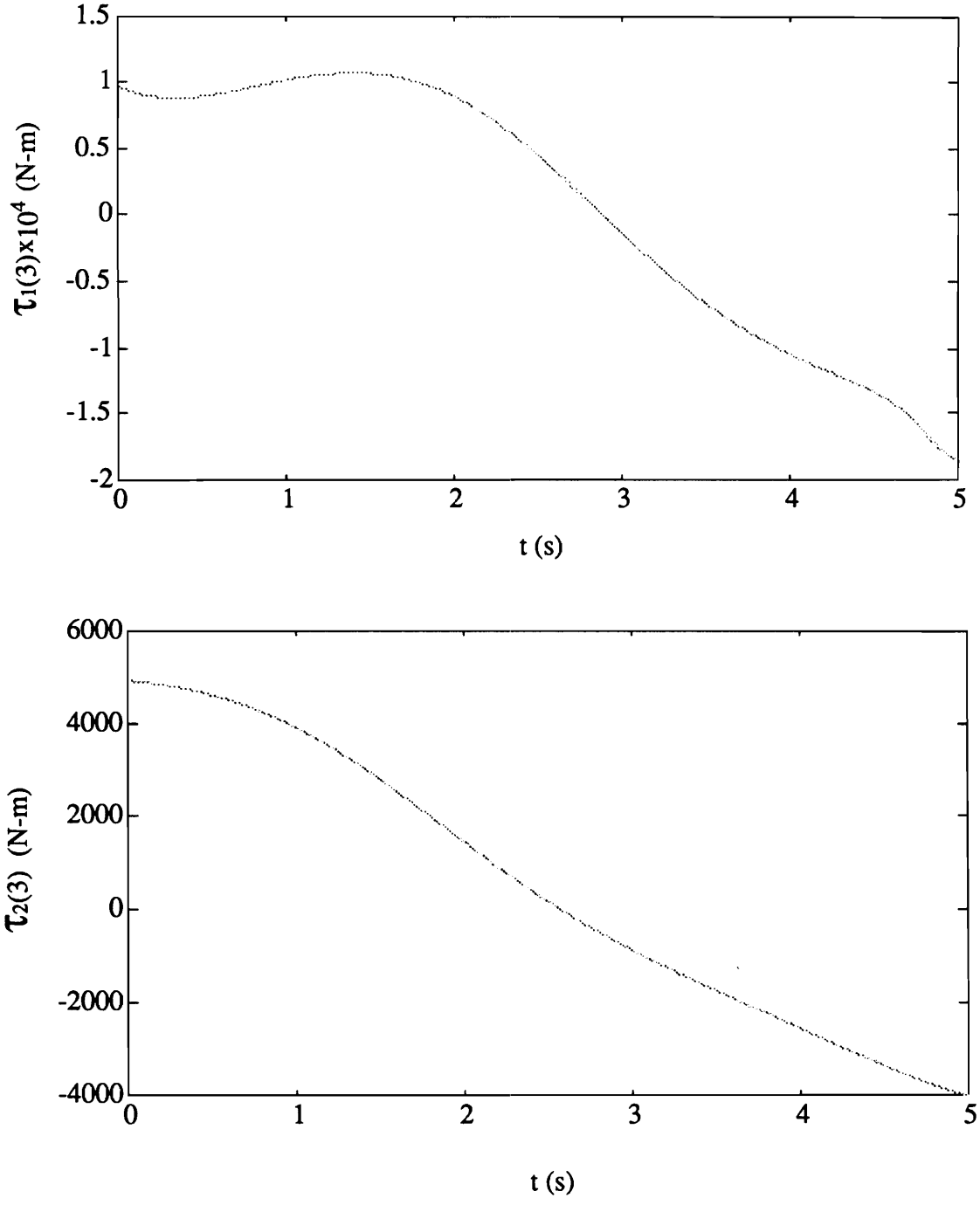

Figure 3.4. Time Histories of the Third Element of the First-Order Control Torques Applied to the Flexible Arms for Disturbance Rejection

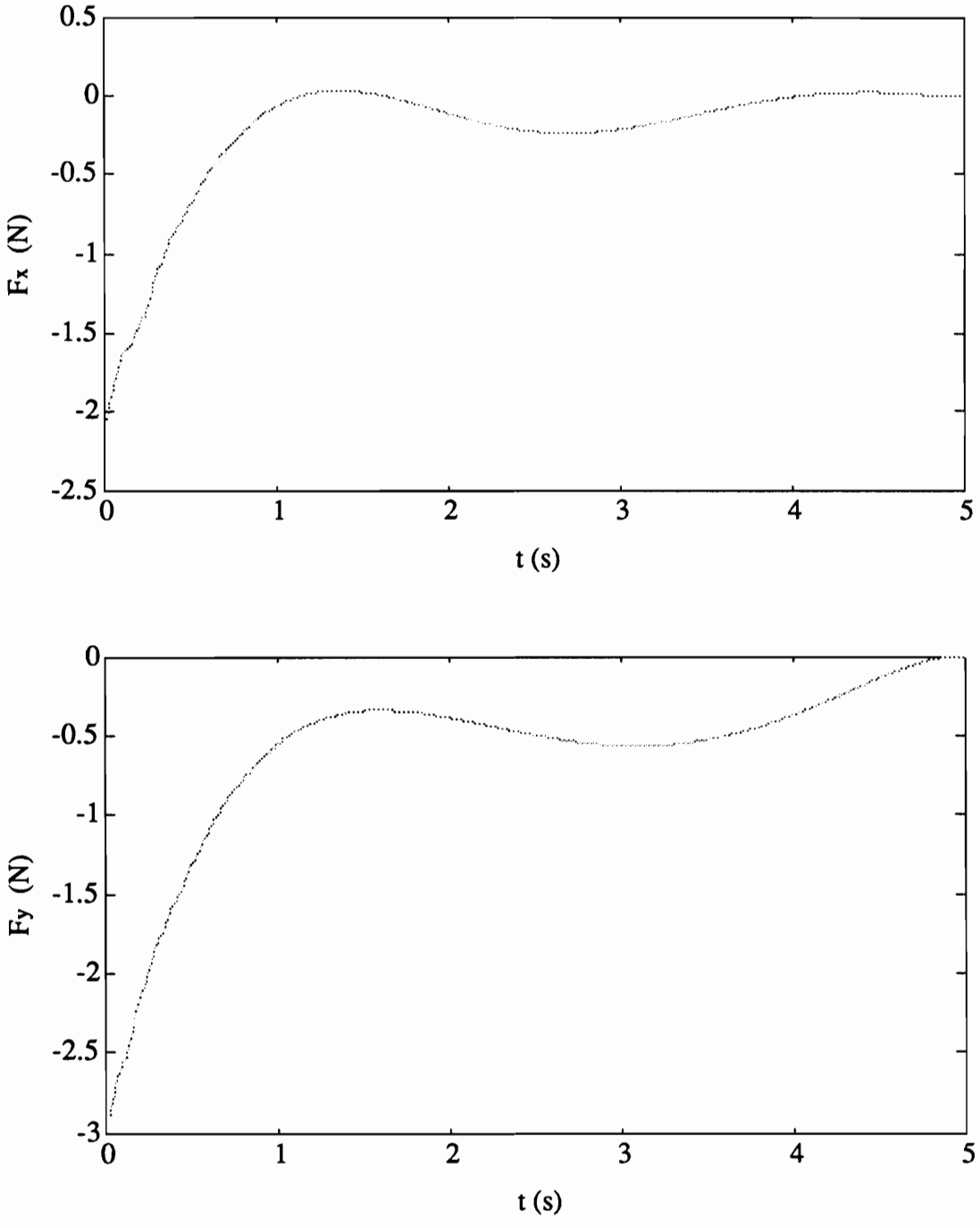

Figure 3.5a. Time Histories of the First-Order Control Forces for LQR Control

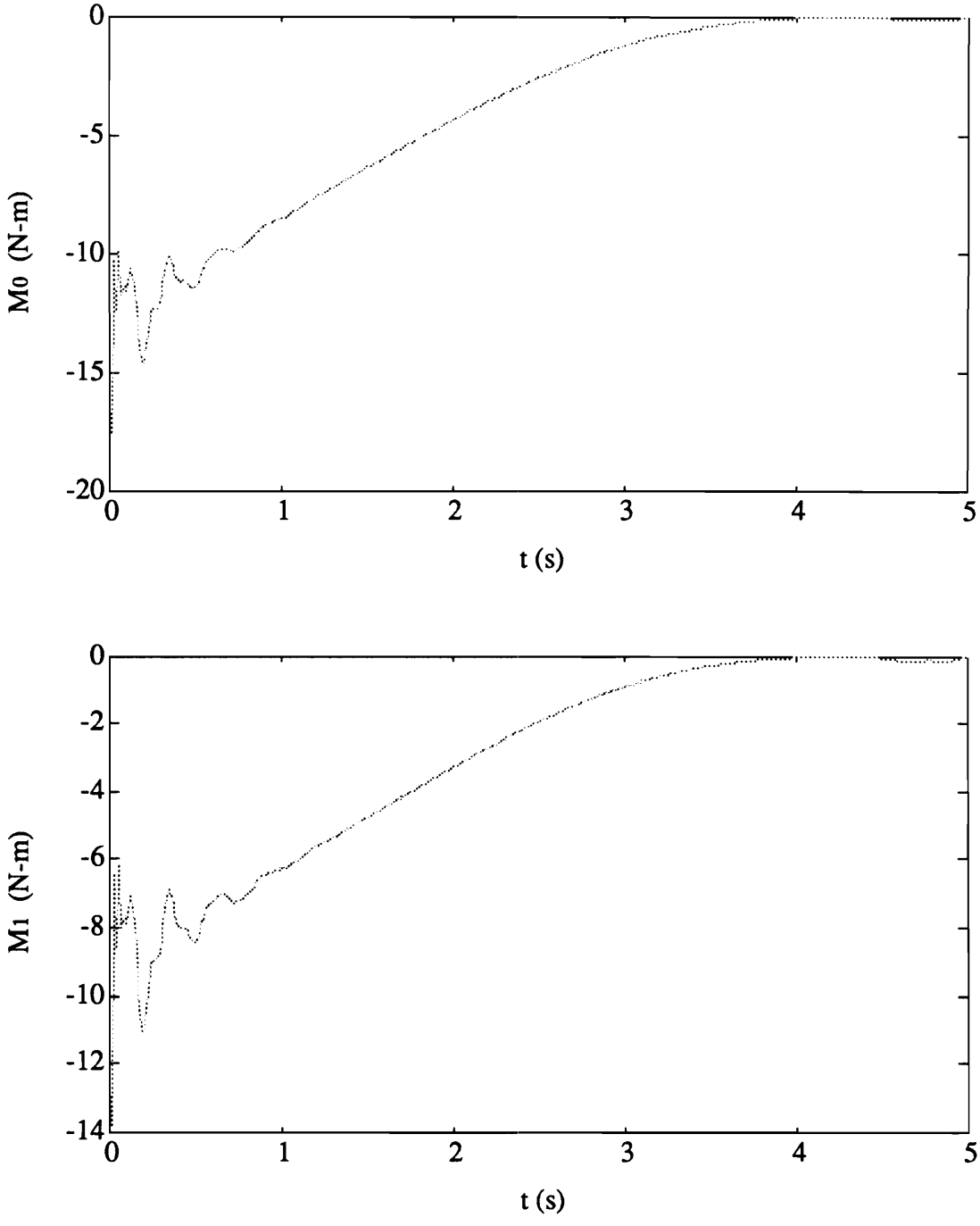

Figure 3.5b. Time Histories of the First-Order Control Torques for LQR Control

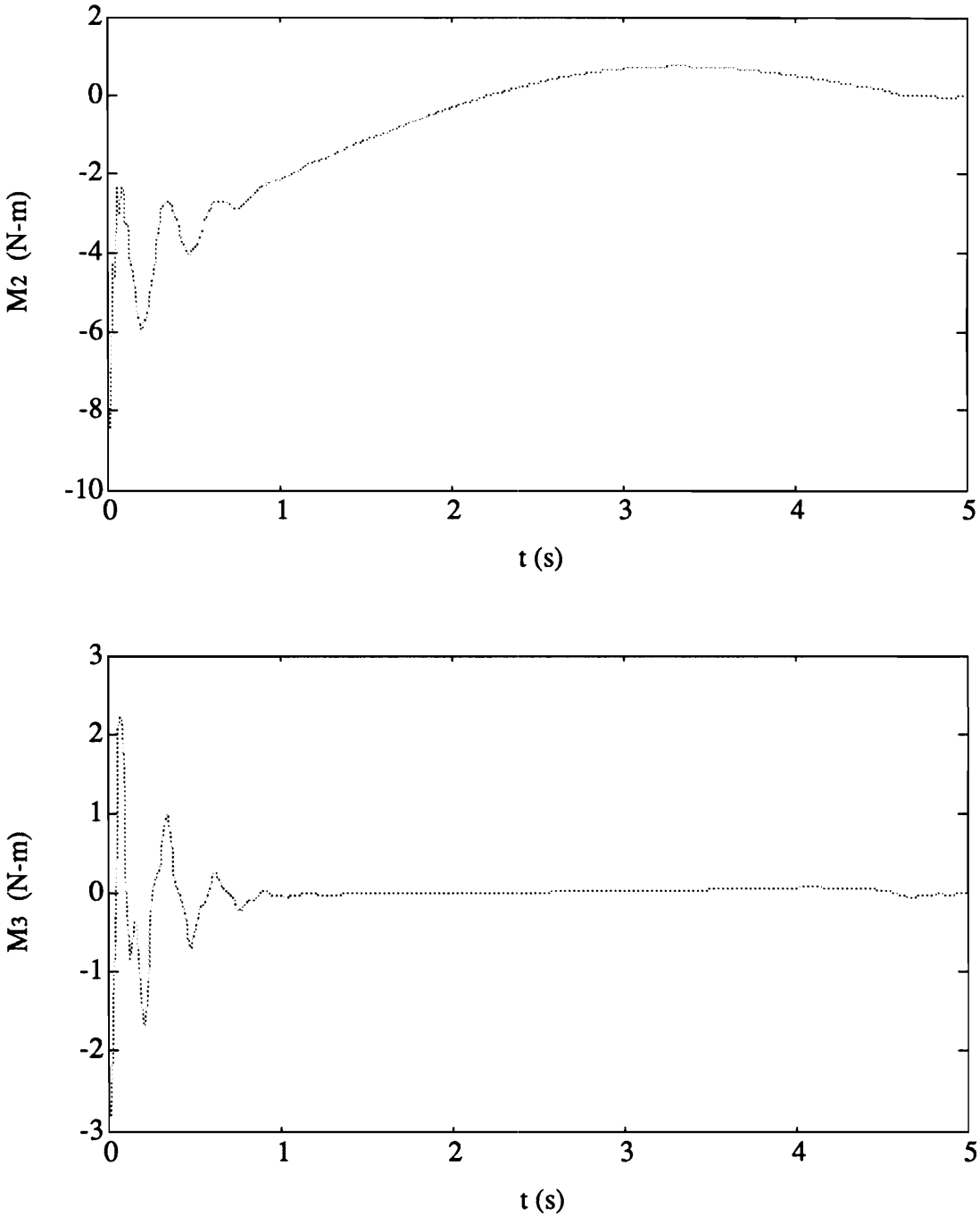

Figure 3.5c. Time Histories of the First-Order Control Torques for LQR Control

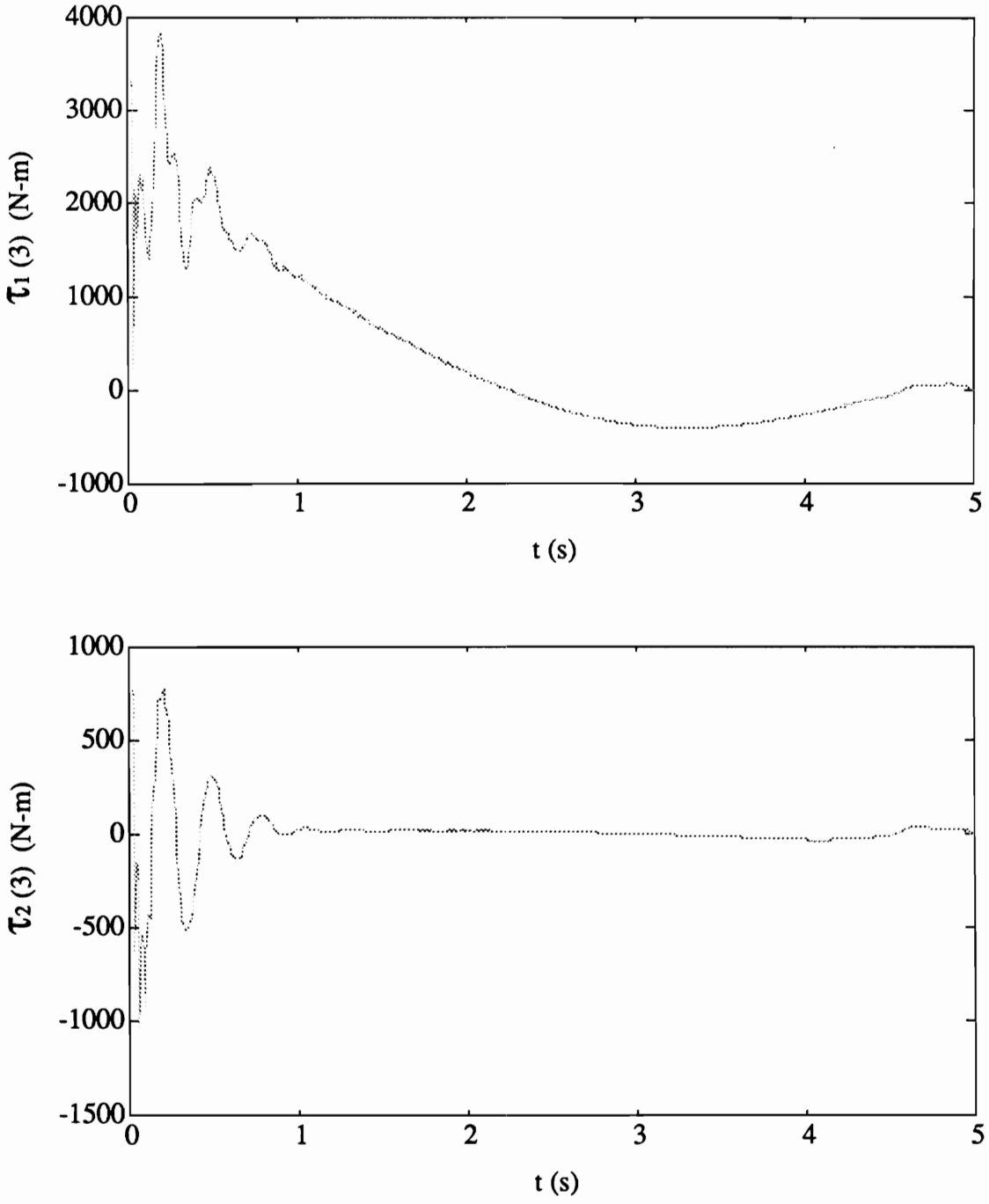

Figure 3.5d. Time Histories of the Third Element of the First-Order Control Torques Applied to the Flexible Arms for LQR Control

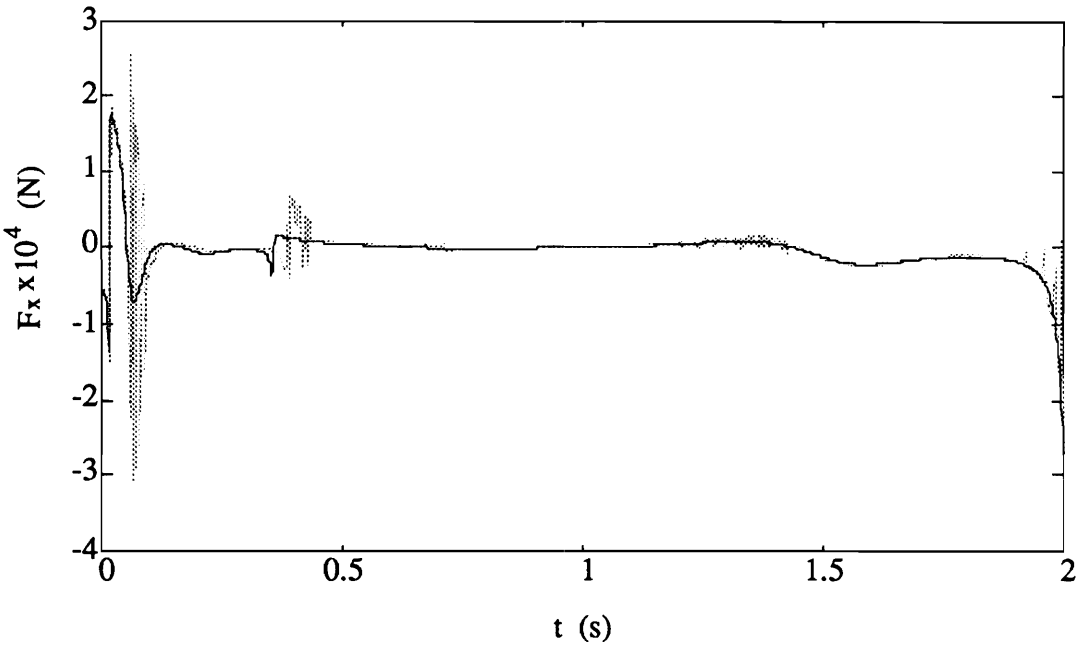

Figure 4.1. Bursting Phenomenon

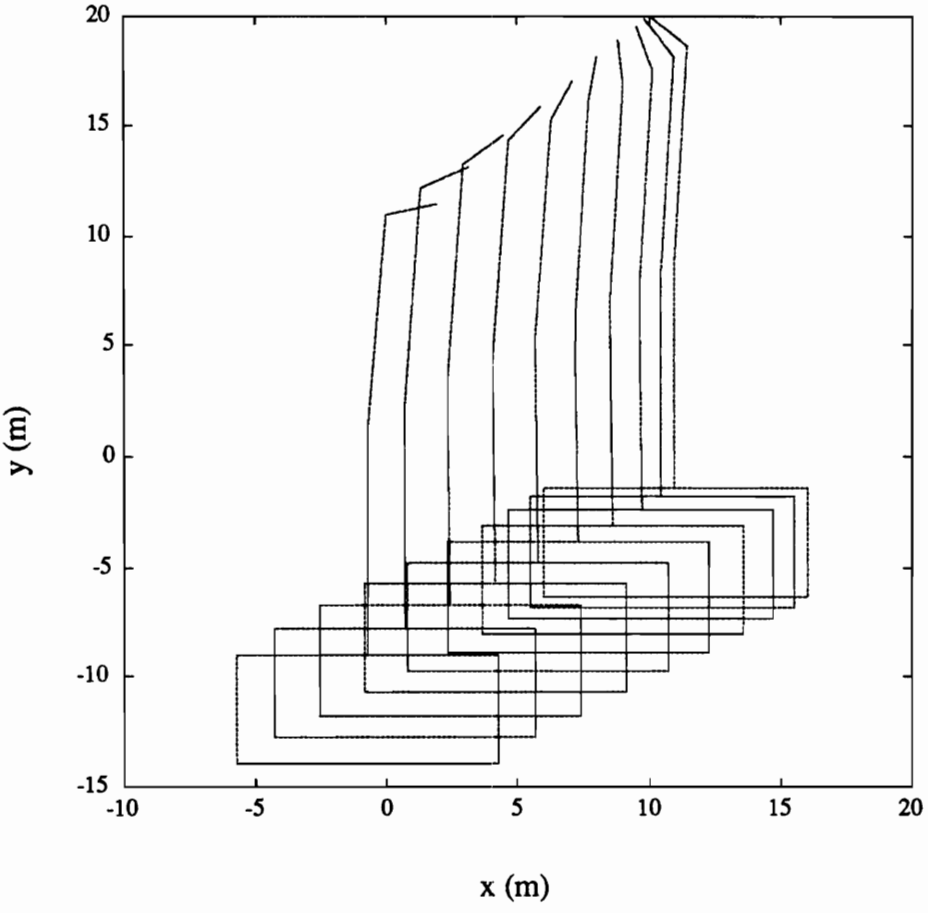

Figure 4.2a. Time-Lapse Picture of Robot Configuration Trajectory for Case 1

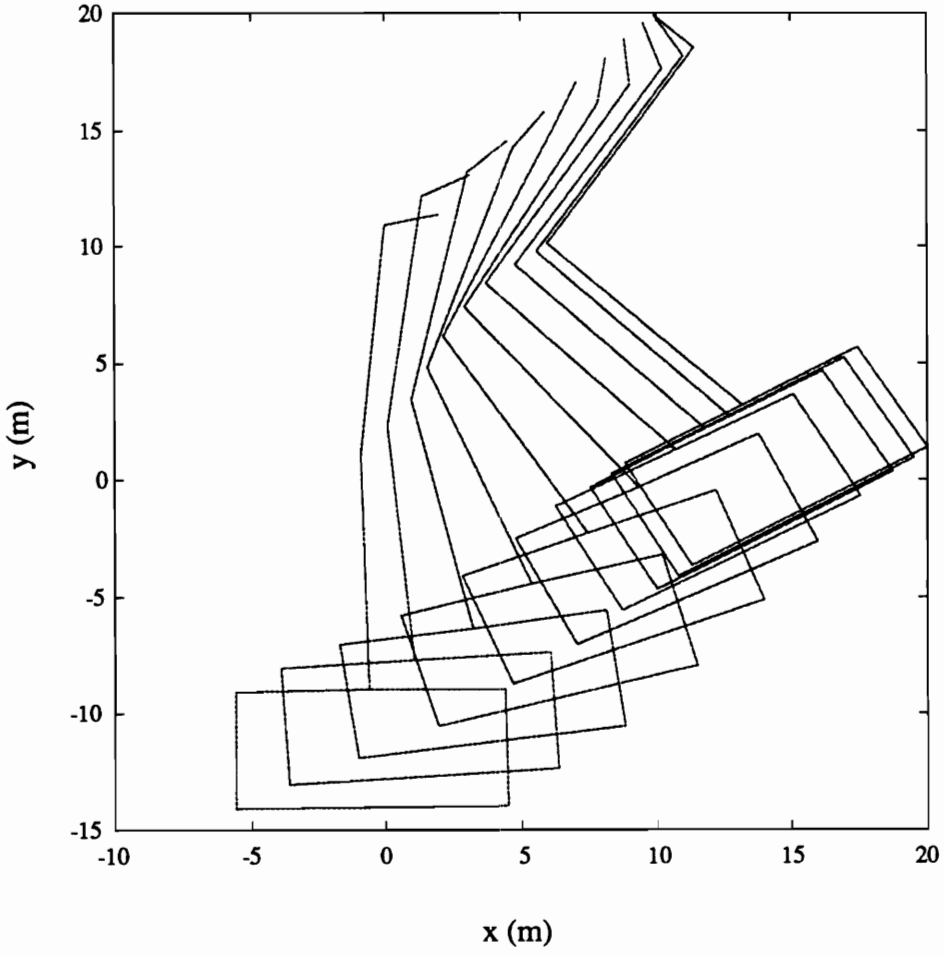

Figure 4.2b. Time-Lapse Picture of Robot Configuration Trajectory for Case 2

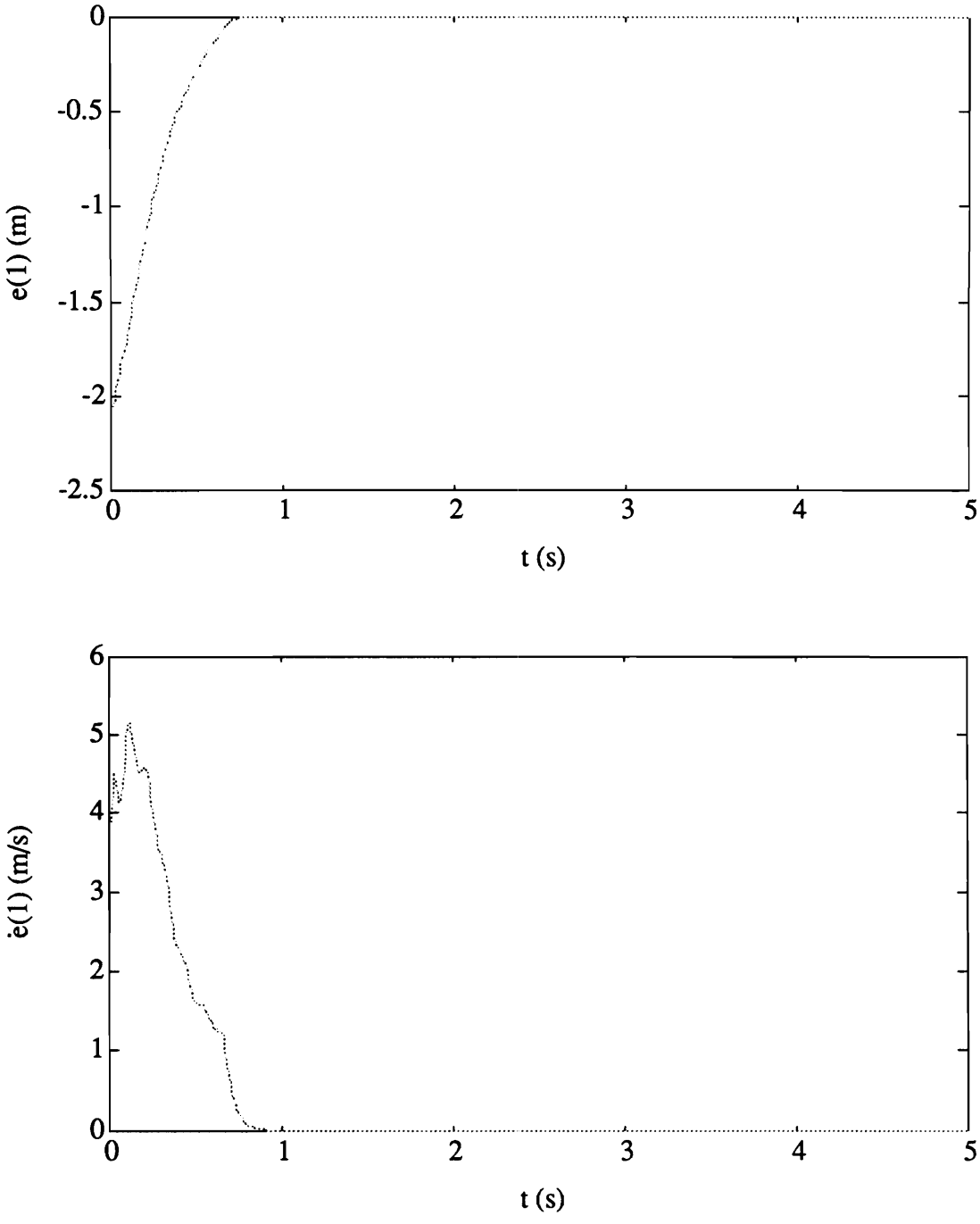

Figure 4.3a. Time Histories of Position Error and its Time Derivative

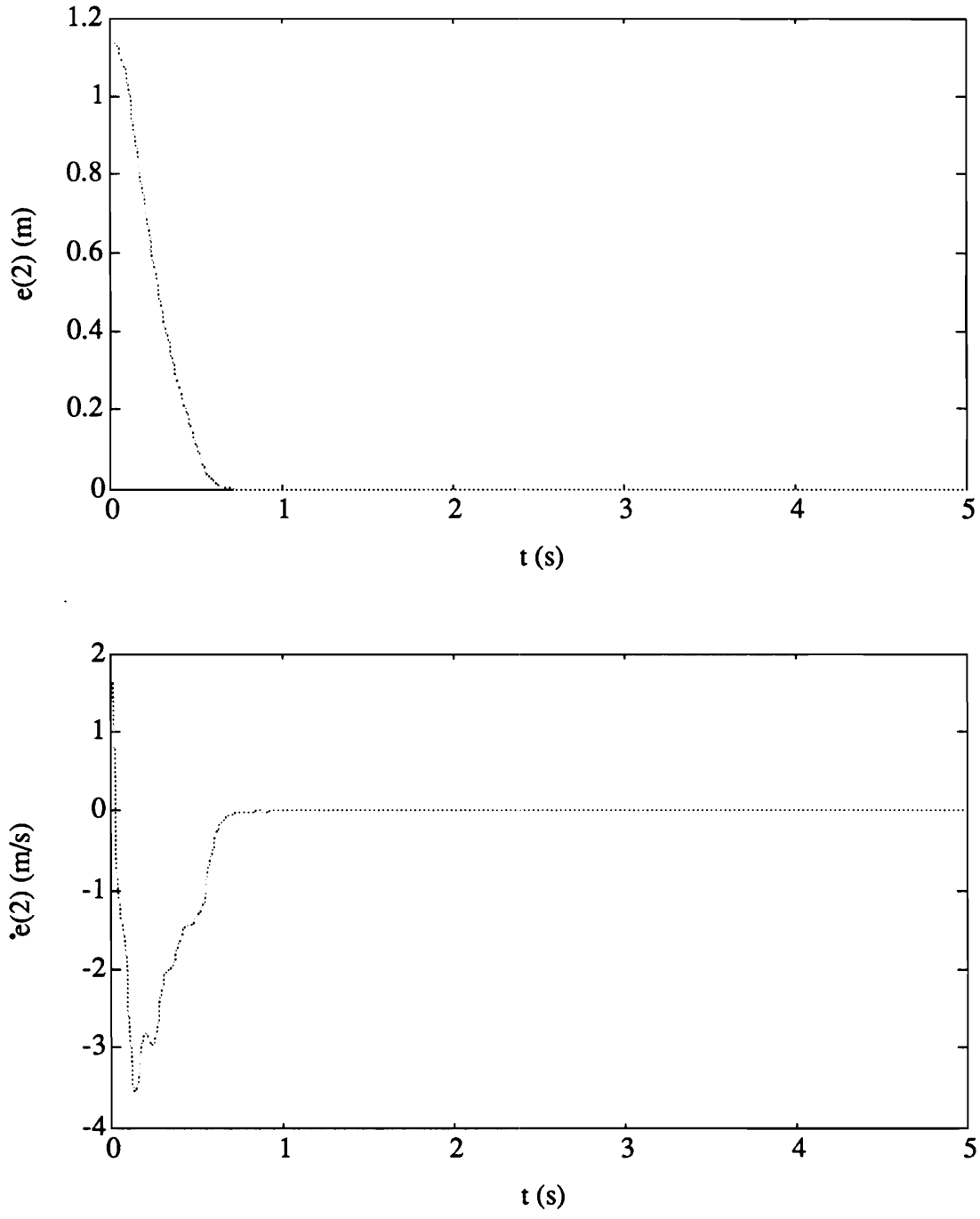

Figure 4.3b. Time Histories of Position Error and its Time Derivative

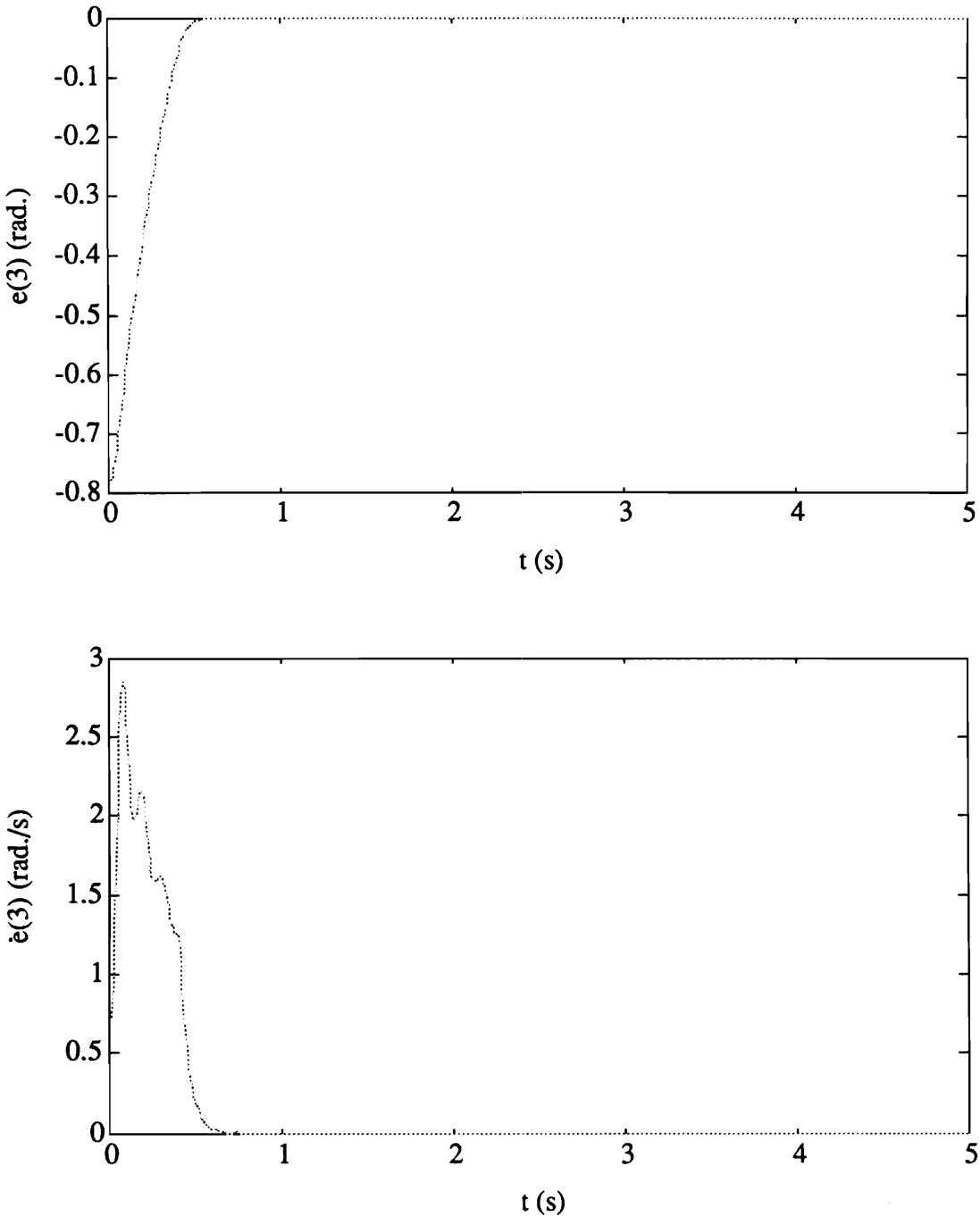

Figure 4.3c. Time Histories of Orientation Error and its Time Derivative

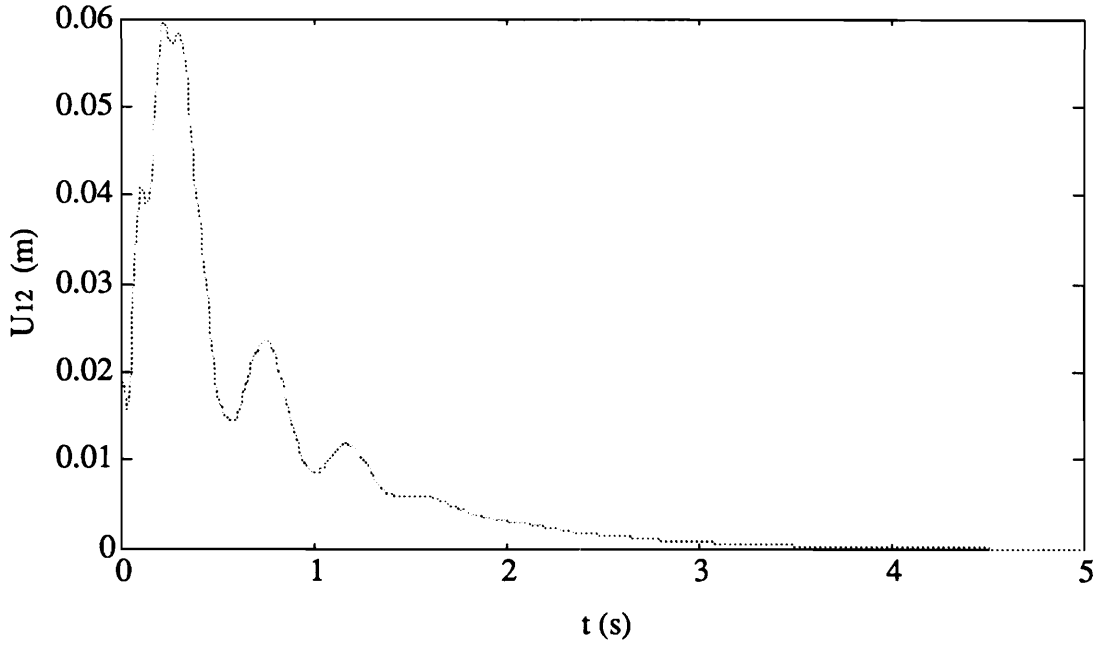

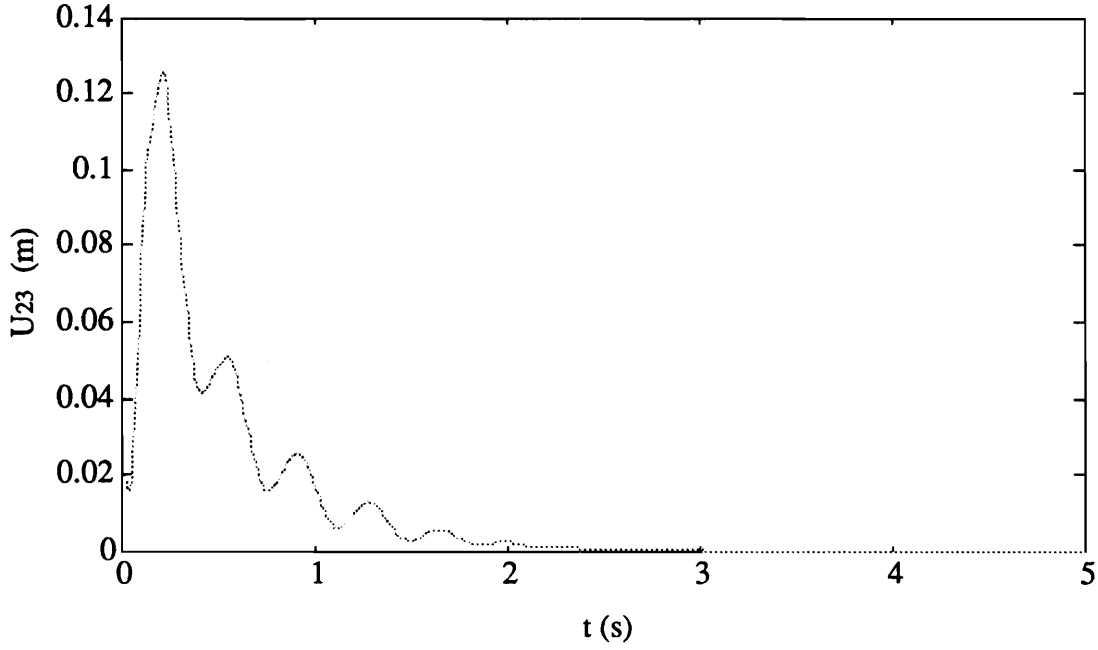

Figure 4.4. Time Histories of the Tip Elastic Displacements

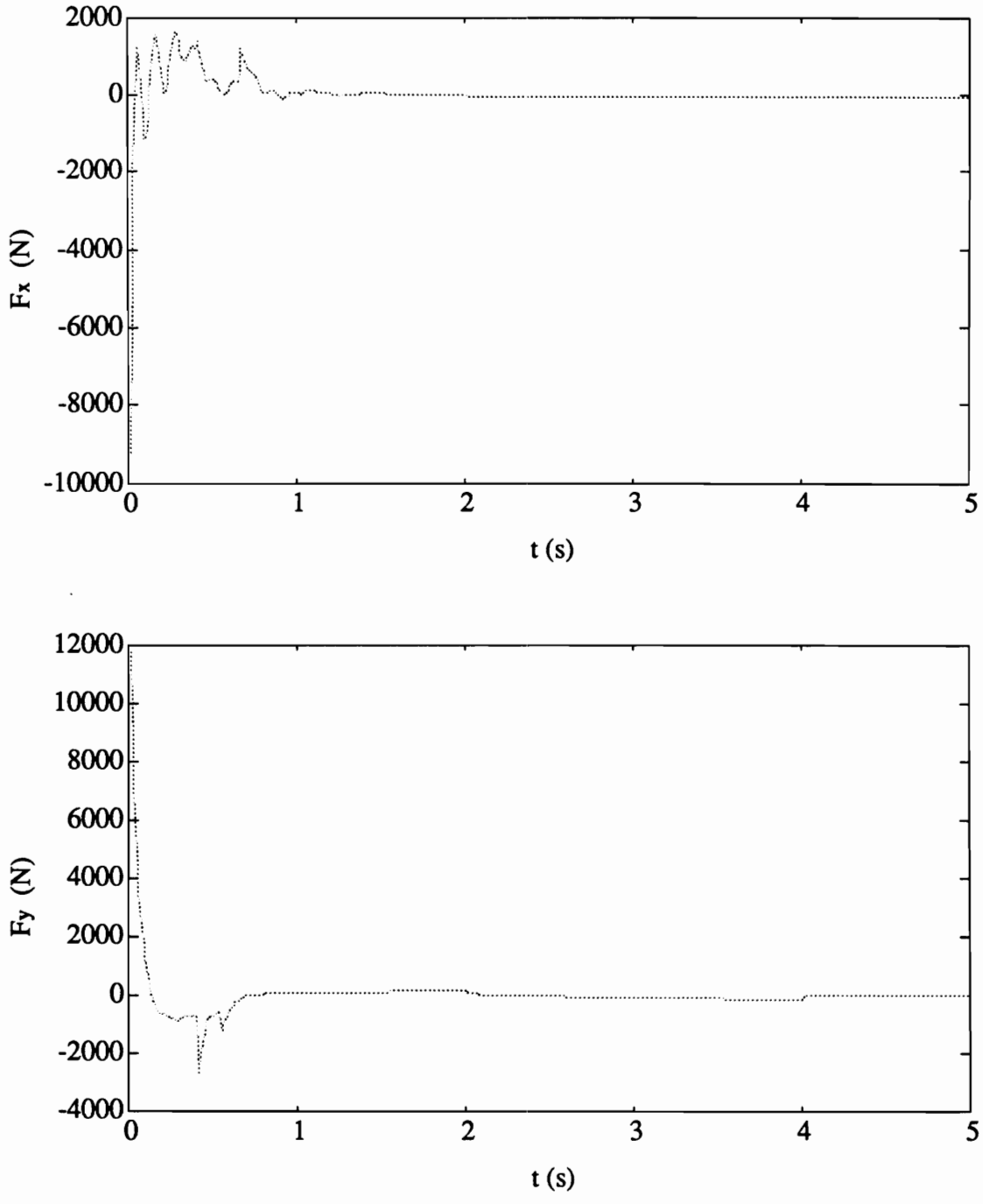

Figure 4.5a. Time Histories of the Control Forces for Rigid-Body Maneuver

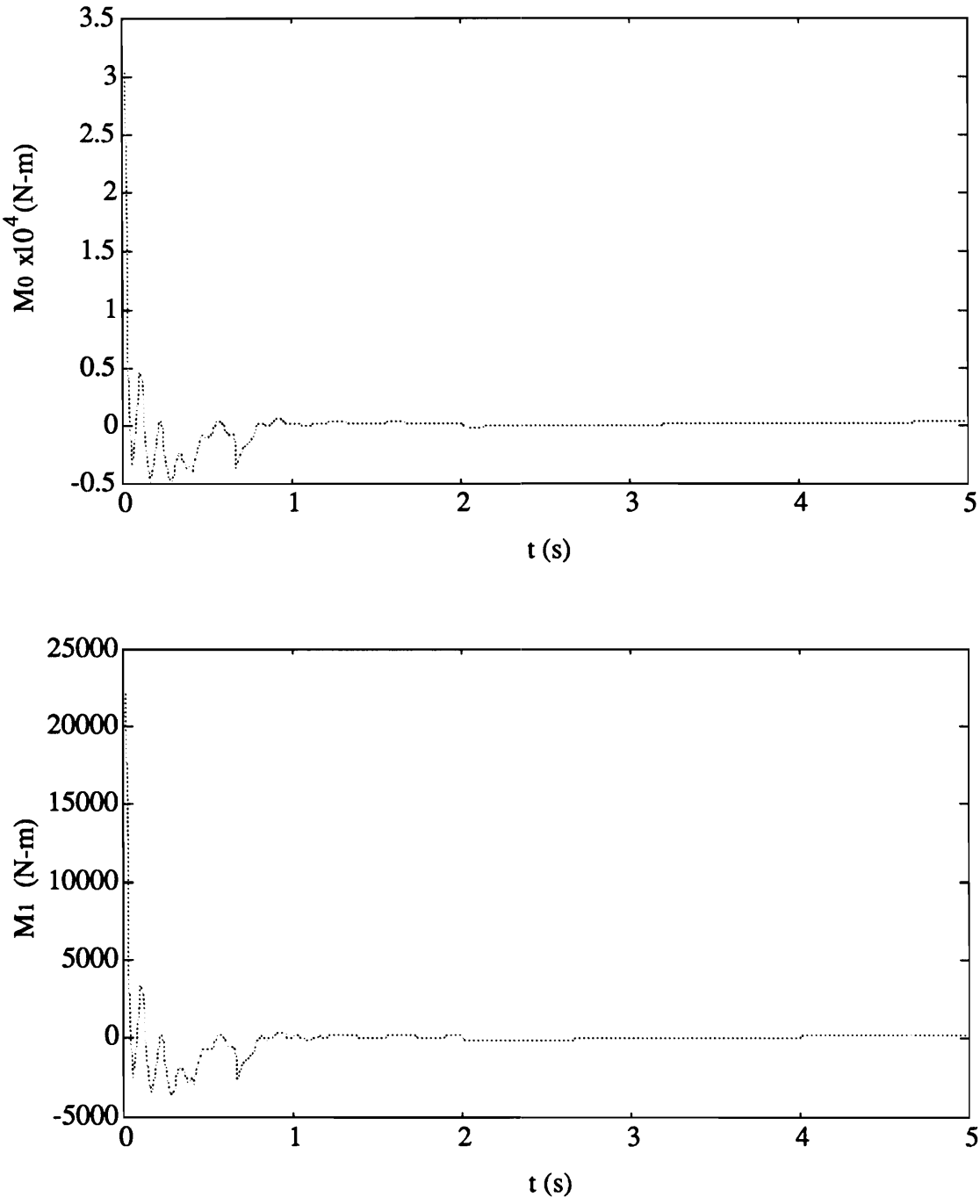

Figure 4.5b. Time Histories of the Control Torques for Rigid-Body Maneuver

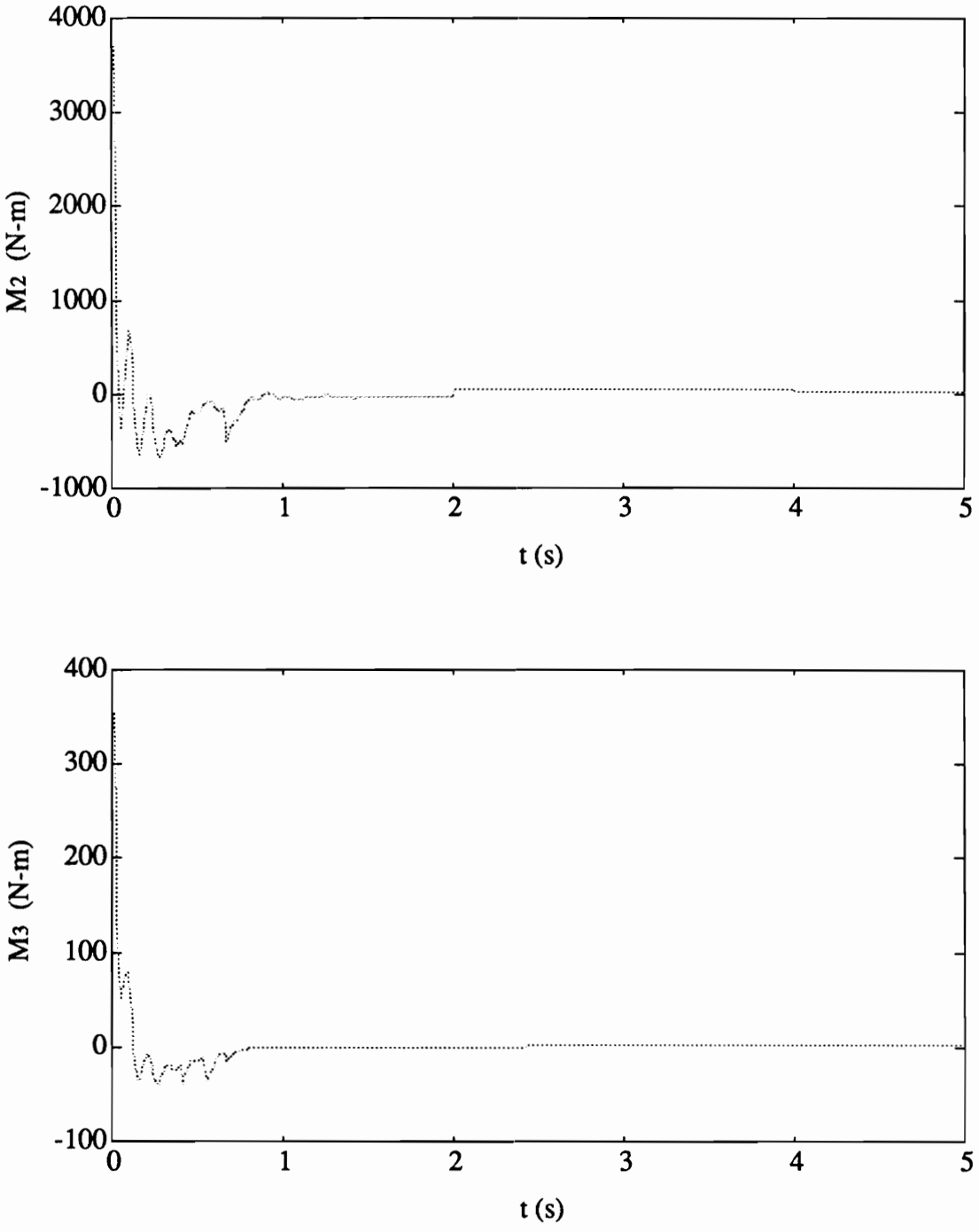

Figure 4.5c. Time Histories of the Control Torques for Rigid-Body Maneuver

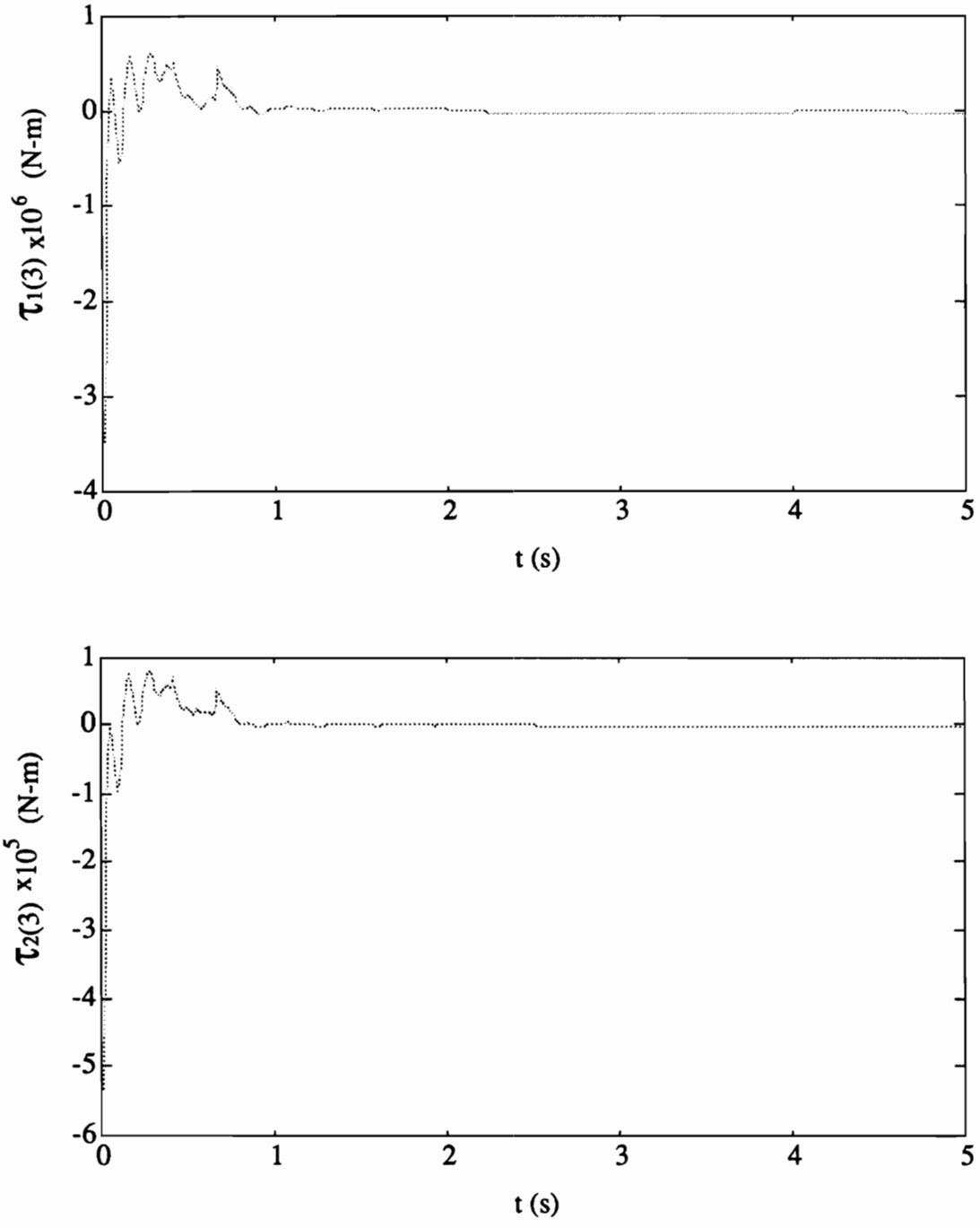

Figure 4.6. Time Histories of the Third Element of Control Torques Applied to the Flexible Arms for Disturbance Rejection

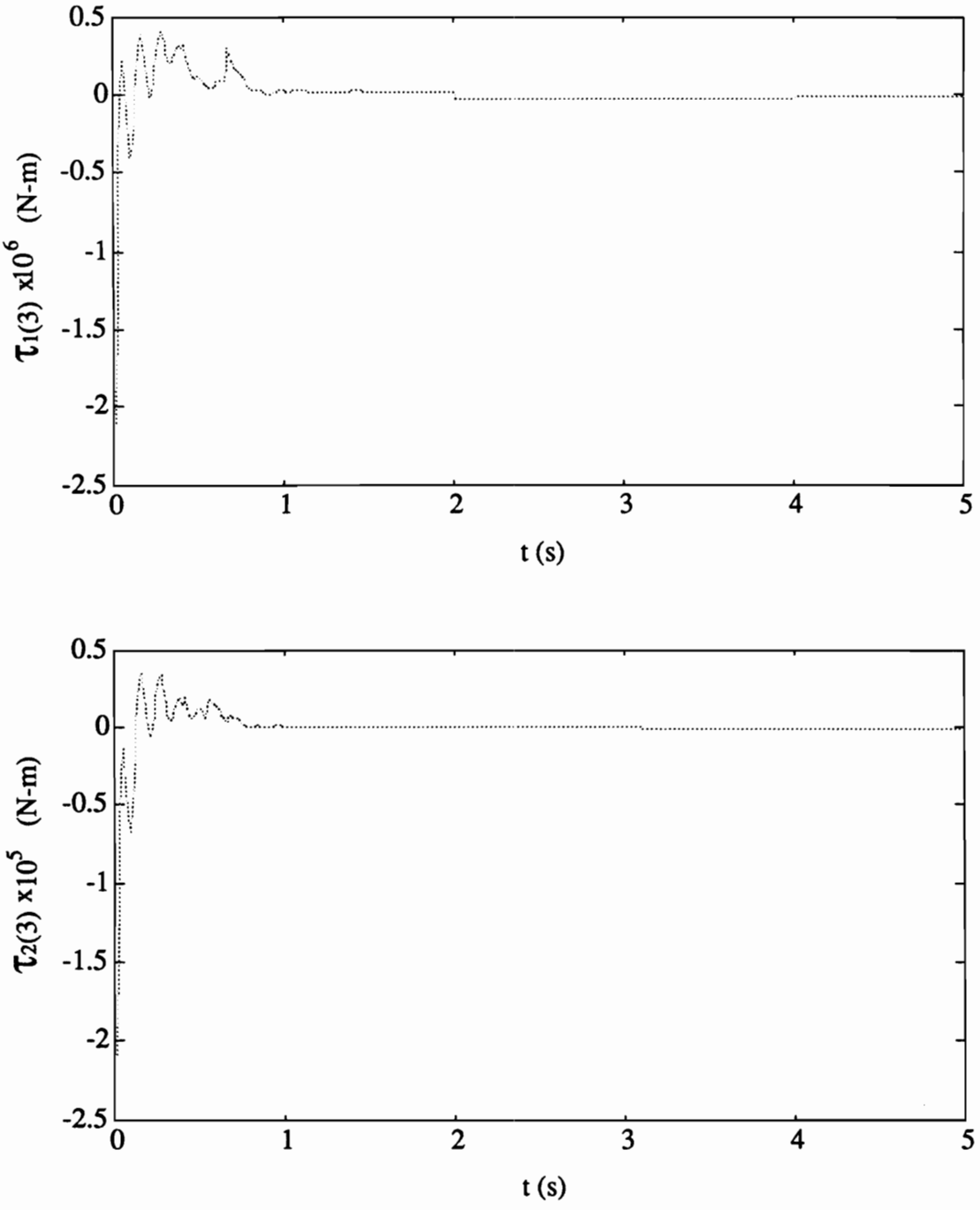

Figure 4.7. Time Histories of the Third Element of Control Torques Applied to the Flexible Arms for LQR Control

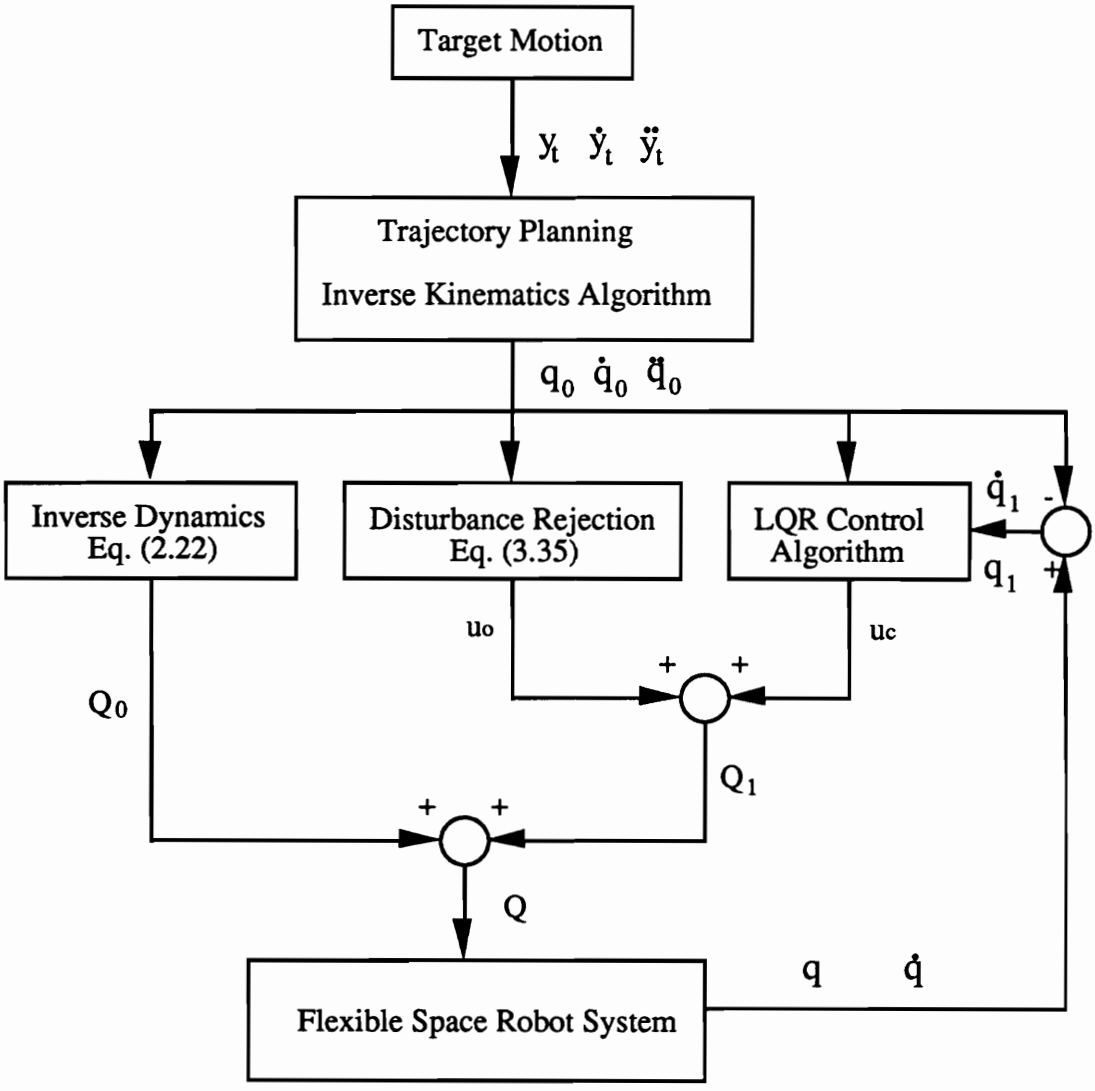

Figure 5.1. Block Diagram of the Control Algorithm for a Flexible Space Robot Tracking a Target Whose Motion is Known

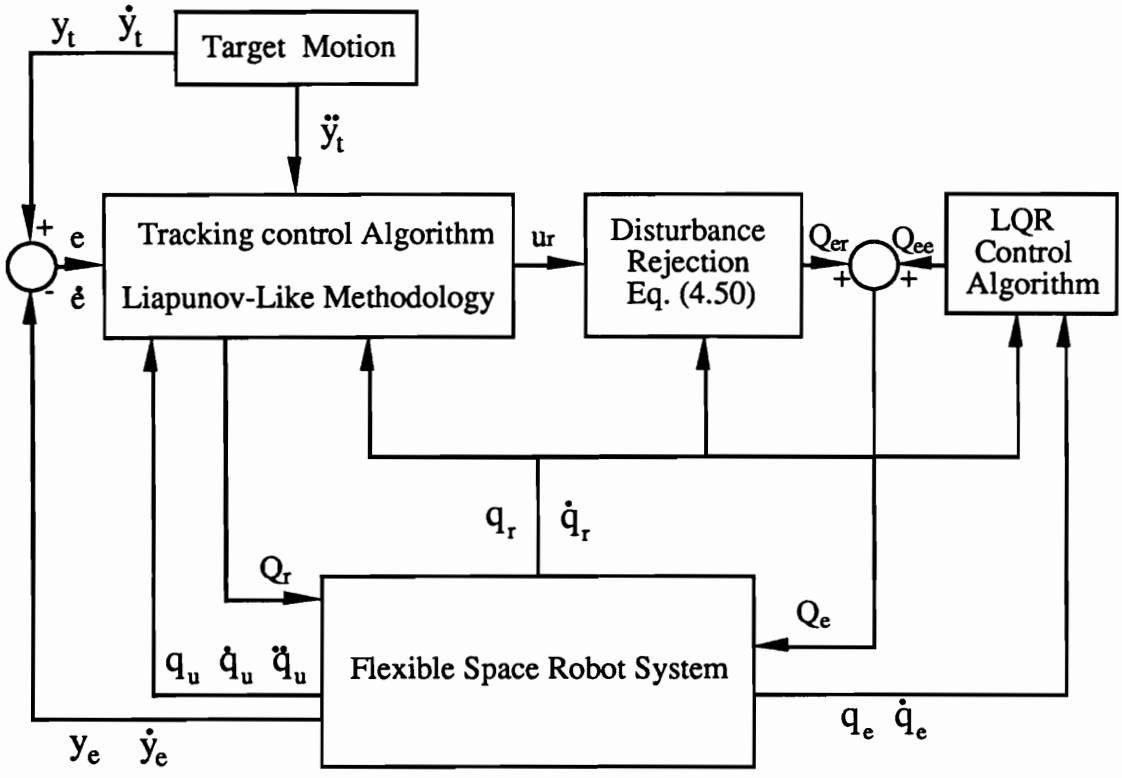

Figure 5.2. Block Diagram of the Control Algorithm for a Flexible Space Robot Tracking a Target Whose Motion is Not Known

Vita

Yifeng Chen was born on March, 19, 1963 in Wuhan, China. She received a Bachelor of Science degree in July, 1984 and a Master of Science degree in May, 1987, both from Northern Jiaotong University, Beijing, China. After spending one year as an engineer in Major Bridge Bureau at Wuhan, China, she entered Duke University in Sept. 1988 and then transfered to VPI&SU in Sept. 1989.

Yifeng Chen